I. RADIANCE AND IRRADIANCE IN FRESHWATER LAKES.

II. THE SPATIAL AND TEMPORAL DISTRIBUTION OF ZOOPLANKTON IN LAKE ITASCA.

A THESIS
SUBMITTED TO THE FACULTY OF THE GRADUATE SCHOOL
OF THE UNIVERSITY OF MINNESOTA
BY

PETER WURTELE VAUGHAN

IN PARTIAL FULFILLMENT OF THE REQUIREMENTS
FOR THE DEGREE OF
DOCTOR OF PHILOSOPHY

1988

ABSTRACT

A model of radiance distributions (RD) in water bodies is presented which is a simplification of the General Theory of Radiative Transfer. All of the parameters of the model may be estimated empirically, permitting the complete description of the RD in any water body. The model is tested by comparing its predicted RDs to measured RDs in three optically disparate lakes in northwestern Minnesota, and by demonstrating that it satisfies three other criteria: it obeys Snell's Law, it simplifies to the Lambert-Bouguer Law, and it predicts an asymptotic RD under certain circumstances.

The shape of natural RDs is shown to depend strongly on sun position and cloud cover. The shape of the RD is also shown to change with depth and to be dependent on water clarity. There is a very weak dependence of the RD shape on proximity to the bottom and to the shore.

The spectral composition of a specific radiance is highly dependent on the direction of the line of sight and on the optical clarity of the lake.

In the most transparent lake (Long Lake), downwelling irradiance is largely attenuated by water itself. In Lake Itasca, chlorophyll _a_ is the major light attenuating substance. Dissolved organic compounds dominate light attenuation in Bog Lake.

The effective, specific attenuation coefficients for chlorophyll _a_ and gilven are shown not to be constants. They are concentration dependent because of competition for light.

Intensive sampling is used to describe the small-scale vertical distribution and large-scale horizontal distribution of zooplankton in Lake Itasca. Patterns in the distribution and mesocosm experiments are used in an attempt to explain the ultimate cause of the observed distributions. It is shown that distribution patterns are specific for

individual populations, not for the entire zooplankton assemblage. In addition, there is a close temporal coupling between the vertical and horizontal distributions of many limnetic organisms. This suggests that the observed distributions are the result of biological interactions rather than large-scale physical factors such as, dark/light cycles and water currents.

TABLE OF CONTENTS

ACKNOWLEDGMENTS

I am indebted to Dr. Robert Megard for providing valuable direction and assistance throughout all phases of my work. He contributed enormously to my understanding of the importance of light in limnology and ecology. Dr. Peter Abrams was kind enough to guide and verify my mathematical efforts. Jeff Curtis listened to and commented on many early versions of my hypotheses about "Snell's Window".

Many undergraduate students helped with my field work. In particular, I would like to thank Steve Householder, Barb Stoner, Dave Delehanty and Amy Manolis for their contributions. Jon Ross, and the staff and students at the Itasca Biological Station made that a very interesting, productive and enjoyable place to work.

My field work was financed with grants from the Dayton Natural History Fund, the Wilkie Fund and the Itasca Biological Station. I would like to thank the Graduate School of the University of Minnesota for supporting me with a Bush Fellowship, a Dissertation Fellowship and four years of teaching assistantships.

Finally, I need to thank my wife, Cathy Anson. She maintained an undaunted enthusiasm and optimism as she listened to the minutiae of my trials and tribulations that are recorded in the following pages.

CHAPTER 1

AN EMPIRICAL MODEL OF RADIANCE DISTRIBUTIONS IN WATER BODIES

Abstract

A model of radiance distributions in water bodies is presented which is a simplification of the General Theory of Radiative Transfer. All of the parameters of the model may be empirically estimated, permitting the complete description of the radiance distribution in any hydrosol. The model is tested by comparing its predicted radiance distributions to measured radiance distributions in three optically disparate lakes in northwestern Minnesota, and by demonstrating that it satisfies three other criteria: it obeys Snell's Law, it simplifies to the Lambert-Bouguer Law in the case of no scattering, and it predicts an asymptotic radiance distribution under certain circumstances.

Introduction

The analysis of radiance distributions in natural water bodies contributes to an understanding of radiation transfer processes and leads directly to knowledge about scalar irradiance. Scalar irradiance is ecologically significant because it is a measure of the amount of energy that is available at a given depth in a water body for primary production (Kirk, 1983 pg. 118). The radiance distribution is of interest in its own right because it constitutes the photic environment in which many light-dependent, biological phenomena occur. It is the radiance distribution which determines the background lighting against which visual vertebrate predators search for their prey (McFarland & Munz, 1975a, 1975b; Janssen, 1981), and it has been invoked as the proximate mechanism used by limnetic zooplankton to detect and hence avoid littoral regions ("uferflucht"), (Siebeck, 1980). Thus, the radiance distribution may be an important structural component of limnetic environments which otherwise lack physical structure.

Preisendorfer (1957, 1958a, 1958b, 1959) has provided an extensive theoretical framework for Radiative Transfer Theory. Whitney (1941), Tyler (1960) and others have contributed detailed field measurements of radiance distributions, and several authors have produced computer models, based on Radiative Transfer Theory, which predict radiance distributions. The most successful class of these models are the "Monte Carlo" models of Plass and Kattawar (1969, 1972), Kattawar and Plass (1972), Gordon and Brown (1973) and Kirk (1981a). Only Kirk (1981b) attempts to test his model by making a comparison between empirical measurements of the vertical attenuation coefficient and the irradiance reflectance with estimates generated by the model.

These models predict the change in the radiance distribution due to transmission through water. Within the water column, the radiance distribution is dependent on two inherent optical properties of the water, the beam attenuation coefficient (c) and the volume scattering function ($\tilde{\beta}_{\theta}$) (Preisendorfer, 1957). Table 1 is a list of all the symbols used in this chapter. Modelers assign values to these parameters

and then derive a probability for a photon being either absorbed or scattered in a unit pathlength. Photons are then introduced as a parallel beam and are tracked until they are either absorbed, scattered back out of the water, or penetrate past a predetermined depth limit. A detailed description of the photic environment is generated by following a large number of photons.

A principal shortcoming of these models is that β_θ is very difficult to measure, and few laboratories are equipped to make the measurements (Kirk, 1981b). Modelers have followed several strategies to circumvent this problem: assumed Rayleigh, isotropic, scattering only (Preisendorfer, 1959); allowed both Rayleigh and Mie, anisotropic, scattering, but set particle size distributions to arbitrary size limits (Plass & Kattawar, 1969); or borrowed measurements from other water bodies (Kirk, 1981). Scattering in natural water bodies is of both the Mie and Rayleigh type, and although the shape of the scattering function should not depend on the concentration of particles in the water, it does depend on the optical nature of the particles present (Kirk, 1983, pg. 87). This makes the extrapolation of parameter values to foreign water bodies uncertain. There is an obvious appeal to a method which incorporates the scattering properties of the water of interest.

A second shortcoming is that these models assume a parallel beam as their radiance source, whereas in some circumstances, diffuse skylight may be of great importance. This problem is minimized in models that treat the atmosphere-ocean system as a single unit of layers with differing scattering characteristics, and then introduce a parallel beam into the atmosphere (Kattawar & Plass, 1972). It may be justified in other models on clear days when radiance is highly directional (Kirk, 1981), but is less realistic on overcast days when source light is diffuse.

In this paper, I develop an empirical simplification of the Radiative Transfer Theory which allows the prediction of radiance at any depth and from any direction provided the following are known: the corresponding sky radiance distribution, a radiance distribution measured just beneath the surface, the beam attenuation coefficient and the scalar irradiance

(vertical) attenuation coefficient. I then test this model with measurements from three optically disparate lakes in northwestern Minnesota.

Model

a) The air-water interface: The radiance distribution just beneath the surface is dependent on the radiance distribution just above the surface and the physical processes of refraction and reflection at the air-water interface. Figure 1 illustrates the two processes, refraction and reflection, which are known to modify the sky radiance distribution at the air-water interface. Radiance of a specified direction at a point in a lake is given by $L_{(z,\theta,\phi)}$, where z is depth, θ is zenith angle and ϕ is azimuth angle measured clockwise from the position of the sun. Incident radiance, $L_{(0,\theta a,\phi)}$ is refracted to zenith angle theta at the air-water interface following Snell's Law

$$\theta = \arcsin((\sin \theta a)/n) \qquad (1)$$

Here, n is the refractive index and can be considered to be a constant equal to 1.33. The result of Snell's refraction is the focussing of sky radiance within the critical angle of 48.6° from the vertical (Snell's Window).

Radiance is also subject to partial reflection at the air-water interface as described by Fresnell's Law. The percent of radiance transmitted across the interface to angle θ (T_θ) is dependent only on the the angle of incidence, shown as

$$T_\theta = 1 - 0.5\left[\frac{\sin^2(\theta a-\theta)}{\sin^2(\theta a+\theta)} + \frac{\tan^2(\theta a-\theta)}{\tan^2(\theta a+\theta)}\right] \qquad (2)$$

b) Radiative Transfer Theory: Radiative Transfer Theory recognizes three processes that modify radiance as it penetrates a medium: absorption and outscatter contribute to a reduction in radiance, and inscatter of radiance from other directions (θ',ϕ') augments the radiance

at direction (θ,ϕ) (Kirk, 1983). Figure 2 illustrates these processes. Radiance incident on thin section dz at g, $L_{(g,\theta,\phi)}$ is only partially transmitted to h. A fraction of the incident light is absorbed, and a separate fraction is scattered out of angle (θ,ϕ). In addition, some radiation is scattered into direction (θ,ϕ) from other directions and is transmitted to h. Absorption and outscatter are inherent optical properties of the medium and may be considered together as a beam attenuation. c is the beam attenuation coefficient (m^{-1}). Inscatter is also an inherent property of the medium that is dependent on β_θ, the volume scattering function. These three processes comprise Radiative Transfer Theory and give rise to the classical formulation for the change of radiance with depth given by Preisendorfer (1957)

$$dL_{(z,\theta,\phi)}/dx = -cL_{(z,\theta,\phi)} + L^*_{(z,\theta,\phi)} \qquad (3)$$

where z is depth and x is the pathlength light travels to depth z ($x=z/\cos\theta$). $L^*_{(z,\theta,\phi)}$ is the path function which is defined as

$$L^*_{(z,\theta,\phi)} = \int_{4\pi} \beta(z,\theta,\phi,\theta',\phi') L_{(z,\theta',\phi')} d\hat{\omega}_{(\theta',\phi')} \qquad (4)$$

Here, β is the proportion of radiance at direction (θ',ϕ') which is scattered into direction (θ,ϕ) at depth z, and $d\hat{\omega}$ is the unit of solid angle around $L_{(\theta',\phi')}$ which is under consideration. Preisendorfer (1957) integrates equation 3 with respect to depth to derive the instantaneous solution for radiance at a depth

$$L_{(z,\theta,\phi)} = L_{(0,\theta,\phi)} e^{-cx} + \left[\frac{L^*_{(0,\theta,\phi)} e^{-kz}}{c + k\cos\theta}\right]\left[1-e^{-(c+k\cos\theta)x}\right] \qquad (5)$$

Equations 1, 2, and 5 may be combined to give an expression for $L(z,\theta,\phi)$ in terms of sky radiance that accounts for reflection and refraction at the surface and absorption and scatter along pathlength x. This summary expression is given as equation 6.

$$L_{(z,\theta,\phi)} = T_{\theta}L_{(a,\theta a,\phi)}e^{-cx} + \left[\frac{L^{*}_{(0,\theta,\phi)}e^{-kz}}{c + k\cos\theta}\right]\left[1-e^{-(cx+kz)}\right] \quad (6)$$

In this equation, radiance at a given depth and direction is comprised of two components: one of light incident at that direction (the first quantity on the right-hand side of equation 6) and one of light scattered into that direction from other incident angles (the second quantity on the right-hand side of equation 6). These components may be represented by the symbols L' and L" respectively, which simplifies equation 6 to

$$L_{(z,\theta,\phi)} = L'_{(z,\theta,\phi)} + L''_{(z,\theta,\phi)} \quad (7)$$

Although L' is a relatively simple value to measure, L" is very complex. One must first know the shape of β_{θ}, which has been measured in a relatively few bodies of water (Petzold, 1972). Secondly, one must know the radiances at all angles (θ',ϕ') and how they change with depth. Lastly, one must calculate k, Schuster's Coefficient that relates backscatter to absorption (Preisendorfer, 1957).

c) Redefinition of the path function: Estimation of L" may be greatly simplified if it is assumed that a single value, scalar irradiance (E) at depth z (rather than the integration of the contribution from all other radiance values), is the source for the inscattered light at depth z. If one next assumes that a constant proportion of scalar irradiance is scattered into direction (θ,ϕ) per unit depth, one may define an inscatter coefficient $s = dL''_{(z,\theta,\phi)}/E_{(z)}dx$ with units of $(m^{-1}\ deg^{-1})$. This assumption is clearly valid once the asymptotic radiance distribution is achieved, but is likely to be somewhat in error at shallower depths (Preisendorfer, 1958a). It is assumed here that this error is small. Each direction requires a unique s that is largely dependent on the angular distance between the principle light source and the direction of interest.

d) A new Radiative Transfer Model: With this new definition of inscatter, it is possible to construct a simple mass balance for photons traversing the thin section, dz, in Figure 2

$$L_{(h,\theta,\phi)} = L_{(g,\theta,\phi)} - L_{(g,\theta,\phi)}cdx + E_{(g)}sdz \tag{8}$$

The change of radiance between g and h ($dL_{(\theta,\phi)}$ is simply the net result of the processes of attenuation and inscatter. Thus, $dL_{(\theta,\phi)}$ is defined as the difference between L_h and L_g. Rearrangement of 8 gives

$$dL_{(\theta,\phi)} = E_{(g)}sdz - L_{(g,\theta,\phi)}cdx \tag{9}$$

Note that $dL_{(\theta,\phi)}$ may be either positive or negative depending on the relative magnitudes of inscatter and attenuation.

Because inscatter is dependent on scalar irradiance, it is important to be able to predict $E_{(g)}$. This can be done because the attenuation of scalar irradiance is accurately modeled by an adaptation of the Lambert-Bouguer Law (Kirk, 1983, pg. 119)

$$E_{(g)} = E_{(0)}e^{-c'g} \tag{10}$$

where c' is the vertical attenuation coefficient for scalar irradiance (m^{-1}).

The instantaneous rate of change of radiance is found by substituting equation 10 into 9 and then dividing equation 9 by $L_{(g,\theta,\phi)}$

$$\frac{dL_{(\theta,\phi)}}{L_{(g,\theta,\phi)}} = \frac{E_{(0)}se^{-c'g}dz}{L_{(g,\theta,\phi)}} - cdx \tag{11}$$

Equation 11 can be integrated from the surface to depth z to show how the radiance is dependent on depth.

$$\int_0^z \frac{dL_{(\theta,\phi)}}{L_{(g,\theta,\phi)}} = \int_0^z \frac{E_{(0)}se^{-c'g}dz}{L_{(g,\theta,\phi)}} - \int_0^z \frac{cdz}{\cos\theta}$$

$$\ln\left[\frac{L_{(z,\theta,\phi)}}{L_{(0,\theta,\phi)}}\right] = \left[\frac{E_{(0)}s}{L_{(0,\theta,\phi)}}\right]\left[\frac{e^{-c'z}}{-c'}\right] - \left[\frac{E_{(0)}s}{-L_{(0,\theta,\phi)}c'}\right] - cx$$

$$\frac{L_{(z,\theta,\phi)}}{L_{(0,\theta,\phi)}} = e^{(E_{(0)}s - E_{(0)}se^{-c'z})/L_{(0,\theta,\phi)}c') - cx} \qquad (12)$$

Next, assume that radiance just below the surface at g is comprised of two components: radiance incident at the surface at the appropriate angle (θa) less that attenuated in distance g, and radiance scattered into that angle in distance dz. This assumption is justified by equation 7, and is expressed as

$$L_{(0,\theta,\phi)} \approx L_{(g,\theta,\phi)} = T_\theta L_{(a,\theta a,\phi)} - T_\theta L_{(a,\theta a,\phi)}cg + E_{(0)}sg \qquad (13)$$

The substitution of equation 13 into equation 12 gives

$$\frac{L_{(z,\theta,\phi)}}{T_\theta L_{(a,\theta a,\phi)} - T_\theta L_{(a,\theta a,\phi)}cg + E_{(0)}sg} =$$

$$e^{\left[\left[\frac{E_{(0)}s - E_{(0)}se^{-c'g}}{c'(T_\theta L_{(a,\theta a,\phi)} - T_\theta L_{(a,\theta a,\phi)}cg + E_0 sg)}\right] - cx\right]} \qquad (14)$$

Finally, to derive a simplified expression for radiance at a given depth, allow b to equal the complex exponent on the right side of equation 14 and solve for $L_{(z,\theta,\phi)}$. This results in an expression for radiance that is dependent only on quantities which can be empirically estimated. This model is given as equation 15.

$$L_{(z,\theta,\phi)} = T_\theta L_{(a,\theta a,\phi)}e^b - T_\theta L_{(a,\theta a,\phi)}cge^b + E_{(0)}sge^b \qquad (15)$$

Methods

The model given as equation 15 was tested by comparing computer generated depth profiles of radiance distributions to measurements made in three optically distinct lakes in northwestern Minnesota: Long Lake is highly transparent (mean summer transparency of 7.0m), Lake Itasca is a highly productive lake (transparency of 2.2m) and Bog Lake is a strongly colored lake (transparency of 1.5m). Empirical radiance measurements were made with a Li-Cor 185 quantum sensor fitted with a Gershun tube (acceptance angle of 13.0°) and then attached to a 3m long PVC pole. Radiance measurements were made above the lake surface and below the surface every 0.5m to a depth of 2.5m. Four azimuth headings were used, two in the plane that included the sun and two normal to that plane (ϕ = 0°, 90°, 180°, and 270°). The radiance in the water was measured at 16 zenith angles at each azimuth heading. Within Snell's Window (0-50°) the angular distance between readings was 5°; there was a larger angular distance between measurements outside Snell's Window. The radiance distribution at each depth is therefore characterized by 64 radiance measurements. Above the water surface, radiance measurements were made at appropriate angles that correspond to the refracted radiance measured in the water.

Care was taken to avoid boat shadow and drift by double anchoring the boat and walking around the boat so that the Gershun tube never pointed at the boat while a reading was being taken. A complete series of measurements (surface to 2.5m) consisted of 364 independent radiance measurements and could be completed in about 1.5 hours. To minimize the effect of sun motion, the readings for a given direction were made sequentially at all depths, so little time elapsed between measurements that were to be compared.

The beam attenuation coefficient may be estimated in one of two ways. The first is to use a beam transmissometer (Kirk, 1983 pg. 76). An alternative method is to assume that inscatter contributes an insignificant amount to direct sunbeam light (s=0,g=0). In this case, equation 15 reduces to the Lambert-Bouguer Law. c may be found by regressing ln (sunbeam radiance) on pathlength x, as given by

$$\ln(L_{(z,sun)}) = \ln(L_{(0,sun)}) - cx \qquad (16)$$

Equation 16 gives a lower value of c than the beam transmissometer because a Gershun tube has a larger acceptance angle and thus does not record all scattering at small angles. Equation 16 was used to estimate c in this paper because it employs the same radiance meter that was used to test the model and thus gives an estimate of c that is most appropriate for the test conditions.

The vertical attenuation coefficient was estimated by fitting a Li-Cor sensor with a spherical collector and measuring scalar irradiance at depth intervals to 2.5m, and then fitting these data to the Lambert-Bouguer Law.

The inscatter coefficient, s, is calculated from equation 13 for radiance at a point just beneath the surface (g). Solving equation 13 for s gives

$$s = \frac{L_{(g,\theta,\phi)} - T_{\theta} L_{(a,\theta a,\phi)} + T_{\theta} L_{(a,\theta a,\phi)} cg}{E_{(0)} g} \qquad (17)$$

Each of the factors on the right-hand side of equation 17 can be measured with relative ease. This definition assumes that radiance that is first scattered into direction (θ,ϕ) and then attenuated before reaching h is negligible.

A Fortran computer program (Appendix 1) was written and compiled to simulate the model presented in equation 15. As input, the model requires the following: two radiance distributions (one made just above the surface and one made just below the surface), estimates of both the beam and the vertical attenuation coefficients, and an estimate of

surface scalar irradiance. These measurements were made on or near the date on which the model was tested.

Results and Discussion

The validity of the model is dependent on its ability to satisfy four criteria. First, it must obey the two tenets of Snell's Law. The first of these tenets is that radiance must be refracted appropriately at the air-water interface. Figure 3 shows a comparison between the model and empirical data at 0.5m in Lake Itasca together with a radiance distribution from just above the surface. The peak of radiance intensity due to sunlight occurs above the surface at about 30°, but is shifted to about 23° in both the model and the empirical data. This indicates that Snell's refraction is properly accounted for. The second tenet is that the angular region that is outside of Snell's Window should not have a direct skylight component to its radiance, but any radiance impinging from that region must be generated only by inscatter. This is demonstrated by setting $L_{(0,\theta a,\phi)}$ equal to 0 for theta outside of Snell's Window ($48.7 < \theta < 331.3$) in equation 15. This eliminates all direct sky radiance as input to these directions, and thus any light that is generated by the model must be attributable to inscatter.

The second criterion which the model must satisfy to be valid is that it should reduce to the Lambert-Bouguer Law in the case s is equal to zero. If s is zero, then g also is zero, and equation 15 does simplify to the Lambert-Bouguer Law as demonstrated previously to derive equation 16.

The third criterion is that the model must accurately predict the radiance distribution under a variety of optical conditions. Figure 4 shows comparisons between the model and empirical data in each of the three lakes. The scale is limited to 0.01 $\mu E\ m^{-2}\ s^{-1}\ deg^{-1}$ because that is the maximum sensitivity of the radiance meter. At 2.0m, only 4.6% of the incident scalar irradiance remains in Bog Lake, and at 2.5m only 15.0% remains in Lake Itasca and 47% in Long Lake. The model is able to predict the attenuation of radiance values over a range of up to two

orders of magnitude in the space of only 2.5m. In addition, there is a marked change in the shape of each of the radiance distributions. In spite of the fact that sunbeam radiance persists as a significant proportion of total irradiance, its relative importance decreases, and the overall shape of each distribution becomes more diffuse with depth. Thus, the model successfully predicts both the overall shape of the radiance distribution as well as its intensity to a depth at which the majority of irradiance has been attenuated in each of the three lakes.

The model can be analyzed statistically by a regression of the empirical data on values generated by the model. The expected results of this regression are a slope of 1.0 and an intercept of 0.0. The results of this analysis are given in Table 2.

In the two turbid lakes, Itasca and Bog Lake, seven of the nine slopes are significantly greater than 1. This implies that in water with a strong scattering component, the model underestimates inscatter. The opposite happens in Long Lake, where three of the five slopes are significantly less than 1, and the model tends to overestimate inscatter. There are two likely sources for this error. First, for heuristic reasons, s is considered here to be a constant, but this is not fully justified until the ARD is achieved. The second, and probably the more important source of this error, is in the measurement of s itself. If the first source of error is most important, it should systematically skew the model in each lake in one direction or the other, but this is not seen. Overall, the regression slopes are close to 1.0, and with a better estimate of s, it is reasonable to assume that the slopes would more closely approximate 1.0. It will be possible to make better estimates of s when more accurate radiance meters, such as the electro-optical device, become available (Voss, personal communication).

In all three lakes, s is highly dependent on theta. Values ranged from $1*10^{-4}$ to 1.0. Figure 5 shows the distribution of s as it depends on theta in Lake Itasca. As expected, the lowest values are for backscatter at 180°, and the highest values are for angles close to the sunbeam radiance. This is because the majority of all scattering is at small angles in the forward direction (Petzold, 1972). There is a

secondary minimum at the angle that corresponds to the solar position because out-scatter dominates the solar beam. The symmetry of Figure 5 implies that s need only be calculated at a few directions, and then it could be estimated for any other direction.

It is noteworthy that there is no trend in the regression slopes that is due to depth, which implies that the model is as accurate at low light levels as it is at high light levels. R^2 values do tend to drop off slightly in deeper water, which implies a decreased precision at low light levels. R^2 values for the regressions are uniformly greater than 0.70, and they average 0.87, which indicates a strong correlation between the predicted and observed values. The majority of the regression intercepts are not significantly different from 0, which is as expected.

The fourth criterion that the model should satisfy is that the shape of the radiance distribution should change with depth only to a point, and then assume a constant form known as the asymptotic radiance distribution (ARD), (Preisendorfer, 1958a). I tested this by calculating the ratio between two radiance values generated by the model (sunbeam and 90° in the same plane) over depths to 10m. If the radiance distribution is approaching an asymptotic radiance distribution, this ratio should also asymptote to an arbitrary number. This is analogous to Kirk's proposal that the asymptotic radiance distribution is reached when irradiance reflectance ceases to increase (Kirk, 1983). Figure 6 demonstrates that this is the case, and that the model predicts the asymptotic radiance distribution to be reached at about 4.0m, or an optical depth of 1.2. The trajectory of the empirical data is consistent with this prediction, although logistic considerations prevented taking measurements at depths greater than 2.5m.

The model fails to predict an asymptotic radiance distribution for either Bog Lake or Lake Itasca even though the empirical RD's clearly show that the ARD exists. The underestimation of s in these lakes results in a continually changing radiance distribution.

Conclusion

The usefulness of this model is that it provides a method to predict radiance distributions in water bodies in which β_θ is not known. The parameters of the model can be estimated with relatively inexpensive and widely available equipment. The model satisfies the three theoretical criteria of light penetration into a lake by obeying Snell's and Fresnell's Laws, simplifying to the Lambert-Bouguer Law and predicting an asymptotic radiance distribution. Finally, it successfully predicts the radiance distribution in three optically disparate lakes.

REFERENCES

Gordon, H.R. and O.B. Brown. 1973. Irradiance reflectivity of a flat ocean as a function of its optical properties. Applied Optics 12(7):1549-1551.

Janssen, J. 1981. Searching for zooplankton just outside Snell's Window. Limn. and Ocean. 26(6):1168-1171.

Kattawar, G.W. and G.N. Plass. 1972. Radiative transfer in the Earth's atmosphere-ocean system: 2. Radiance in the atmosphere and ocean. J. of Physical Oceanography. 2:146-156.

Kirk, J.T.O. 1981a. Monte Carlo procedures for simulating the penetration of light into natural waters. CSIRO (Aust.) Division of Plant Industry. Technical paper #36.

Kirk, J.T.O. 1981b. Monte Carlo study of the nature of the underwater light field in, and the relationships between optical properties of, turbid yellow waters. Aust. J. Mar. Freshwater Res. 32:517-32.

Kirk, J.T.O. 1983. Light and photosynthesis in aquatic ecosystems. Cambridge U. Press. Cambridge.

McFarland, W.N. and F.W. Munz. 1975a. The visible spectrum during twilight and its implications to vision. In Light as an Ecological Factor. (G.C. Evans, O. Rackham and R. Bainbridge, eds.) Vol. 2. Blackwell, Oxford Press.

McFarland, W.N. and F.W. Munz. 1975b. Part 3: The evolution of photopic visual pigments in fishes. Vision Res. 15:1071-1080.

Petzold, T.J. 1972. Volume scattering functions for selected ocean waters. Visibility Lab, Scripps Institute of oceanography, U. of CA. SIO Ref. 72-78.

Plass, G.N. and G.W. Kattawar. 1969. Radiative transfer in an atmosphere-ocean system. Applied Optics 8(2):455-466.

Plass, G.N. and G.W. Kattawar. 1972. Monte Carlo calculations of radiative transfer in the Earth's atmosphere-ocean system: 1. Flux in the atmosphere and ocean. J. of Physical Ocean. 2:139-145.

Preisendorfer, R.W. 1957. Model for radiance distributions in natural hydrosols. Visibility Lab, Scripps Institute of Oceanography, U. of CA. SIO Ref. 58-42.

Preisendorfer, R.W. 1958a. A proof of the asymptotic radiance hypothesis. Visibility Lab, Scripps Institute of Oceanography, U. of CA. SIO Ref. 58-57.

Preisendorfer, R.W. 1958b. Some practical consequences of the asymptotic radiance hypothesis. Visibility Lab Report, Scripps Institute of Oceanography, U. of CA. SIO Ref. 58-60.

Preisendorfer, R.W. 1959. Theoretical proof of the existence of characteristic diffuse light in natural waters. J. of Marine Res. 18(1):1-9.

Siebeck, H.O. 1980. Optical orientation of pelagic crustaceans and its consequences in the pelagic and littoral zones. In Evolution and Ecology of Zooplankton Communities. (W.C. Kerfoot ed.) New England Press.

Tyler, J.E. 1960. Radiance distributions as a function of depth in an underwater environment. Bull. Scripps Institute of Oceanography, U. of CA. 7(5):363-412.

Whitney, L.V. 1941. The angular distribution of characteristic diffuse light in natural waters. J. of Marine Res. 4:122-131.

TABLE 1

b.....Complex exponent used to simplify equation 15.
c.....Beam attenuation coefficient.
c'.....Vertical attenuation coefficient for scalar irradiance.
E.....Scalar irradiance.
g, h.....Depths that define the thin plane dz.
k.....Schuster's coefficient.
L, L',L"...Radiance values.
L*.....Path function which determines inscatter.
n.....Snell's refractive index; 1.33 for air-water interfaces.
T_θ.....Percent of radiance incident at θ_a that is transmitted to θ.
x.....Pathlength of radiance to depth z.
z.....Depth.
β_θ.....Volume scattering function.
ϕ,ϕ'.....Azimuth angle of radiance.
θ,θ'.....Zenith angle of radiance in water.
θ_a.....Zenith angle of radiance in air.
Ω.....Unit of solid angle around radiance L.

Table 1: Summary of symbols used in this paper.

TABLE 2

	DEPTH	n	SLOPE (±95% CI)	INTERCEPT (±95% CI)	R^2
LAKE ITASCA:	0.5	64	1.60 (0.08)	-3.1 (3.9)	.96
	1.0	64	1.09 (0.10)	3.3 (2.9)	.87
	1.5	64	0.76 (0.10)	4.3 (1.3)	.82
	2.0	64	0.80 (0.10)	3.2 (0.8)	.78
	2.5	64	0.86 (0.14)	2.4 (0.5)	.72
	COMBINED	320	1.42 (0.05)	0.5 (1.2)	.91
LONG LAKE:	0.5	64	0.94 (0.06)	-2.4 (10.4)	.94
	1.0	64	0.76 (0.02)	-1.2 (4.1)	.98
	1.5	63	0.68 (0.06)	2.7 (8.8)	.90
	2.0	63	0.57 (0.06)	2.7 (5.5)	.85
	2.5	62	0.94 (0.08)	-0.5 (3.7)	.90
	COMBINED	317	0.80 (0.03)	-0.8 (3.7)	.90
BOG LAKE:	0.5	64	1.63 (0.05)	0.7 (2.9)	.99
	1.0	64	1.36 (0.11)	3.1 (1.9)	.91
	1.5	64	1.27 (0.18)	3.1 (1.4)	.76
	2.0	64	1.56 (0.20)	1.8 (0.6)	.79
	COMBINED	256	1.54 (0.04)	1.6 (0.1)	.86

Table 2: Results of regression analysis in which the empirical data are regressed on values predicted by the model. The "combined" row is a regression of the same data used in the individual depth analyses combined into a single data set. The expected slope is 1.0 and the expected intercept is 0.0 in each case.

FIGURE CAPTIONS

Figure 1: a) Radiance incident on a surface at angle θ_a is subject to partial reflection following Fresnell's Law and partial refraction to angle θ following Snell's Law. b) Refraction at the surface results in the focussing of skylight into Snell's Window.

Figure 2: Radiance incident on thin slab dz at g from direction (θ,ϕ) is partially absorbed and partially scattered to other directions along pathlength dx. Radiance in direction (θ,ϕ) is augmented by inscatter from all other radiance directions.

Figure 3: Empirical radiance distributions made in Lake Itasca from just above the lake surface (open triangles) and at 0.5m (open circles) compared with a model radiance distribution at 0.5m (closed circles). Note the shift in peak radiance from about 30° above the surface to about 25° in both the model and empirical data at 0.5m. Measurements were made in the vertical plane that includes the sun's azimuth; theta equal to 0° and 360° is pointing straight up, theta equal to 180° is straight down. Snell's Window is the region from 0 to 50° and from 310 to 360°.

Figure 4: Comparison of the model (solid lines) to empirical data (dashed lines) in three lakes at three depths. All figures are from the plane that includes the sun.

Figure 5: Values of s from Lake Itasca which demonstrate that s is highly dependent on theta. The highest values are at angles near the sunbeam, as most scattering is at small angles in the forward direction. The closed circles are data from a plane that includes the sun, and the open circles are values of s from a plane normal to the sun's direction.

Figure 6: A ratio calculated in Long Lake by dividing radiance at 25° (sunbeam) by radiance at 90°. The open circles are empirical data, the closed circles are predictions generated by the model. The model clearly demonstrates that the ratio asymptotes to a value of about 5.0 at 4m.

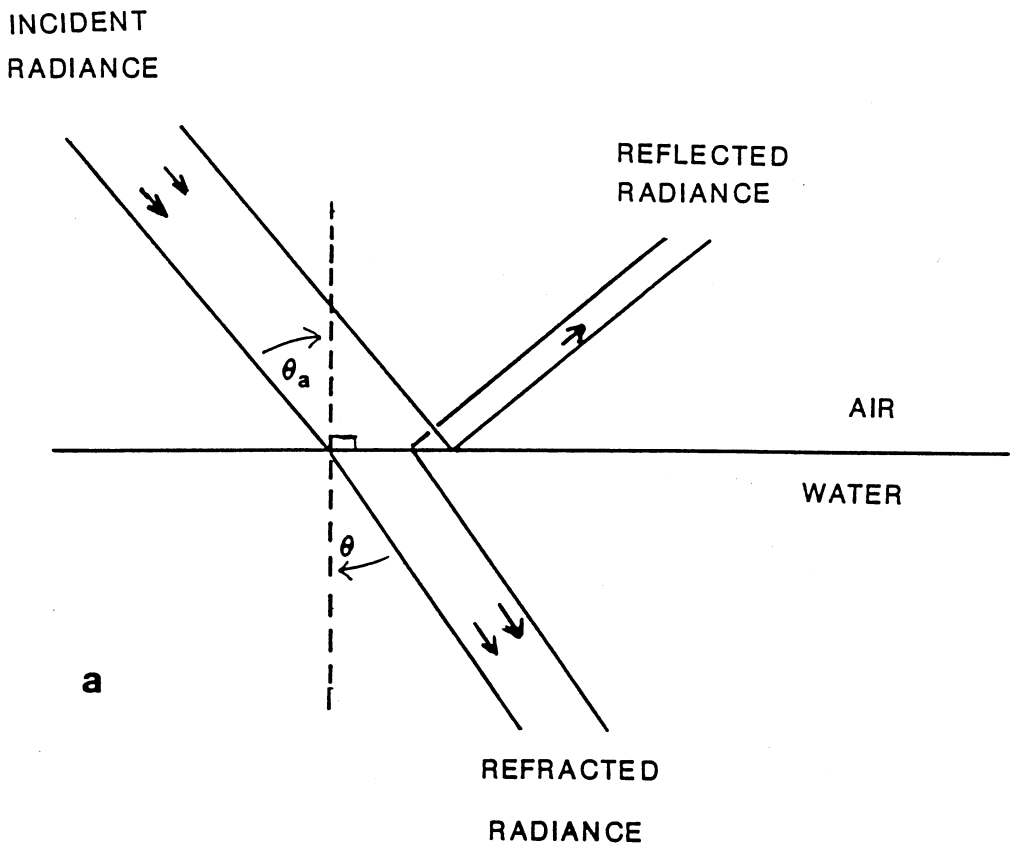

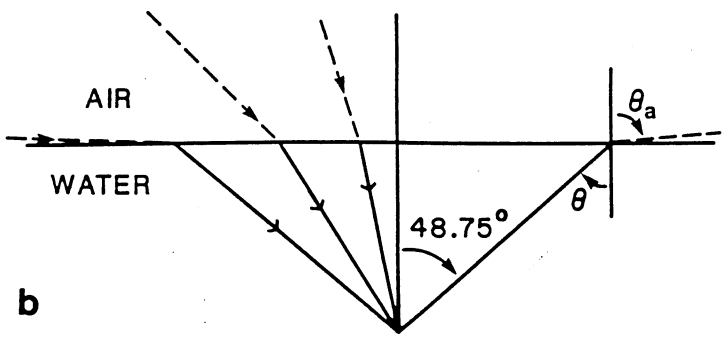

SNELL'S WINDOW

FIGURE 1

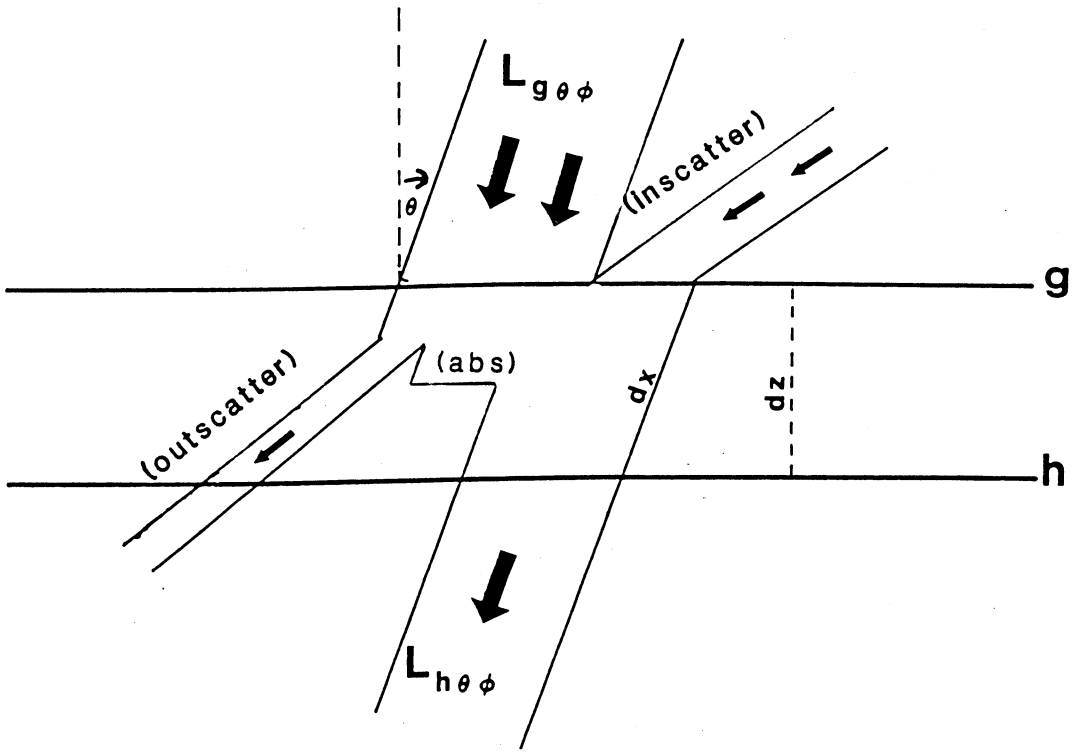

FIGURE 2

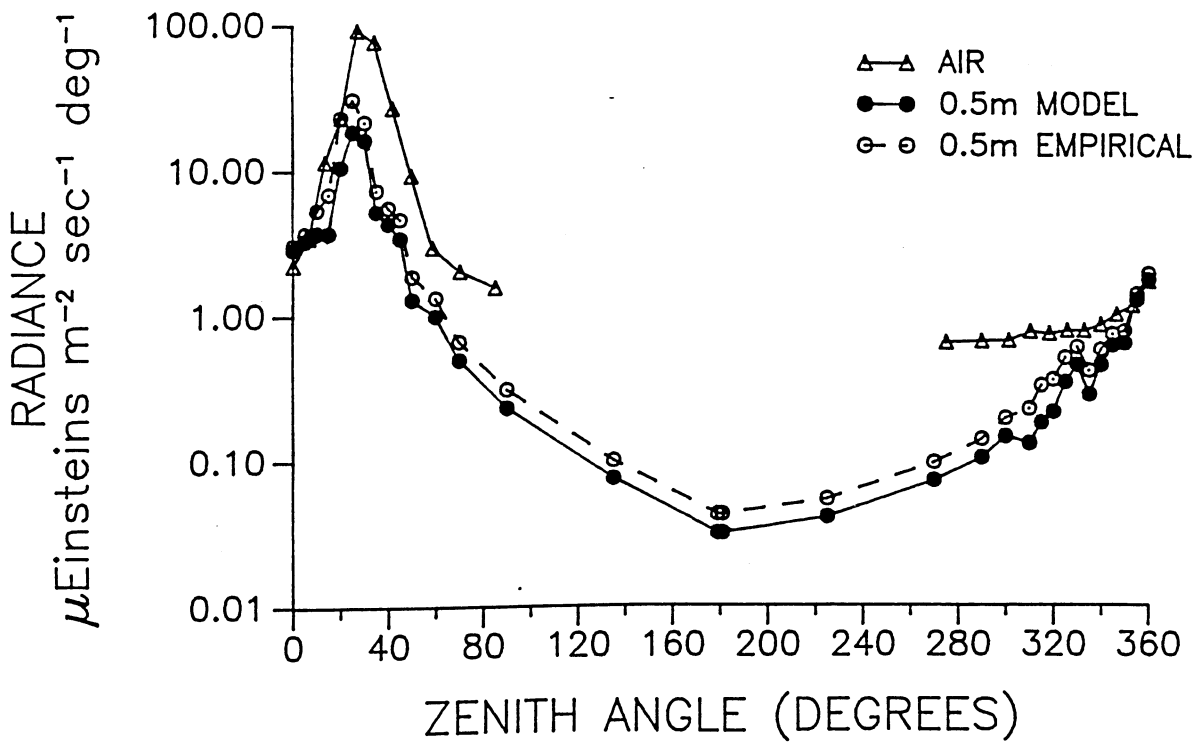
RADIANCE
μEinsteins m⁻² sec⁻¹ deg⁻¹
100.00
10.00
1.00
0.10
0.01
0
40
80
120
160
200
240
280
320
360
ZENITH ANGLE (DEGREES)
AIR
0.5m MODEL
0.5m EMPIRICAL

FIGURE 3

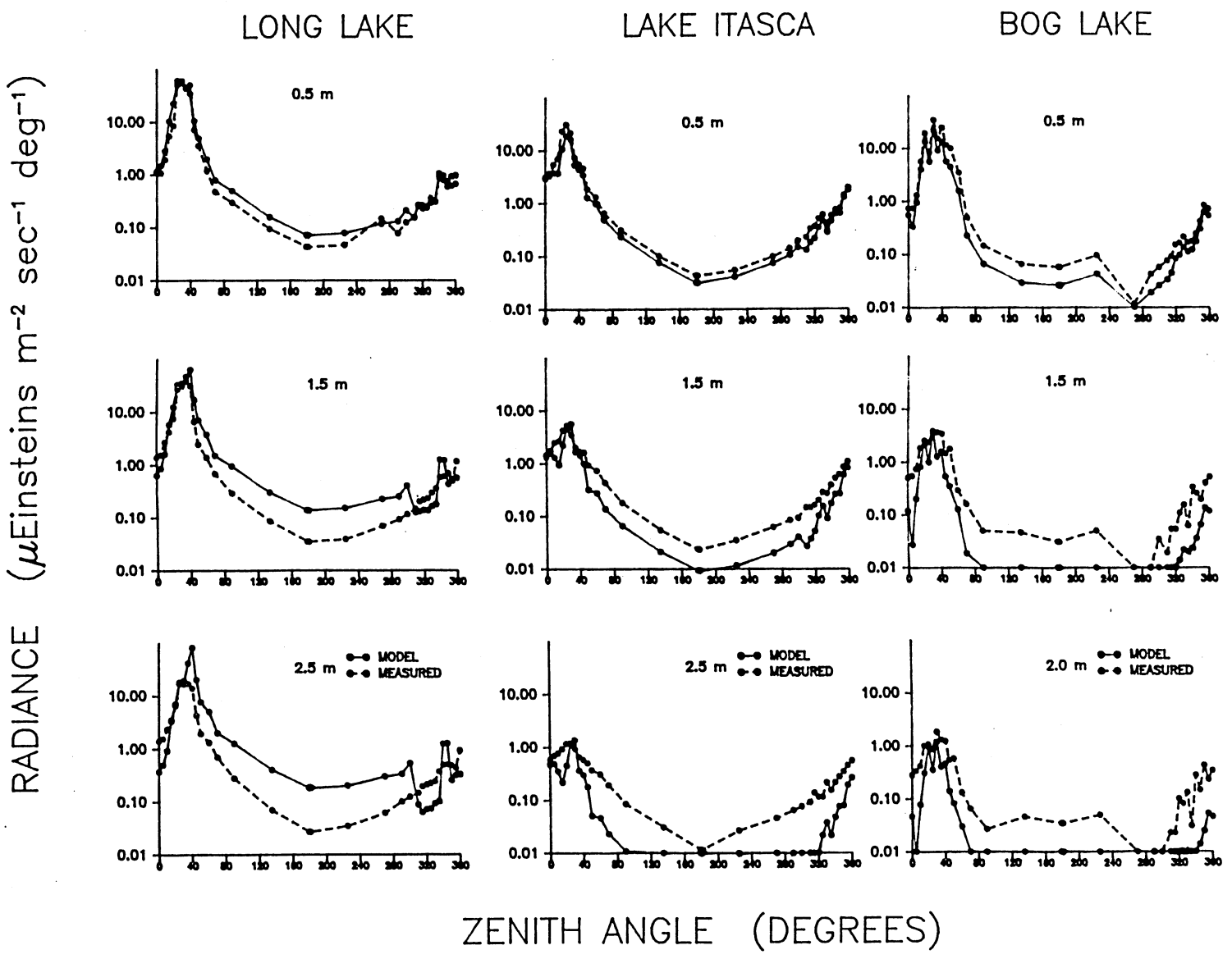
LONG LAKE
LAKE ITASCA
BOG LAKE
0.5 m
1.5 m
2.5 m
2.0 m
MODEL
MEASURED
10.00
1.00
0.10
0.01
0
40
80
120
160
200
240
280
320
360
RADIANCE (μEinsteins m⁻² sec⁻¹ deg⁻¹)
ZENITH ANGLE (DEGREES)

FIGURE 4

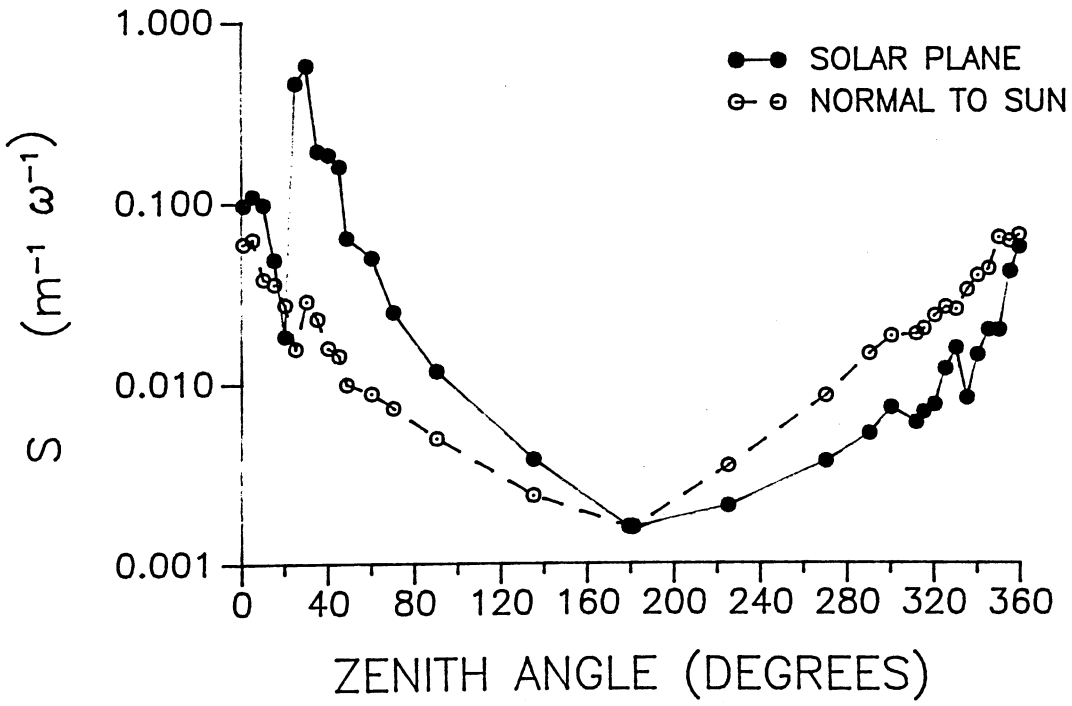
1.000
0.100
0.010
0.001
S (m⁻¹ ω⁻¹)
SOLAR PLANE
NORMAL TO SUN
0
40
80
120
160
200
240
280
320
360
ZENITH ANGLE (DEGREES)

FIGURE 5

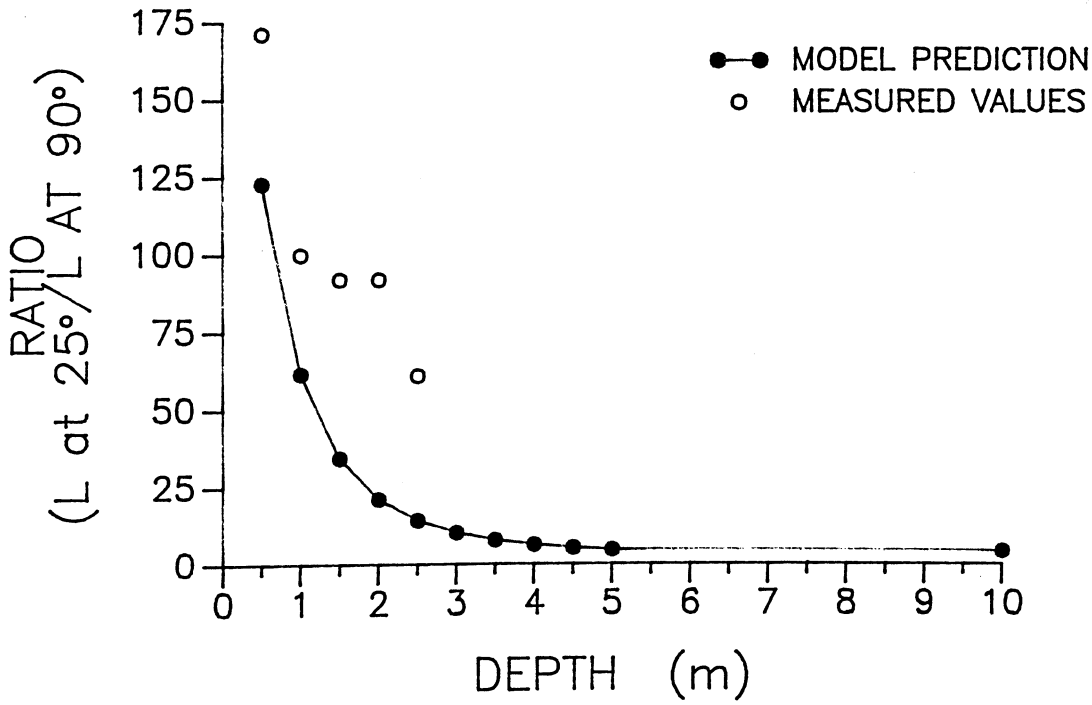
MODEL PREDICTION
MEASURED VALUES
RATIO
(L at 25°/L AT 90°)
175
150
125
100
75
50
25
0
0
1
2
3
4
5
6
7
8
9
10
DEPTH (m)

FIGURE 6

APPENDIX 1

```
*                    PROGRAM ID
*
*  This program computes the radiance distribution at any depth in
* a hydrosol from the radiance distribution above the surface.  It
* solicits the following information: depth (z), beam attenuation
* coefficient (c)(0.00), the diffuse attenuation coefficient (k)
* (0.00), and irradiance just below the surface (IR)(0000.00).  Each
* input file must have: incident angle, incident radiance for S-N
* and E-W data and radiance just below the surface for S-N and E-W
* data.
*
*
*    The following real variables are used:
*        Theta:  The angle of incidence in degrees.
*        Thetar: The angle of incidence in radians.
*        Thetaw: The angle of light in the water in degrees.
*        SN:     Irradiance input data for S-N data (mE/m**2/s)
*        EW:     Irradiance input data for E-W data (mE/m**2/s).
*        SN0,EW0:  Radiance measured just beneath the surface.
*        SNI,EWI:  Radiance transmitted across the surface.
*        T:      Percent of light transmitted across the interface.
*        X:      Pathlength of light.
*        Z:      Depth (m).
*        K:      diffuse attenuation coefficient.
*        C:      Beam attenuation coefficient.
*        F,G,H,I,J,M:  Partial solutions to Fresnell's Law.
*        AS,AP:  Partial solutions for A1.
*        AE,AQ:  Partial solutions for A2.
*        A1,A2:  Exponents for master equation.
*        IR:     Irradiance just below the surface.
*        S1:     Inscatter coefficient for SN.
*        S2:     Inscatter coefficient for EW.
*        LZSN,LZEW:  Radiance at depth z.
*
*   The following real parameters are used:
*        Rad:   Converts degrees to radians.
*        N:     Snell's index of refraction.
*        E:     Base of the natural logarithms.
*
*  BEGIN THE PROGRAM AND DECLARE THE VARIABLES
*
      PROGRAM ID
$NOTRUNCATE
$DEBUG
      REAL THETA,THETAR,THETAW,SNI,EWI,SN,EW,RAD,N
      REAL X,C,Z,A1,A2,E,LZSN,LZEW
      REAL*8 S1,S2,F,G,H,I,J,K,T
```

```
      REAL*8 AP,AS,AE,AQ,IR,SN0,EW0,M
      PARAMETER (RAD=0.01745,N=1.33,E=2.718)
*
* OPEN AND NAME THE INPUT AND OUTPUT DATA FILES
*
*     WRITE (*,001)
      OPEN (UNIT=2,FILE=' ',ACCESS='SEQUENTIAL')
*     WRITE (*,002)
      OPEN (UNIT=3,FILE=' ',ACCESS='SEQUENTIAL')
*
* SOLICIT THE INPUT INFORMATION
*
      WRITE (*,003)
      READ *,Z,C
      WRITE (*,004)
      READ *,IR,K
  001 FORMAT (2X,'WHAT IS THE INPUT FILE?')
  002 FORMAT (2X,'WHAT IS THE OUTPUT FILE?')
  003 FORMAT (2X,'GIVE THE DEPTH AND C')
  004 FORMAT (2X,'GIVE THE IRRADIANCE AND K')
*
* COMMANDS TO READ THE DATA SET.
*
  005 READ (2,10,END=20) THETA,SN,EW,SN0,EW0
  010 FORMAT (F4.1,2X,F6.2,2X,F6.2,2X,F6.2,2X,F6.2)
*
* CALCULATE THE LIGHT ANGLE IN THE WATER (SNELL'S LAW)
*
      THETAR=THETA*RAD
      IF (THETA .LT. 60.0 .OR. THETA .EQ. 70.1 .OR.
     +THETA .EQ. 85.0) THEN
      THETAW=(DASIN(DSIN(THETAR)/N))/RAD
      ELSEIF (THETA .GT. 300.0 .OR. THETA .EQ. 275.0 .OR.
     +THETA .EQ. 289.9) THEN
      THETAW=(DASIN(DSIN(THETAR)/N))/RAD+360.0
      ELSE
      THETAW=THETA
      ENDIF
*
* CALCULATE THE PERCENT OF LIGHT TRANSMITTED AT ANGLE THETA.
*
      IF (THETA .EQ. THETAW) THEN
      T=0.0
      ELSE
      G=(DSIN((THETA+THETAW)*RAD))**2
      H=(DTAN((THETA-THETAW)*RAD))**2
      I=(DTAN((THETA+THETAW)*RAD))**2
      J=F/G
      M=H/I
*
      T=1.0-(0.5*(J+M))
```

```
*
      ENDIF
*
*
* CALCULATE THE LIGHT PATHLENGTHS
*
      IF (THETAW .LT. 50 .OR. THETAW .GT. 310) THEN
      X=Z/COS(THETAW*RAD)
      ELSE
      X=Z/COS(.838)
      ENDIF
*
* CALCULATE THE COEFFICIENT S.
*
      SNI = T*SN
      EWI = T*EW
*
*
      S1 = ((SN0-SNI+(SNI*.5*C))/(IR*.5))
      IF (S1 .LT. 0) THEN
      S1=0.001
      ELSEIF (S1 .GT. 1.0) THEN
       S1=.99
      ENDIF
      S2 =((EW0-EWI+(EWI*.5*C))/(IR*.5))
      IF (S2 .LT. 0) THEN
      S2 = 0.001
      ELSEIF (S2 .GT. 1.0) THEN
      S2 = .99
      ENDIF
* CALCULATE THE EXPONENT A
      AS = (IR*S1) - (IR*S1*(E**(-K*Z)))
      AP = ((SN*T) + (.5*IR*S1) -(SNI*.5*C))*K
      IF (AP .EQ. 0.0) THEN
      A1=-C*X
      ELSE
      A1=(-C*X)+(AS/AP)
      ENDIF
*
*
      AE = (IR*S2) - (IR*S2*(E**(-K*Z)))
      AQ = ((EW*T) + (.5*IR*S2) - (EWI*.5*C))*K
      IF (AQ .EQ. 0.0) THEN
      A2=-C*X
      ELSE
      A2=(-C*X)+(AE/AQ)
      ENDIF
*
*
* CALCULATE THE NEW RADIANCE VALUES
*
      LZSN=T*SN*(E**A1) + (IR*S1*0.5*(E**A1))- SNI*.5*C*(E**A1)
```

```
      LZEW= T*EW*(E**A2) + (IR*S2*0.5*(E**A2)) - EWI*.5*C*(E**A2)
      WRITE (3,15) THETAW,LZSN,LZEW,S1,S2
  015 FORMAT (F5.1,2X,F9.4,2X,F9.4,2X,F8.6,2X,F8.6)
      GO TO 5
*
* TERMINATE THE PROGRAM
*
  020 CONTINUE
      STOP
      END
```

CHAPTER 2

RADIANCE DISTRIBUTIONS IN FOUR OPTICALLY DISPARATE MINNESOTA LAKES

ABSTRACT

Natural radiance distributions (RD) were studied in four optically disparate lakes in Minnesota. The shape of the radiance distribution is shown to depend strongly on sun position and cloud cover. The shape of the radiance distribution is also shown to change with depth and to be dependent on water clarity. There is a very weak dependence of the RD shape on proximity to the bottom and to the shore.

The spectral composition of a specific radiance is highly dependent on the direction of the line of sight and on the optical clarity of the lake. A horizontal line of sight in transparent lakes is dominated by blue and green light, while horizontal light in turbid lakes is dominated by green and red light. In all lakes, a line of sight within Snell's Window is comprised of all wavelengths.

INTRODUCTION

Essentially all light in a lake is derived from skylight that is transmitted across the air-water interface into the water column. Light is refracted at this interface according to Snell's Law. The result is that all transmitted light has an initial zenith angle of between 0° and 48.75° from the vertical. The radiance distribution (RD) at any point below the surface, therefore, has the shape of an inverted cone, which is known as "Snell's Window". Light impinges on any point only from within Snell's Window, and therefore regions that are outside of Snell's Window appear black. Snell's Law is illustrated in Figure 1.

This idealized schematic is not realized in lakes because water is optically impure and light is scattered into new angles, including angles that are outside of Snell's Window (Petzold, 1972). Together, the processes of scatter and absorption change the radiance distribution as light is transmitted through the water column until the asymptotic radiance distribution (ARD) is reached (Preisendorfer, 1959). Once the ARD is established, the magnitude of each directional radiance decreases at a rate that is proportional to the decrease of all other radiances. Thus, the shape of the ARD does not change although the magnitudes of both the individual radiances and the total irradiance continues to decline.

A common paradigm of aquatic ecology is that there is no structure in the epilimnion of lakes due to turbulent mixing of the water and the absence of physical structure. This homogeneous region is thought to contrast sharply with terrestrial ecosystems where physical structure is known to play a significant role in the function of the community (Krebbs, 1978; pg. 408). It has been shown previously, however, that the radiance distribution is not homogeneous (spherical), but is highly asymmetrical (Whitney, 1941a). This asymmetry introduces an optical structure that is unique to aquatic habitats, and which may be important to a variety of light-dependent systems.

McFarland & Munz (1975a, 1975b) recognized this optical structure and demonstrated that piscivorous fish take advantage of it through behavioral and physiological mechanisms which enhance the contrast between their prey and the visual background. Similarly, the widespread phenomenon of countershading in fishes is an adaptation to reduce this contrast, and thus their visibility to predators (Hemmings, 1966). Janssen (1981) showed that zooplanktivorous fish increase the visibility of their prey by searching for them in the region just outside Snell's Window. To fish that use this strategy, these highly transparent organisms would appear as bright reflective objects against a dark background. Finally, Siebeck (1980) suggested that differences between inshore and mid-lake radiance distributions are a reliable source of information to an organism of its horizontal position in a lake. He proposed that limnetic zooplankton use these indicators to detect the shore and then swim away from it, thereby avoiding littoral predators.

Thus, it may be that optical structure is an ecologically important component of the pelagic habitat. Unfortunately, both Janssen and Siebeck assumed that Snell's Window is uniformly bright, and that water is more or less optically pure. This paper is a study of natural radiance distributions in four lakes in Minnesota to examine what type of optical structure the RD might provide. An empirical approach is used to examine the effect of meteorology, lake type, and location within a lake in the determination of the radiance distribution.

METHODS

Radiance distributions were studied in Bush Lake (93° 20' W; 45° N) during 1984, and in Lake Itasca, Long Lake and Bog Lake (95° 10' W; 47° 15' N) during 1985 and 1986. Table 1 gives a summary of the basic optical parameters of water from each lake. An extensive review of the optical conditions in these lakes is given elsewhere (Chapter 3). In general, Bush Lake and Lake Itasca are shallow, productive lakes with a low summer transparency. Bog Lake is very shallow, and has distinctly colored water. Long Lake is a deep and highly transparent lake.

A Li-Cor 185 quantum irradiance meter and cosine sensor (Lambda Inst.) that responds only to wavelengths between 400-700nm (PAR) was converted into a radiance meter by the attachment of a 15cm by 3.5cm black Gershun tube to the sensor. This tube created an acceptance angle for the sensor of 13°. The radiance meter was lowered into the water by attaching it to a 3m long PVC pole equipped with a compass and a protractor for measuring both the zenith and azimuth orientation of the radiance meter.

Each radiance distribution consists of 64 independent radiance measurements. Four azimuth directions were used: two in the vertical plane that included the sun's azimuth, and two in the plane normal to the sun's azimuth. Sixteen zenith angles were measured at each azimuth setting: within Snell's Window the angular distance between readings was 5°, and then measurements were made at 60°, 70°, 90°, 135°, and 179° from the zenith. The RD for specific wavelengths was measured by inserting an interference filter, with a bandwidth of less than 10nm (Andover Corp.), into the Gershun tube.

Care was taken to avoid boat drift and shadow by double anchoring the boat and working around the bow of the boat so that the Gershun tube never pointed at the boat during a reading. The measurement of a radiance distribution is completed in about fifteen minutes, which represents about 3° of arc motion by the sun. A total of 137 radiance distribution measurements were made in the four lakes during the summers of 1984, 1985 and 1986. All solar elevations were calculated from the equations of Spencer (given in Kirk, 1983; pg. 33).

RESULTS

Solar position: Figure 2 illustrates three important and related points about radiance distributions on clear days. First, note the extreme asymmetry of the RD. The peak radiance is three to four orders of magnitude greater than other directions. Second, peak radiance is extremely narrow. Direct solar beam light is demonstrated to be responsible for this peakedness by a correlation between the solar elevation and the direction of the highest measured radiance. For

example, at 10:25 A.M. the solar elevation was 43° towards the southeast. Allowing for Snell's refraction at the air-water interface, the solar beam should assume an angle of 33° in the water. Peak radiance was measured at 35° (±6°). Obviously, the peak radiance should track the sun's position over the course of the day. For the radiance distribution made at 19:00, just fifty minutes before sunset, the solar elevation is 7° towards the southwest, and the measured peak is right at the edge of Snell's Window at 48° (shown as 312° in Fig. 2). Relative to the morning measurement, the absolute magnitude of the evening measurement is reduced; in part, because light incident at the water surface at high angles is strongly reflected rather than transmitted into the water (Kirk, 1983, pg. 39).

Figure 3 shows that as the sun continues to set, not only does the magnitude of the peak decrease, but it shifts away from the edge of Snell's Window towards the vertical (towards 360°) and becomes broader. This is because the solar beam is at increasingly high angles of incidence and is mostly reflected. Skylight becomes gradually more important. Just after sunset, Snell's Window becomes uniformly bright and the RD is nearly spherical, although at extremely low radiance levels.

Cloud cover: Figure 4 is a radiance distribution made on a heavily overcast day in Bush Lake. Both a south/north and an east/west distribution are shown. Figure 4 contrasts sharply with Figure 2. Not only is there not just a single, sharp peak, but Snell's Window is almost uniformly illuminated. This uniformity is represented by the four broad and nearly equal peaks in each quadrat of Snell's Window. The highest radiance is at about 290° towards the north, where there was a patch of blue sky. In all four quadrats of Snell's Window, the zenith radiance is lower than at slightly larger angles, and most distributions peak at about 30°. This is counter-intuitive, because a radiance at theta equal to 30° must travel farther through the water to reach 0.5m than a vertical radiance (0.58m vs 0.5m), and thus is subject to greater attenuation. However, a greater area of sky light is focussed into a given arc at 30° than it is at 0°. The interval from 0 to 5° contains

sky light that was incident on the surface from 0 to 6.66°, whereas the interval from 30 to 35° contains sky light that was incident from 41.68 to 49.72° (a total of 8.04°). Thus, if the sky is uniformly bright, refraction alone will make 30° brighter than the zenith because it contains more skylight. At angles of incidence greater than 50°, reflection at the air-water interface is very strong, and thus theta larger than 30° (in the water) are less bright because most of the incident sky light is reflected back to the sky rather than refracted into the water.

The overall effect of clouds is to act as both a strong attenuator and diffuser of light. The clouds do not change the importance of Snell's Law in structuring underwater light, however, and Snell's Window retains its importance in the underwater RD.

Depth: Figure 5 shows that the shape of the RD in Bog Lake is qualitatively maintained to a depth of 2.5m, despite a large reduction in total irradiance. The irradiance at 2.5m in Bog Lake is only 2% of the irradiance just below the surface, and yet the general shape of the radiance distribution is similar at 2.5m to what it was at 0.5m. For example, the direction of the peak radiance does not change, and its magnitude is still significantly greater than upwelling light. The light is more diffuse at 2.5m, as the peak radiance is only one or two orders of magnitude greater than upwelling light, whereas it is two to three orders of magnitude greater at 0.5m. Both Long Lake and Lake Itasca also retain the integrity of the shape of their RD to a depth of 2.5m, where total irradiance is 50% and 11% of the subsurface values, respectively.

Although radiance distributions qualitatively retain their shape at depth, it is possible to measure changes in the shape of the RD as it assumes its asymptotic distribution. First, the breadth of the solar beam increases with depth in all three lakes. This is shown in Figure 6. The solar beam is defined as that region of the RD where radiance is at 50% or more of the maximum observed radiance at that depth. Thus, the breadth of the beam is simply the arc between the 50% level on one side of the beam, through the peak to the 50% level on the other side. All three lakes have a beam width of between five and ten degrees at the

surface. Itasca shows the greatest increase, and by 2.5m the beam is 45° of arc. Bog Lake behaves very similarly, and also shows a nearly linear increase in beam breadth with depth. A linear regression analysis of beam breadth on depth shows that there is no statistical difference between Itasca and Bog Lake. (p for a T-test is greater than 0.1 for both slope and intercept; regression R^2 values are equal to .88 and .80 respectively). This implies that scattering is equally strong in both lakes. In Long Lake, there is an initial broadening of the beam as it enters the water, but thereafter the beam breadth does not measurably increase. This suggests that scattering is less strong in Long Lake than in the other two lakes.

A second way to measure the change of shape of the RD is to determine the rate at which it assumes its asymptotic shape. The ratio of the radiance in one direction to the radiance in any other direction is such a measure. This ratio will converge on an arbitrary number as the asymptotic RD is reached, and then should remain unchanged at greater depths. Figure 7a shows the ratio of solar beam radiance to the radiance at 90° in the same azimuth direction. In all three lakes, the ratio decreases with depth in an asymptotic manner. Each lake appears to converge on a unique number. In Itasca, beam light becomes the least important, because light is strongly scattered into new directions. Light is also scattered in Bog Lake, but it is much more strongly absorbed (see Table 1) and thus the ratio does not decrease as much as in Itasca. Although scatter is small in Long Lake, what is scattered out is weakly absorbed, and thus the relative importance of the solar beam decreases more strongly than in Bog Lake, but not as much as in Itasca.

Figure 7b shows the ratios of two other arbitrary directions, 10° east and 90° east. In both Itasca and Long Lake, this ratio decreases very slowly, and it appears that, for this part of the RD, the asymptotic distribution is nearly reached. In Bog Lake, this part of the RD is actively changing between 0.5m and 2.0m, but appears to be leveling off by 2.5m.

Figures 7a and 7b demonstrate that not all components of the RD change at the same rate, or even in the same way. Thus, in Figure 7b, the Bog Lake ratio increases initially before it begins to decrease.

In several instances, radiance at a given direction shows an initial increase with depth. Figure 8 shows depth profiles of RDs that are normal to those given in Figure 5 (i.e. normal to the plane that includes the solar beam). In all three lakes, there is a characteristic Snell's Window shape. In Itasca, all radiance directions decrease at about the same rate, which means that there is little change in the shape of the RD in these regions with depth. In Long Lake, there is no measurable decrease in radiance due to depth. This explains why both Long Lake and Itasca show nearly flat ratio curves in Figure 7b. In Itasca, much of the RD has already reached the ARD by 0.5m (except for the solar beam), and although the radiance values continue to decrease, they do so at a rate proportional to each other. In Long Lake, the ARD has not yet been reached because the radiance values are not decreasing. In much of the RD, scatter into each radiance from the solar beam is equally offset by attenuation. This implies that most of the reduction in irradiance between the surface and 2.5m (about 50%) in Long Lake is due to a decrease in beam light, which was seen in Figure 5.

In Bog Lake, upwelling radiance is greater than horizontal radiance. This is probably caused by reflection of light off of the very shallow bottom (3m). Secondly, some radiance directions show an initial increase with depth, which is indicated by the crossing of the radiance lines. This is most likely caused by scatter of light into those directions that exceeds attenuation. This effect is most pronounced in the region within Snell's Window.

Proximity to shore: Fifteen radiance distributions were measured to study the effect of proximity of the shore and the bottom on the RD shape. In each case, an RD measured close to the shore was compared to a contemporaneous RD measured in the middle of the lake. Figure 9 is a representative example showing three RDs from Bush Lake in 1984. One was made near the east shore, one in the middle of the lake, and one on the west shore. If the shore imposes a shadow, the RD should be depressed in

the azimuth direction towards the shore. For example, in Fig 9a, if the east shore imposed a shadow, one would expect to see the east RD (panel A, between 20° and 50°) reduced relative to both the mid-lake and the west RD. There is no obvious depression in 9a, in fact, the east RD is slightly higher in this region. It is possible to demonstrate this statistically by subtracting the east curve from the mid-lake curve in the region between 20° and 50°, and then testing the average difference in this region to see if it is different from zero. In only one of the fifteen cases was this difference significantly different from zero.

That case is shown as Figure 10, which was made under those conditions that are most favorable to detecting a shore shadow. These conditions are heavy cloud cover (to make the Snell's Window uniformly bright), clear water (to transmit the shadow) and a high shore horizon. The western shore of Long Lake can be detected between 270° and about 320°, where radiance is reduced an average of 0.34 $\mu E\ m^{-2}\ s^{-1}\ deg^{-1}$ (±0.31).

In twelve out of fifteen RDs made near shore, the upwelling radiance (135° to 225°) is higher in shallow water than it is in the open water (see Figure 9). Distance to the bottom was not controlled in these experiments, and two of the distributions that did not show this upwelling were from Long Lake, where the bottom drops off very steeply near the shore (Fig. 10). The bottom effect is very small, averaging only 0.035 $\mu E\ m^{-2}\ s^{-1}\ deg^{-1}$ (±0.02), and is presumed to be caused by reflection off of the bottom.

Water color: Water color is determined by the wavelength of light that is dominant in that region of the RD. It is an apparent optical property, and thus is dependent on the line of sight (Kirk, 1983). Figure 11 shows characteristic RD for PAR, 450, 560 and 670nm wavelengths in each of the three study lakes in northwestern Minnesota. Between six and eight RDs were made for each color in each lake under a variety of conditions. The RDs are very stable in each lake in that the colors of light that dominate a given region of the RD do not change significantly over the summer or with the weather. This implies that the color pattern of the photoenvironment in each lake is highly predictable.

In Long Lake, Snell's Window contains all three colors, although red is somewhat reduced relative to the other colors. Red disappears completely in the region outside of Snell's Window. The region from 60° to 300° is equally dominated by blue and green light. There is a slight tendency for green to dominate the region from Snell's Window edge to the horizontal, and blue light to dominate upwelling light.

Itasca and Bog Lake have color distributions that are similar to each other. Blue light is restricted to a narrow vertical region of Snell's Window. Red light is present throughout Snell's Window, but is not present in upwelling light. In both lakes, green light is dominant in the whole region outside of Snell's Window. The major difference between Itasca and Bog Lake is that in Bog Lake upwelling radiance is an order of magnitude less than at the same optical depth in Lake Itasca.

DISCUSSION

Snell's Law imposes a physical constraint on RDs such that they are always asymmetrical (non-spherical). The highest measured radiances are within Snell's Window. The precise location of the peak radiance is determined primarily by the location of the sun (and presumably by the moon at night). If the sun is occluded, then patchiness of the cloud cover can be important. Even if the sky is uniformly bright, the processes of refraction, reflection and attenuation over differential pathlengths will create non-uniformity in the RD in the water.

It is also clear that the RD changes shape with depth, but that this change is relatively minor, even at depths where the majority of light has been attenuated. The general tendency is for the RD to become more diffuse due to the proportionally greater decrease of the solar beam. This tendency of the RD to change shape decreases with depth as the RD approaches the ARD, and the RD shape stabilizes.

A true ARD was not measured in any lake because I was unable to measure a shift in the direction of the peak radiance from the solar direction towards the zenith. This shift is predicted by Radiative Transfer Theory (Preisendorfer, 1959) which states that the ARD is

independent of the sky RD and is only dependent on the inherent optical properties of the water body (Preisendorfer, 1958). This shift has been observed in highly transparent water bodies where the ARD is reached at great depth (Tyler, 1960), but only with difficulty in less transparent water (Whitney, 1941b). The shift towards the vertical is the result of differential pathlengths for radiances at different directions. The most plausible reason that I did not notice the shift is that my study lakes were so turbid that light is attenuated very rapidly. Thus, I only studied RDs to a depth of 2.5m, which is too shallow for the pathlength differential to cause a shift of greater than 5° (my minimum resolution). In these lakes, the asymmetry imposed at the surface is largely maintained throughout the photic region.

Finally, the proximity to shore or the bottom can have an effect on the RD, but these effects are very small. These shore effects are easily overwhelmed by other factors, such as the sun. This implies that RDs are not reliable indicators to an organism of either horizontal or vertical position in a lake. Any zooplanktor that followed Siebeck's (1980) rule to bodily orient itself such as to make the RD symmetrical (i.e. point towards the peak radiance) and swim until the peak was directly overhead would be misled by changes in the solar position and cloud cover. If zooplankton do actively avoid the shore (Preissler, 1977), they must use a different mechanism.

RD measurements do suggest that Janssen's (1981) foraging strategy for zooplanktivorous fish is appropriate in my study lakes. The darkest visual background is achieved in most cases by looking straight down. The direction to which a zooplankton scatters most light is not likely to be straight up, however, due to their lateral body compression and vertical body orientation. Therefore, for a foraging fish the maximum contrast (some mix of dark background and light scattered from the zooplankton) between prey and background is likely to be along a line of sight between the horizontal and the edge of Snell's Window. In addition, fish could be expected to forage away from the direction of peak radiance, as that bright spot would reduce contrast and create

glare. Attempts to observe this prediction *in situ* have not been successful, however.

Observed color RDs also suggest that the physiological strategy of offset visual pigments (McFarland & Munz; 1975a, 1975b) could be operative in lakes as well as oceans. Fish which forage in Long Lake according to Janssen's model (searching outside Snell's Window) could be expected to have visual pigments which are maximally sensitive at longer wavelengths, because background light is primarily short wavelength light. In more turbid lakes, background light is dominated by longer wavelength light, and thus the visual pigments are expected to show a shift in maximum sensitivity to shorter wavelengths.

CONCLUSION

This study supports the idea that there is a predictable structure in the underwater radiance distribution in lakes. This structure may be important in interactions between zooplanktivorous fish and their prey, and suggests that there are both behavioral and physiological ways that fish could enhance their foraging efficacy. The optical structure is not likely, however, to be a reliable signal for limnetic zooplankton to use in order to avoid the shore.

REFERENCES

Hemmings, C.C. 1966. Factors influencing the visibility of objects underwater. Pg. 359-374. In Light as an Ecological Factor, R. Bainbridge Ed. Brit. Ecol. Soc. Symp. #6.

Janssen, J. 1981. Searching for zooplankton just outside Snell's Window. Limnol. Oceanogr. 26(6):1168-1171.

Kirk, J.T.O. 1983. Light and Photosynthesis in Aquatic Ecosystems. Cambridge U. Press.

Krebbs, C.J. 1978. Ecology: The Experimental Analysis of Distribution and Abundance. Harper and Row. NYC.

McFarland, W.N. and F.W. Munz. 1975a. Part 2: The photic environment of clear tropical seas during the day. Vision Res. 15:1063-1070.

McFarland, W.N. and F.W. Munz. 1975b. Part 3: The evolution of photopic visual pigments in fishes. Vision Res. 15:1071-1080.

Petzold, T.J. 1972. Volume scattering functions for selected ocean waters. SIO Ref. 72-78. Scripps Inst. Ocean.

Preisendorfer, R.W. 1958. A proof of the asymptotic radiance hypothesis. SIO Ref. 58-57.

Preisendorfer, R.W. 1959. Theoretical proof of the existence of characteristic diffuse light in natural waters. J. Mar. Res. 18(1):1-9.

Preissler, K. 1977. Horizontal distribution and "avoidance of shore" by rotifers. Arch. Hydrobiol. Beih. 8:43-46.

Siebeck, H.O. 1980. Optical orientation in pelagic crustaceans and its consequence in the pelagic and littoral zones. In Evolution and Ecology of Zooplankton Communities. W.C. Kerfoot, Ed. pg. 28-38. New England
Press.

Tyler, J.E. 1960. Radiance distributions as a function of depth in an underwater environment. SIO Ref. 7(5):363-412.

Whitney, L.V. 1941a. The angular distribution of characteristic diffuse light in natural waters. J. of Mar. Res. 4(2):122-131.

Whitney, L.V. 1941b. A general law of diminution of light intensity in natural waters and the percent of diffuse light at different depths. J. Opt. Soc. of Amer. 31:714-722.

TABLE 1

	Bush	Itasca	Long	Bog
Mean Secchi depth (m)	2.9	2.4	6.9	1.5
Mean Summer [Chl. *a*.] (mg m^{-3})	-	13.3	1.3	14.7
Mean k_{PAR} (m^{-1})	-	0.87	0.26	1.59
A_{350}	-	0.184	0.035	0.952

Table 1. Summary of the mean summer values for four optical parameters in the study lakes. k_{PAR} is the vertical attenuation coefficient for downwelling photosynthetically active radiation (PAR). A_{350} is the absorbance of 350nm wavelength light in a 10cm cuvette by filtered water, and is a relative measure of the concentration of dissolved yellow compounds.

FIGURE CAPTIONS

Figure 1. Radiance incident at the air-water interface at angle θ_a is refracted to angle θ according to Snell's Law. Light is refracted only slightly at low angles of incidence (near the vertical), but the degree of refraction increases towards the horizontal. The result is that all skylight impinging on point A is focused into an inverse cone, which is called Snell's Window. A line of sight towards the region outside of Snell's Window is dark.

Figure 2. Radiance distributions at 0.5m in Bush Lake at 10:25 A.M. on 8/24/84 and at 19:00 P.M. on 8/27/84. Both 0° and 360° on the abscissa are the zenith direction, and 180° is the nadir direction. Snell's Window is the region from 0° to 49° and from 311° to 360°. For each RD, only an ark through the plane that includes the sun's azimuth is shown. All radiance measurements at 10:25 are divided by 10 to fit the scale.

Figure 3. Radiance distributions at 0.5m in the solar plane made in Bush Lake on 8/27/84 at: 19:00, 19:22, 19:33, 19:42, and 19:52. Sunset was at 19:49. Note the shift in the peak from 315° at 19:00 to 320° at 19:52.

Figure 4. Radiance distribution at 1.0m made in Bush Lake at 13:10 P.M. on 8/17/84. The closed circles are from an east/west plane, and the open circles are from a south/north plane. 0° to 180° represents the east and south directions and 180° to 360° are the west and north directions. The sky was heavily overcast except for a large clear area to the north, which is seen as generally higher radiance values between 240° and 350° in the south-north transect.

Figure 5. The effect of depth on the RD in three of the study lakes. The RD was measured at each of five depths in each lake: 0.5m, 1.5m, and 2.5m are shown here.

Figure 6. The breadth of the solar beam is plotted against depth. The breadth is measured as the arc (in degrees) between the 50% of maximum radiance on one side of the beam to the 50% of maximum radiance value on the other side of the beam in the solar plane.

Figure 7. a) The ratio between radiance in the solar beam to radiance at 90° in the solar azimuth plotted against depth. b) The ratio between the radiance at 10° east to the radiance at 90° east.

Figure 8. Depth profiles of RD that were made normal to the plane of the measurements in Figure 5. Three depths are shown for each lake between 0.5m and 2.5m.

Figure 9. Representative sample of attempts to demonstrate the imposition of a shadow on the RD by the shore. A is an east/west plane, B is a south/north plane that includes the sun. Three separate radiance distributions are shown, one made 14m from the east shore, one in mid-lake, and one made 30m from the west shore. In each case, the near-shore measurements were made just outside the margin of macrophytes. If a shore shadow were present, it should be visible as a depressed radiance between 20° and 50° in panel A for the east shore, and 310° and 350° in panel A for the west shore. The high upwelling light (135° to 225°) for the east shore RD is presumed to be caused by reflection off of the bottom.

Figure 10. Radiance distributions made in Long Lake under heavily overcast conditions. A shore shadow appears, where it is predicted, at 310° (at the western edge of Snell's Window).

Figure 11. Radiance distribution made with no filter (PAR), 450nm (blue), 560nm (green), and 670nm (red) filters in the three study lakes. The radiance values are to a log scale. These radiance distributions were made at the optical depth where 50% of surface irradiance remains.

FIGURE 1

SNELL'S WINDOW

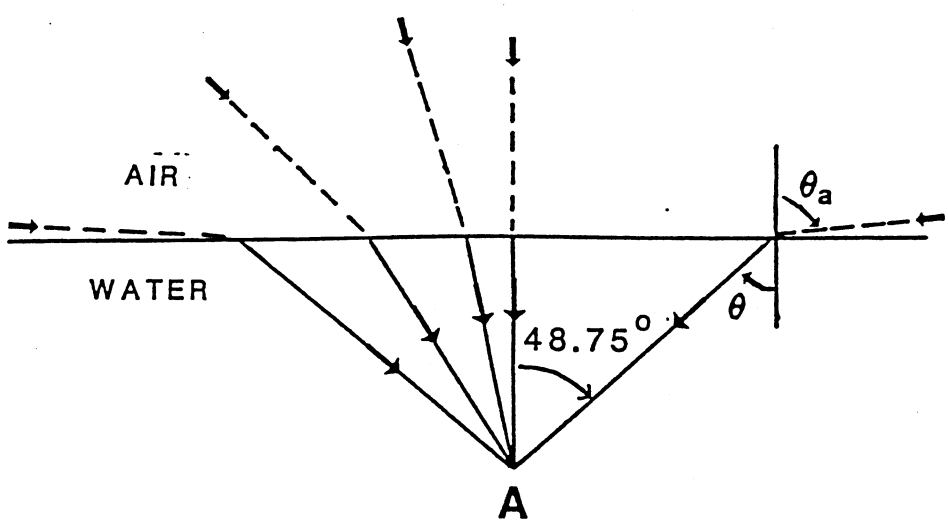

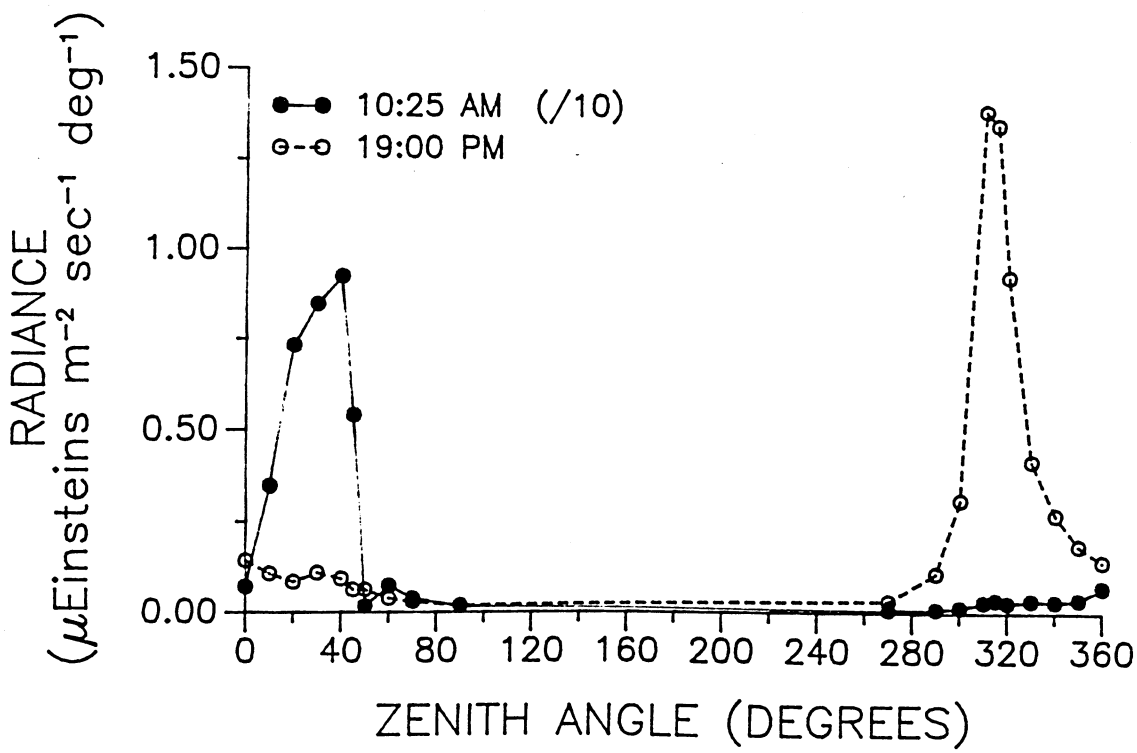
RADIANCE
(μEinsteins m⁻² sec⁻¹ deg⁻¹)
1.50
1.00
0.50
0.00
10:25 AM (/10)
19:00 PM
0
40
80
120
160
200
240
280
320
360
ZENITH ANGLE (DEGREES)

FIGURE 2

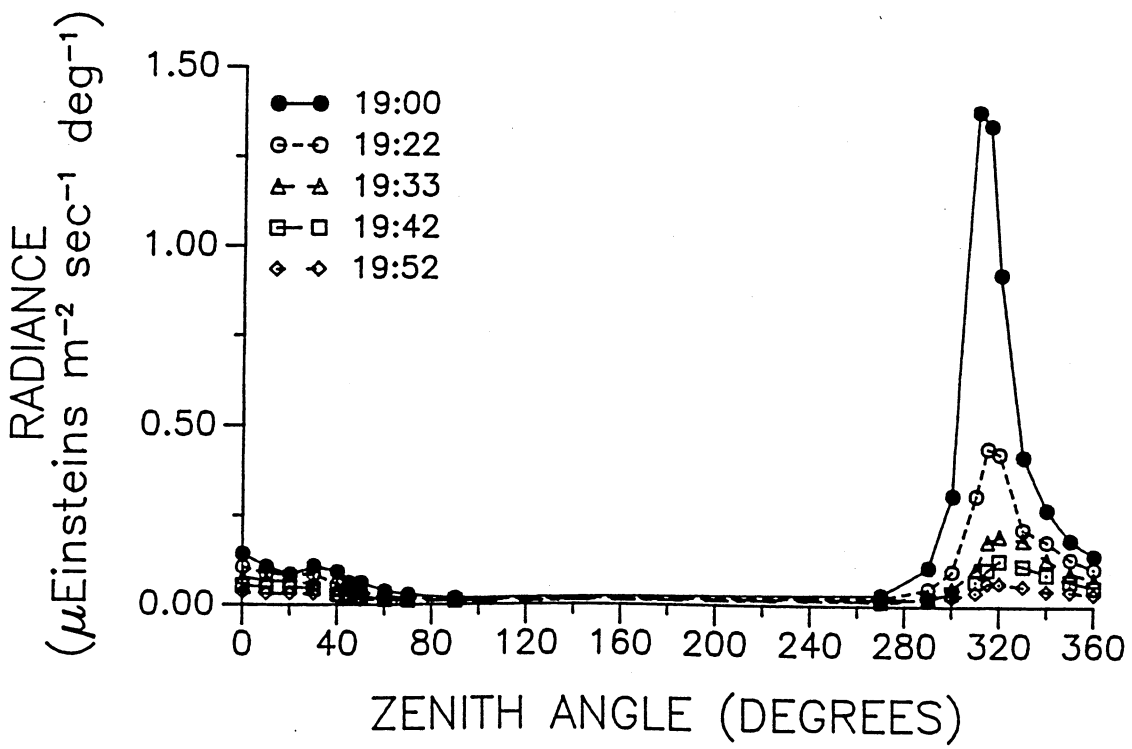
RADIANCE
(μEinsteins m⁻² sec⁻¹ deg⁻¹)
1.50
1.00
0.50
0.00
19:00
19:22
19:33
19:42
19:52
0
40
80
120
160
200
240
280
320
360
ZENITH ANGLE (DEGREES)

FIGURE 3

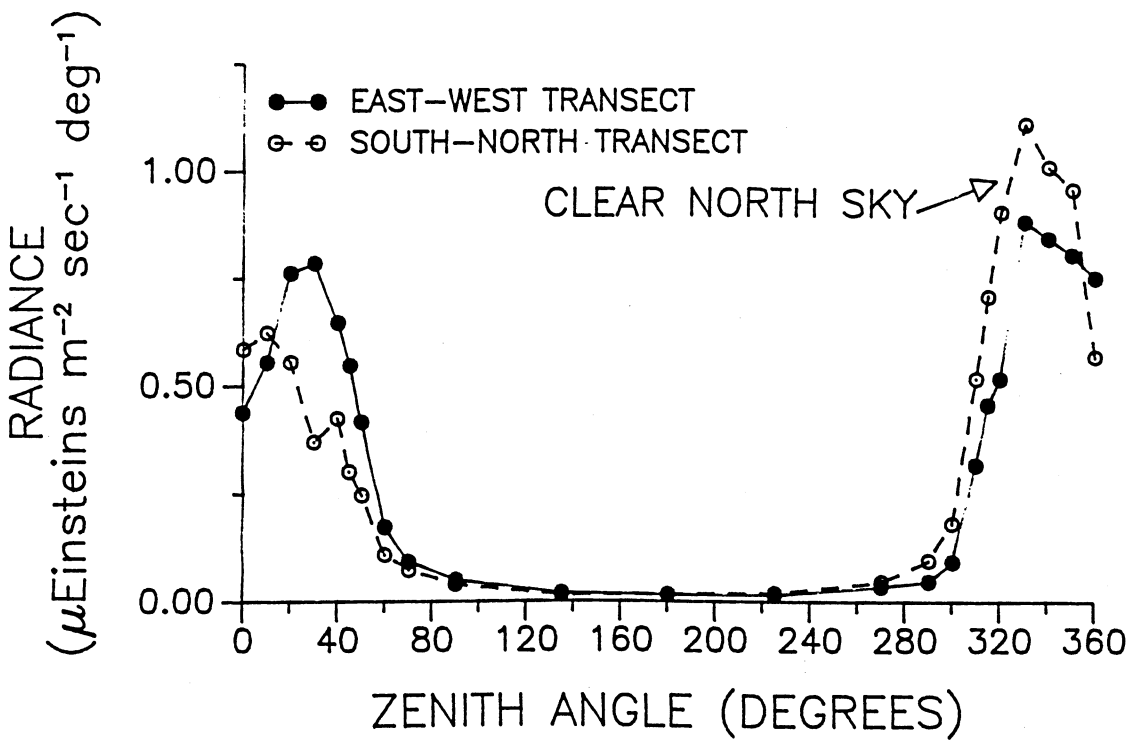
EAST–WEST TRANSECT
SOUTH–NORTH TRANSECT
CLEAR NORTH SKY
RADIANCE
(μEinsteins m⁻² sec⁻¹ deg⁻¹)
1.00
0.50
0.00
0
40
80
120
160
200
240
280
320
360
ZENITH ANGLE (DEGREES)

FIGURE 4

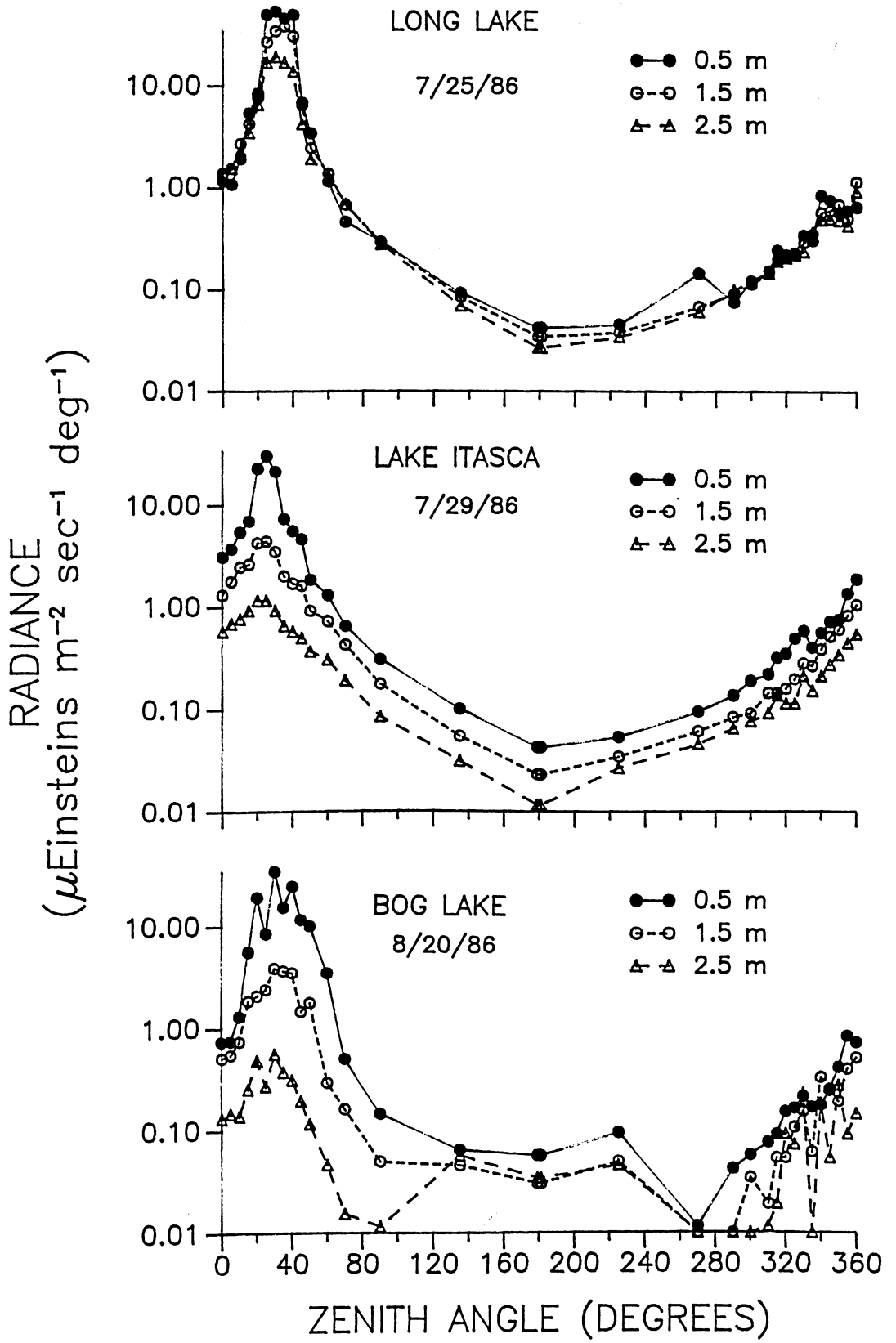
LONG LAKE
7/25/86
0.5 m
1.5 m
2.5 m
LAKE ITASCA
7/29/86
BOG LAKE
8/20/86
10.00
1.00
0.10
0.01
0
40
80
120
160
200
240
280
320
360
RADIANCE
(μEinsteins m⁻² sec⁻¹ deg⁻¹)
ZENITH ANGLE (DEGREES)

FIGURE 5

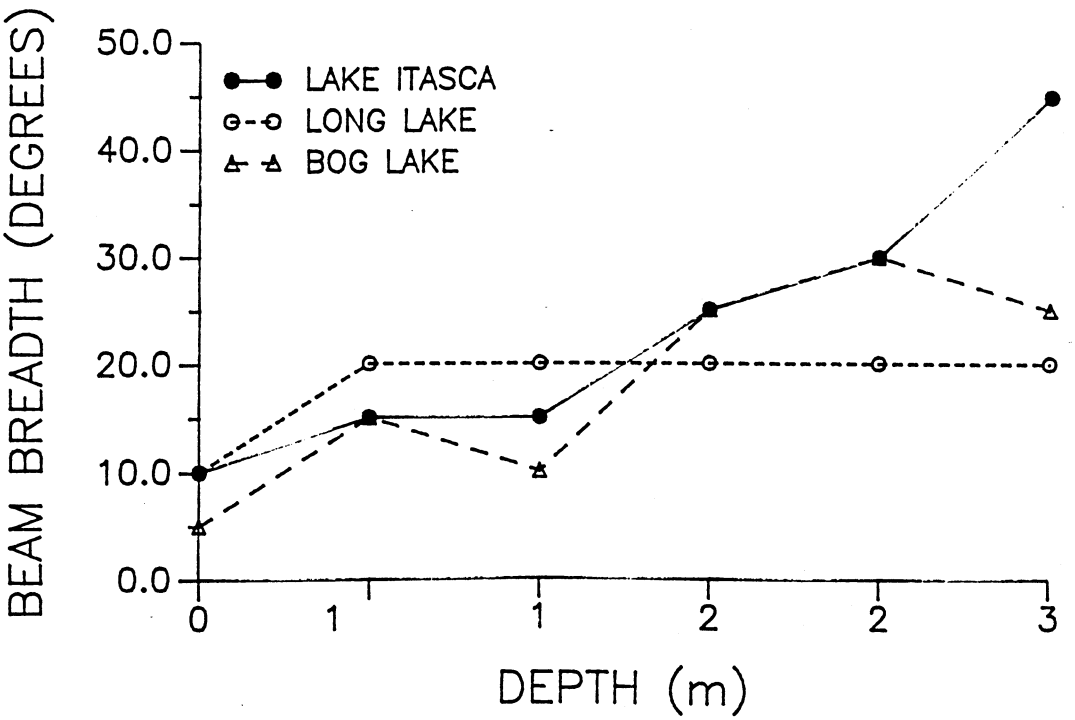
BEAM BREADTH (DEGREES)
50.0
40.0
30.0
20.0
10.0
0.0
LAKE ITASCA
LONG LAKE
BOG LAKE
0
1
1
2
2
3
DEPTH (m)

FIGURE 6

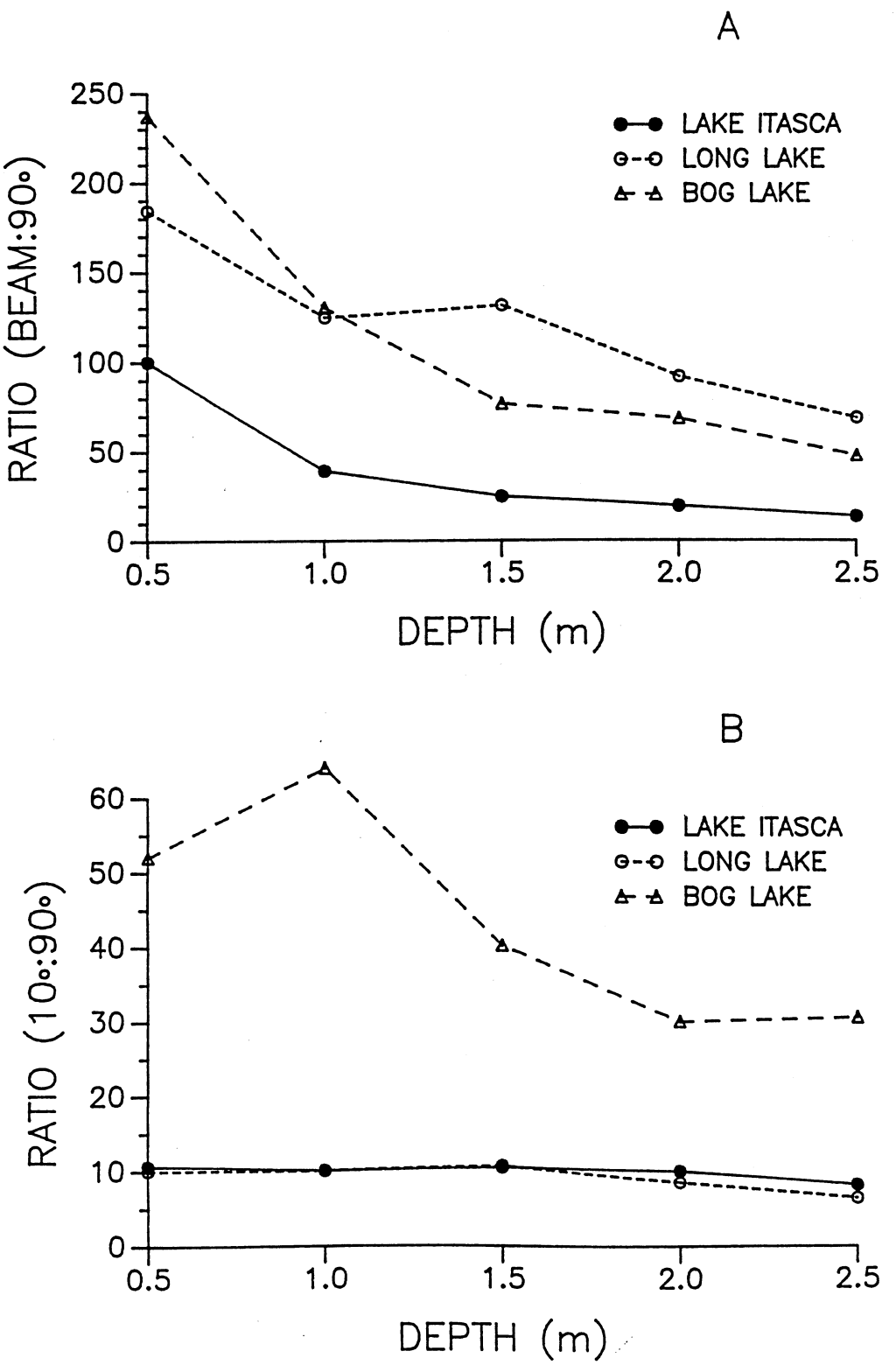
A
250
200
150
100
50
0
RATIO (BEAM:90°)
LAKE ITASCA
LONG LAKE
BOG LAKE
0.5
1.0
1.5
2.0
2.5
DEPTH (m)
B
60
50
40
30
20
10
0
RATIO (10°:90°)
LAKE ITASCA
LONG LAKE
BOG LAKE
0.5
1.0
1.5
2.0
2.5
DEPTH (m)

FIGURE 7

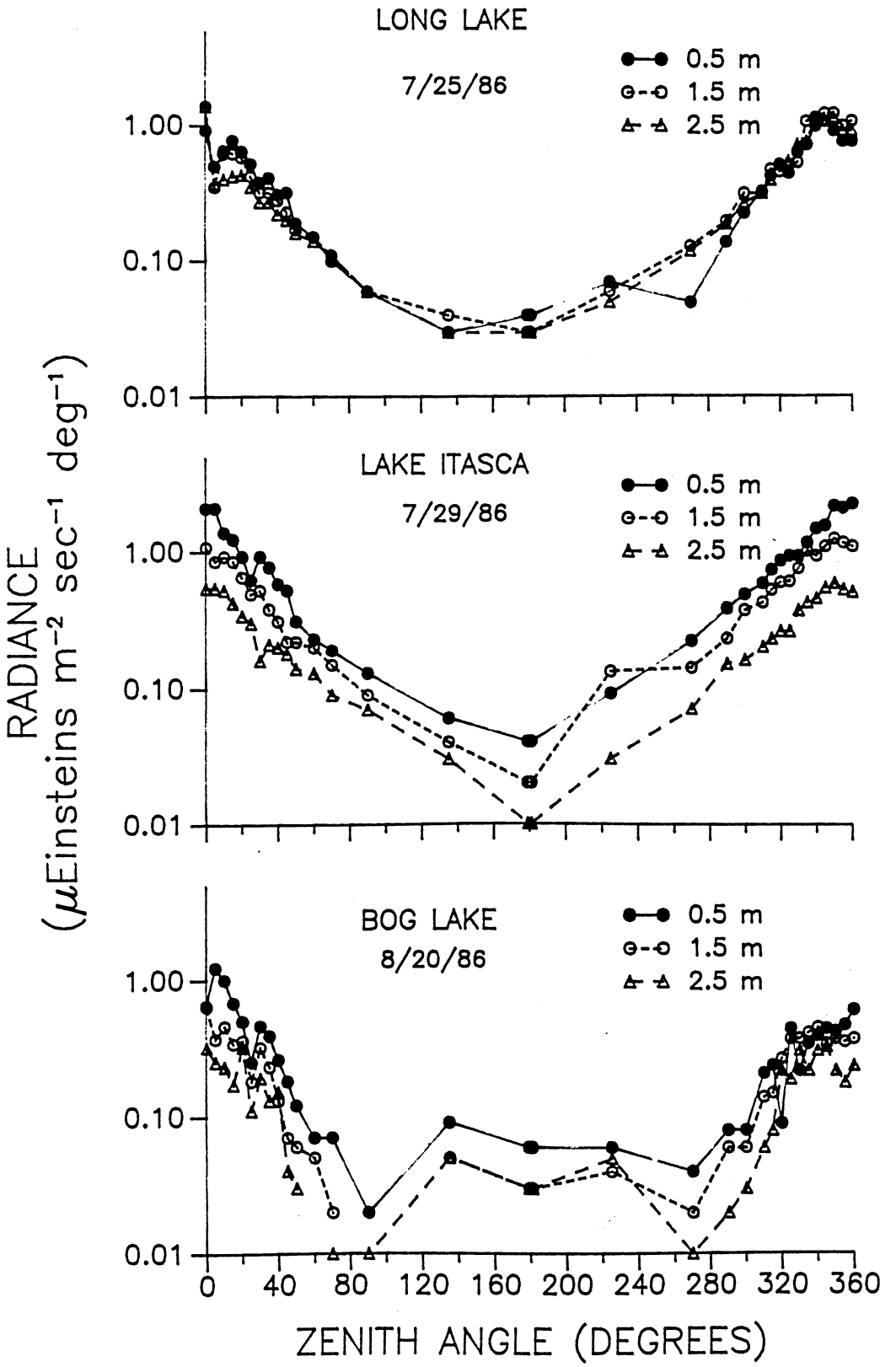
LONG LAKE
7/25/86
0.5 m
1.5 m
2.5 m
1.00
0.10
0.01
LAKE ITASCA
7/29/86
0.5 m
1.5 m
2.5 m
1.00
0.10
0.01
BOG LAKE
8/20/86
0.5 m
1.5 m
2.5 m
1.00
0.10
0.01
0
40
80
120
160
200
240
280
320
360
ZENITH ANGLE (DEGREES)
RADIANCE
(μEinsteins m⁻² sec⁻¹ deg⁻¹)

FIGURE 8

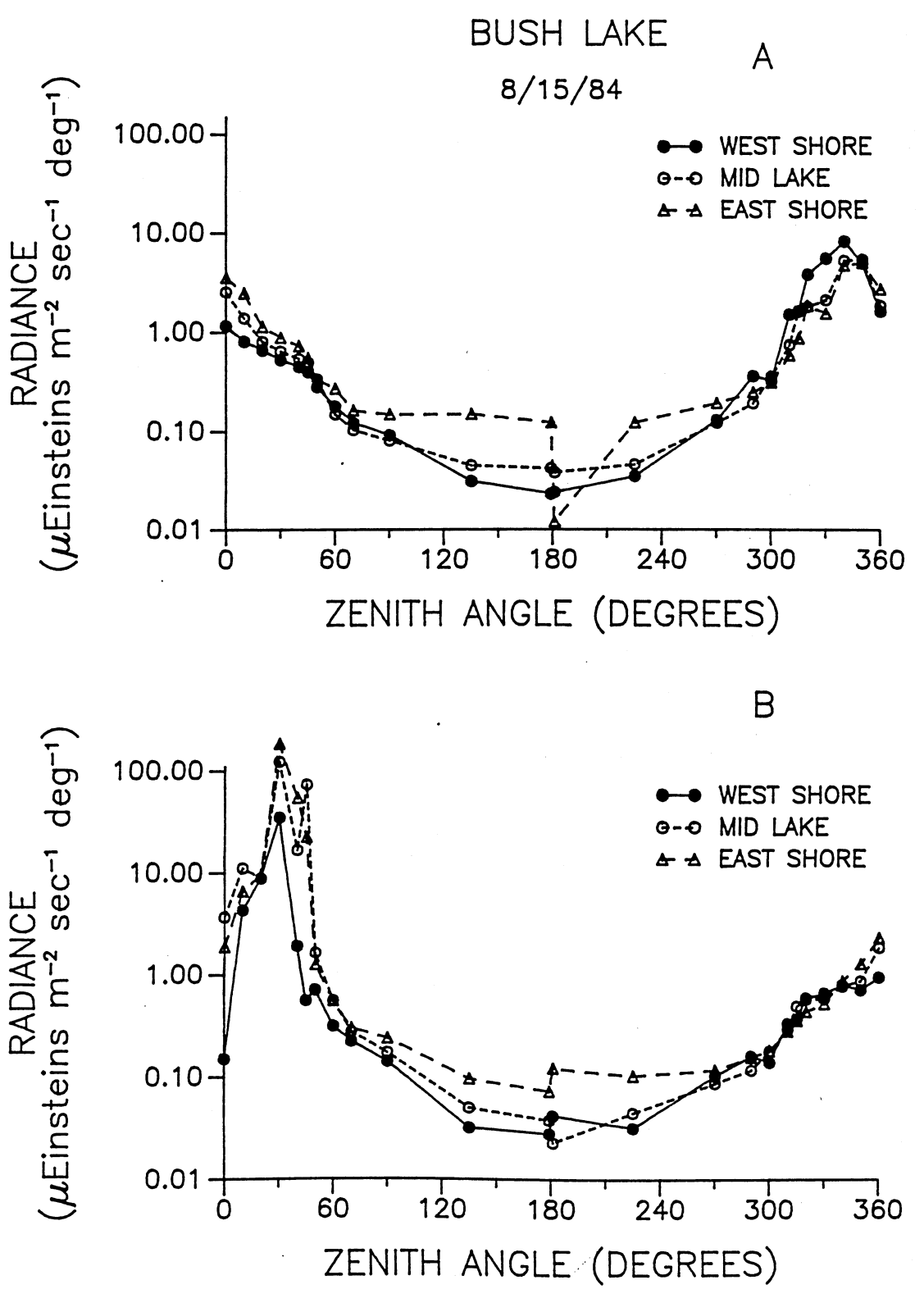
BUSH LAKE
A
8/15/84
WEST SHORE
MID LAKE
EAST SHORE
RADIANCE
(μEinsteins m⁻² sec⁻¹ deg⁻¹)
100.00
10.00
1.00
0.10
0.01
0
60
120
180
240
300
360
ZENITH ANGLE (DEGREES)
B
WEST SHORE
MID LAKE
EAST SHORE
RADIANCE
(μEinsteins m⁻² sec⁻¹ deg⁻¹)
100.00
10.00
1.00
0.10
0.01
0
60
120
180
240
300
360
ZENITH ANGLE (DEGREES)

FIGURE 9

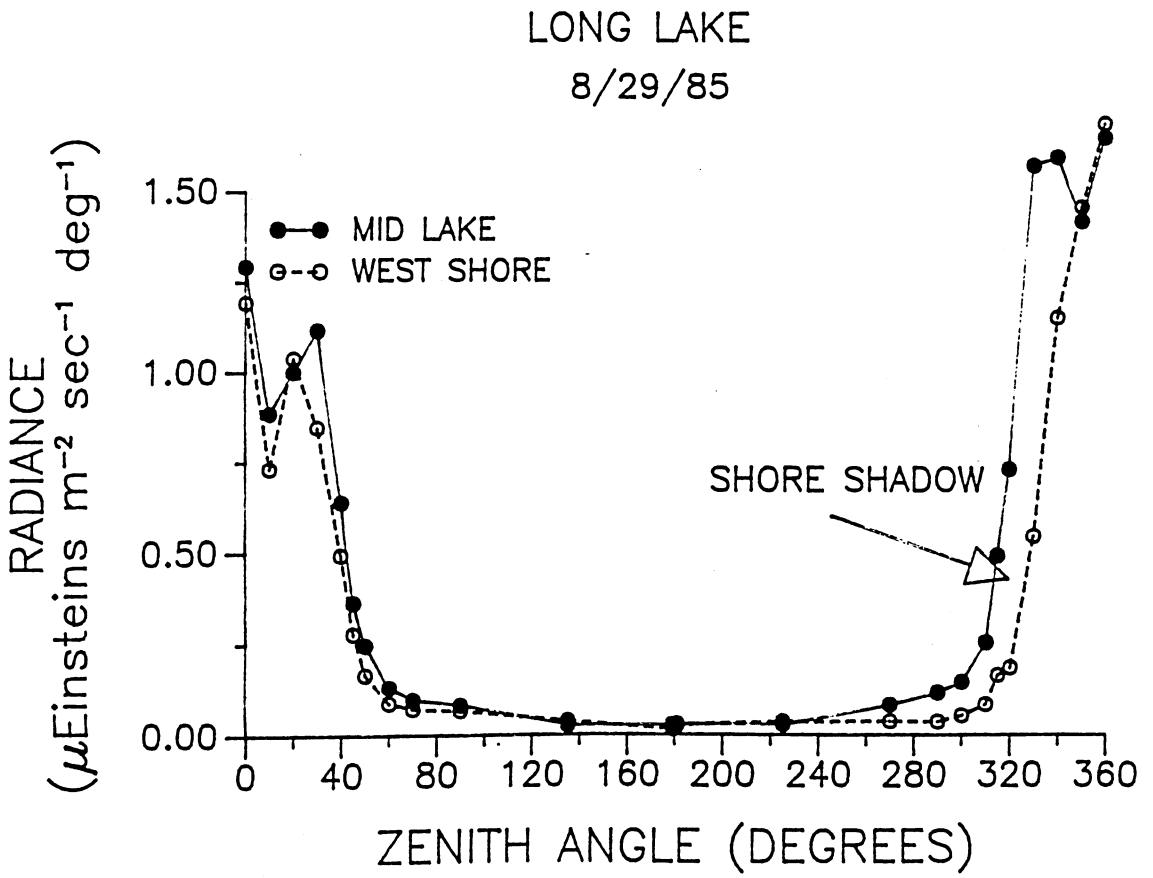
LONG LAKE
8/29/85
RADIANCE
(μEinsteins m⁻² sec⁻¹ deg⁻¹)
1.50
1.00
0.50
0.00
MID LAKE
WEST SHORE
SHORE SHADOW
0
40
80
120
160
200
240
280
320
360
ZENITH ANGLE (DEGREES)

FIGURE 10

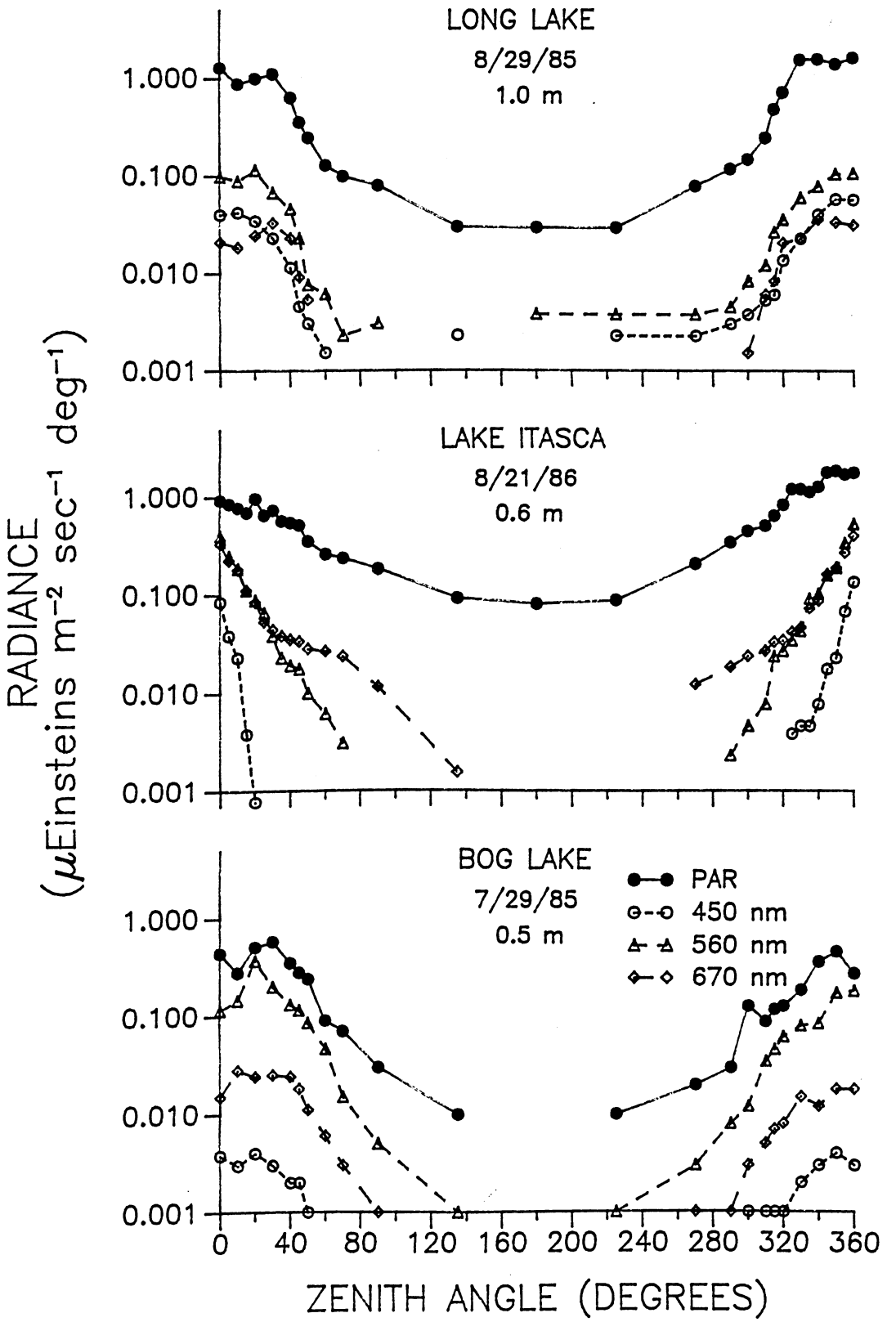
LONG LAKE
8/29/85
1.0 m
LAKE ITASCA
8/21/86
0.6 m
BOG LAKE
7/29/85
0.5 m
PAR
450 nm
560 nm
670 nm
1.000
0.100
0.010
0.001
0
40
80
120
160
200
240
280
320
360
RADIANCE
(μEinsteins m⁻² sec⁻¹ deg⁻¹)
ZENITH ANGLE (DEGREES)

FIGURE 11

CHAPTER 3

THE ATTENUATION OF IRRADIANCE IN THREE LAKES IN NORTHWESTERN MINNESOTA

ABSTRACT

Three lakes in northwestern Minnesota were studied over a two-year period to determine what factors control the attenuation of irradiance in them. Long Lake is shown to be an optical analog of highly transparent oceanic water; downwelling irradiance is largely controlled by water itself, but is also responsive to changes in the concentration of chlorophyll *a* and dissolved organic compounds (gilven). In Lake Itasca, chlorophyll *a* and possibly tripton are the major light attenuating substances. Finally, gilven dominates light attenuation in Bog Lake.

The effective, specific attenuation coefficients for chlorophyll *a* and gilven are shown not to be constants, but to be concentration dependent due to competition for light.

Finally, the relationship between Secchi transparency (s) and the vertical attenuation coefficient for downwelling irradiance (k_d) is shown not to be a simple inverse relationship, but to be of the form $k_d = (1.39 + 1.27/s)/s$.

INTRODUCTION

Both photosynthesis and vision depend on the same narrow range of electromagnetic radiation in order to function. This range, 400nm to 700nm, is referred to as photosynthetically active radiation (PAR). The most ecologically significant measure of PAR is irradiance (or scalar irradiance) because it is a measure of the total amount of light impinging on a point. There are four major constituents of a water body that are known to contribute to the attenuation of PAR: water, phytoplankton, dissolved organic compounds (gilven) and inanimate particulates (tripton). Each of these constituents contributes to the absorption and scatter of PAR in a unique way, thereby changing the optical structure of the waterbody. This optical structure includes the penetration, spectral composition and radiance distribution of PAR. This structure can have broad ecological consequences for primary production (Megard et al., 1979), algal species composition (Kirk, 1983) and predator-prey interactions (McFarland & Munz, 1975; Wright et al., 1980).

This paper examines those factors which control the attenuation and the spectral composition of PAR in three optically disparate lakes in northwestern Minnesota.

THEORY

Radiative Transfer Theory: A general body of theory has been developed which makes use of two fundamental optical processes, absorption and scattering, to describe how radiation is transmitted through water. Beam absorption is the loss of directed radiant energy (radiance) by conversion into another energy form. Beam absorption is normally described by a rate parameter called the beam absorption coefficient, a (m^{-1}). Beam scattering is the loss of radiance by redirection of the energy through the processes of reflection and refraction. An individual photon may be scattered many times before it is finally absorbed or scattered out of the water column. The beam scattering coefficient, b (m^{-1}) is defined in analogy to the absorption

coefficient. Both a and b are inherent optical properties of a water body because they depend only on factors that are intrinsic to the water. They may be summed to give a third inherent optical property, the beam attenuation coefficient, c (m^{-1}).

Unfortunately, Radiative Transfer Theory is complex. First, it is empirically difficult to distinguish between absorption and scattering, and they are therefore hard to measure independently (Plass & Kattawar, 1972). Second, both a and b are wavelength dependent, which makes attempts to understand the full spectrum of PAR more difficult. Lastly, irradiance can only be estimated by integrating the individual radiance values over all directions.

Lambert-Bouguer Law: Fortunately, the attenuation of irradiance over depth in the water column is very nearly exponential. The Lambert-Bouguer Law is an empirical model which estimates irradiance at a depth with a high degree of precision (Kirk, 1983, pg. 104)

$$E_{d(z)} = E_{d(0)} * EXP(-k_d * z) \qquad (1)$$

In this equation, $E_{d(z)}$ is the downward irradiance (μEinsteins m^{-2} s^{-1}) at depth z (m), $E_{d(0)}$ is the downward irradiance just below the surface, and k_d is the vertical attenuation coefficient for PAR (m^{-1}). k_d is analogous to c in that it is the sum of absorption and scattering, but k_d is an apparent optical property because it is dependent on factors that are external to the water column (Kirk, 1983). However, these extrinsic influences are relatively weak, and knowledge of k_d allows a robust estimate of $E_{d(z)}$. In the remainder of this paper I consider only downward irradiance, and so for simplicity, I will not use the subscript d.

k is normally found empirically from the slope of a plot of $\ln(E_{(z)})$ vs z. Such plots for PAR are usually nonlinear near the surface, but become linear a short distance below the surface. This is caused by the rapid attenuation of wavelengths with high beam attenuation coefficients. Thus, irradiance becomes increasingly monochromatic with

depth. Therefore, Equation 1 is most appropriate at depths where the irradiance is monochromatic (Kirk, 1983, pg. 111).

k can be partitioned into the four constituents of a waterbody which are known to contribute to the attenuation of light: water itself (k_w), tripton (k_t), gilven (k_g), and phytoplankton (k_p) (Kirk, 1980). The total attenuation coefficient for PAR may therefore be written as the sum of four partial coefficients,

$$k = k_w + k_t + k_g + k_p \qquad (2)$$

Pure water has a standard attenuation spectrum, and thus k_w is a constant with a value of about 0.027 (Smith & Baker, 1978). This constant is shared by all water bodies, and establishes a minimum level for the value of k. Although k_w may or may not be a significant fraction of k in a particular lake, it is not primarily responsible for the unique attenuation characteristics observed in various water bodies (Smith & Baker, 1981).

Tripton is difficult to separate from phytoplankton, and tends to be of less importance than gilven and phytoplankton in many waters (Kirk, 1980) and so was not measured independently in this study.

The peak of the gilven attenuation curve occurs in the UV, but its attenuation spectrum does extend into the PAR region. In some cases gilven can contribute significantly to the overall attenuation of PAR (Kirk, 1980).

The attenuation of light by phytoplankton is complex because it depends on such factors as algal species composition, plant pigment composition, cell size and cell pigment concentration (see Kirk, 1983 for review). However, for heuristic reasons, only the concentration of chlorophyll a is considered. Chlorophyll a is a widely used index of phytoplankton abundance and is primarily responsible for the absorption of PAR in most algal species.

The partial coefficients for gilven and phytoplankton can be thought of as the product of a concentration and a specific attenuation coefficient. Thus, $k_g = k_y * A_{350}$ and $k_p = k_c * Chl.$, where k_y (m^{-1}) and k_c

(m^2 mg^{-1}) are the specific attenuation coefficients of gilven and chlorophyll a respectively. A_{350} is a relative measure of the concentration of gilven (arbitrary units), and Chl. is the concentration of chlorophyll a (mg m^{-3}).

Correlation between k and s: Poole and Atkins (1929) first suggested that k is correlated to another apparent optical property, the Secchi disk transparency, s (m), through the simple inverse relationship

$$k = A*(1/s) \qquad (3)$$

In their model, A is a constant which is empirically shown to have a value of 1.70 (amended to 1.51 by Megard & Berman, in prep.). Holmes (1970) suggests a value of 1.44 for A in turbid coastal water. Megard and Berman (in prep) derive equation 3 from the Lambert-Bouguer Law, and show that A is equal to $-\ln(E_{(s)}/E_{(0)})$, where $E_{(s)}$ is the irradiance at the Secchi depth. They suggest a universal mean value of 1.54 for A. They also emphasize that the appropriate coefficient to use in Equations 1 and 2 is that for the most penetrating waveband (k'), because light is largely monochromatic at the Secchi depth.

METHODS

Following a survey of lakes near the Itasca Biological Station, three lakes were selected for study. These three lakes represent the full breadth of optical conditions in the region. Bog Lake is a small, shallow (z_{max} = 3m) and highly discolored lake. Lake Itasca is larger, deeper (z_{max} = 13m) and productive, but is more transparent than Bog Lake. Long Lake is a large, deep (z_{max} = 20m) and very transparent lake. All three lakes are located within a few miles of the biology station (at 95° 15' W; 47° 15' N), surrounded by a mixed deciduous/evergreen forest that is minimally impacted by human development, and lie within the same geological formation, the Itasca Moraine.

Water transparency data were collected in each of the three study lakes at approximately ten-day intervals between mid-June and late September, 1985 and 1986. Secchi disk transparency was measured with a standard, white 20cm Secchi disk (Wildco) on the shaded side of the boat. Attenuation coefficients for PAR were estimated by making measurements of irradiance at depth intervals within the mixed layer with a Li-Cor 185 quantum meter and cosine collector that responds only to PAR (Lambda Instruments). Measurements of attenuation coefficients for specific wavelengths were made by attaching interference filters, with a bandwidth of less than 10nm (Andover Corp.), to the sensor. The midpoints of the wavelengths used were: 400, 450, 500, 520, 540, 560, 610 and 670nm.

Water samples for measurements of gilven and phytoplankton were collected at 1m depth. One liter of sample was filtered through Gelman type A/E, glass fiber filters. Chlorophyll a was then extracted from the filters in methanol and its concentration estimated following the procedure of Holm-Hansen & Reiman (1978).

The concentration of gilven was estimated by measuring the absorbance of the filtrate at 350nm in a 10cm cuvette against a distilled, deionized water blank, in a Bausch & Lomb spectronic 70 spectrophotometer. The absorbance of a filtered sample at 350nm (A_{350}) is used throughout this paper as a relative measure of the concentration of gilven. The beam attenuation spectra due to gilven were made by measuring the absorbance of the filtrate at 10nm intervals between 330 and 750nm.

RESULTS

Measure of water clarity: As shown in Table 1, Bog Lake is the least transparent of the three lakes, with a mean Secchi transparency of about 1.5m; Itasca has a mean s of about 2.4m, and Long Lake is the most transparent of the three with a mean s of about 7.0m. These means are highly consistent between years, and each lake is optically unique based on ANOVA of seasonal mean s ($p < .001$).

Figure 1 shows the seasonal variation of reciprocal transparency (1/s) in the three study lakes during 1985. All three lakes show significant variation in 1/s during the four months of the study. Reciprocal transparency is most variable in Lake Itasca, with a CV of 30.4%. The CV for 1/s in Long Lake is 21.3% and in Bog Lake it is 12.7%. In Itasca, 1/s increases (clarity decreases) through July and August and then decreases (clarity increases) during September and October. The trends in 1/s are less symmetrical in the other two lakes. All lakes show an increase in 1/s during late July or early August; but the timing of the onset of the increase and its duration vary amongst the lakes. Thus, transparency is poorly synchronized amongst them. This implies that meteorology and other external factors that are common to the lakes are not the only important determinants of transparency, but that endogenous factors are important as well.

Table 1 indicates that the ranking of the three study lakes with respect to water clarity is the same when k is the criteria rather than s. Figure 2 shows seasonal trends in k. Long Lake is most transparent to PAR with a seasonal mean attenuation coefficient of about .25 m^{-1}; Itasca is second with a mean seasonal k of about .85 m^{-1}; and Bog Lake is least transparent with a mean seasonal k of about 1.55 m^{-1}. Again, these means are significantly different from each other ($p < .00001$).

Gilven: Figure 3 shows spectrophotometric scans of the beam attenuation coefficient due to gilven in the three study lakes from the early summer of 1985. It is clear that gilven is very important in both Bog Lake and Lake Itasca at wavelengths below 500nm.

Beam attenuation by gilven is due in part to absorption and part to scatter. It is possible to isolate these two components if one uses the adaptation by Davies-Colley and Vant (1987) of Bricaud et al's. (1981) equation for the calculation of the absorption coefficient from attenuation measured in a spectrophotometer. Davies-Colley and Vant (1987) assume that scatter by gilven is inversely proportional to wavelength and that attenuation at long wavelengths (e.g. 750nm) is all due to scatter. Figure 4 is a plot of the beam scattering coefficient due to gilven (found using Eq. 5 of Davies-Colley and Vant, 1987) vs

wavelength. These scattering coefficients for gilven are between two and three orders of magnitude larger than scattering coefficients of pure water (Smith and Baker, 1981). Thus, even at wavelengths where PAR is weakly absorbed by gilven, it can contribute to attenuation through scattering.

The beam absorption coefficient due to gilven can be calculated by subtracting the scattering coefficient from the attenuation coefficient (Fig. 3- Fig. 4) at each wavelength. Figure 5 shows a semi-log plot of the beam absorption due to gilven, calculated in this manner, vs wavelength: the near linear nature of the three plots, and their similar slopes, suggests that they fit the general equation derived by Bricaud et al. (1981) for gilven in the sea

$$a(\lambda) = A_{350} * EXP(-S*(\lambda-\lambda_{350})) \qquad (4)$$

In this equation, $a(\lambda)$ is the portion of the beam absorption coefficient attributable to gilven (m^{-1}) at a specific wavelength, λ (nm), and A_{350} is the spectrophotometric absorbance at a reference wavelength in a region of strong absorbance (350nm). S is the slope parameter (nm^{-1}), and is simply the slope of the curves in Figure 5. Estimates of S are consistent from a wide range of water types and gilven concentrations. Bricaud et al. (1981) reported a range of S from .010 to .020 with a mean value of .014 from several different ocean waters, and other workers have reported values that lie within this range from fresh water (e.g. Davies-Colley and Vant, 1987). My estimate of S from Long Lake was .021 (± 0.002), from Lake Itasca it was .013 (± 0.0006) and from Bog Lake it was .014 (± 0.0004). These data fall within the observed values from other water bodies, but Bog Lake and Itasca are significantly different from Long Lake ($p < .001$). Thus, there is some indication that there is a difference in the nature of the dissolved organics in Long Lake. Its higher value of S indicates that the gilven in Long Lake absorb less strongly at longer wavelengths than in the other two lakes.

Figure 6 shows that there is relatively little seasonal variation in gilven concentration in any of these lakes. Bog Lake's seasonal average was .956 and was the least variable with a CV of 3.13%. Itasca had a seasonal average of .192, and a CV of 15.67%. Long Lake had a seasonal average of .035 and a CV of 17.87%. In all three lakes, the highest concentrations of gilven occurred in the middle of the summer. However, as with the transparency measurements, the gilven dynamics are poorly synchronized amongst the three basins.

Phytoplankton: Figure 7 shows the seasonal trends in chlorophyll a concentration in the three study lakes during 1985. Both Bog Lake and Itasca have high mean summer concentrations of Chl. a, while Long Lake has a very low concentration. All three lakes show a gradual increase in Chl. a until late August. The concentration of Chl. a is highly variable with CVs in all three lakes ranging from 31.5% to 63.5%. There is no correlation between gilven (A_{350}) and chlorophyll a in any of the three lakes.

Spectral distribution of irradiance: Figure 8 shows the spectral distribution of irradiance at various depths in each lake on a single day in 1985. The depths shown were chosen to represent 100%, 50%, 10% and 1% of surface PAR. 1% PAR is reached at 3.01m in Bog Lake, and not until 15.35m in Long Lake. In all lakes, there is a selective loss of blue light. This is most pronounced in Lake Itasca. Itasca and Bog Lake show an overall shift towards red light with depth. Long Lake shows a shift towards green light with depth, as both blue and red light are selectively attenuated.

Correlation between k and s: Figure 9 is a scatter plot of data from 55 days on which both k and s were measured in the three lakes. A least-squares linear regression in which the regression line is constrained to pass through the origin (Megard, personal communication) supports the general form of Equation 3 (R^2=.956). My observed value of A is 2.10. This is significantly higher than those found by previous investigators. Most authors have worked primarily on marine waters that are significantly more transparent than the lakes considered here. Poole & Atkin's (1929) highest measured k is 0.22, Holme's (1970) highest k is

.68, and Megard & Berman (in prep.) have only one value of k greater than 0.70.

On 42 of the 55 days plotted in Figure 9, interference filters were used to measure k for discrete wavelengths between 400nm and 670nm. Figure 10 is a plot of the attenuation coefficient for the most penetrating waveband (k') vs 1/s. Five data appear as outliers, and if they are omitted, the R^2 value of the regression is .965, which is slightly higher than the regression for k vs 1/s. The estimate of A is 1.96, which is not significantly different than the estimate of 2.10 ($0.2 > p > 0.1$) obtained from the regression of k on 1/s. This result implies that in inland waters, 1/s can be used to predict k and not just k'. k is a more biologically significant parameter than k' because both photosynthetic and visual systems can utilize all of the wavelengths, to a greater or lesser degree, between 400 and 700 nm.

DISCUSSION

Measure of water clarity: Secchi disk transparency is widely used as an index of water clarity. Secchi disks are quick and easy to use, and provide a relative measure of PAR penetration in lakes, regardless of the nature of the principal attenuating components. However, there are advantages to using k, rather than s, as an estimate of water clarity. First, k is a more conservative parameter. Although there is seasonal variation of k in each lake, the CVs are smaller than they are for s. The CVs are given in Table 1, and for two years the CVs for k averaged 30% lower than the CVs for s. This implies that any single measurement of k is more likely to give a better estimate of the mean seasonal water clarity than is any single estimate of s. Secondly, k enables the direct calculation of irradiance at any depth. k can also be partitioned into its component parts to show the relative importance of each to overall transparency. Because irradiance meters are now widely available and are nearly as easy to use as a Secchi disk, k is the superior parameter to estimate water clarity.

Components of k: Attempts to partition k into its four component parts are frustrated, in part, by the relative insensitivity of k to changes in these parameters. The best approach is to assume that tripton does not vary in either quantity or quality during a season in each lake. Attenuation attributable to it then becomes a constant, and Equation 2 simplifies to

$$k = k_{w+t} + k_y * A_{350} + k_c * Chl. \qquad (5)$$

Equation 5 suggests that a multiple regression of k on A_{350} and Chl. will provide estimates of the coefficients k_y and k_c as well as the constant k_{w+t}. At the same time, this approach obviates the concern that gilven and chlorophyll might covary, even though an independent analysis has shown that they do not covary in any of the lakes. These regressions were done in each lake for data collected in 1985, and the results are given in Table 2.

In Long Lake, changes in k are clearly related to seasonal changes in chlorophyll concentration, and somewhat less clearly to changes in A_{350}. The multiple regression of k on Chl. and A_{350} explains 72% of the seasonal variance in k, and estimates k_c to be .088.

In Lake Itasca, seasonal changes in k are very responsive to chlorophyll, but not to gilven, as k_y is not statistically significant. k_c is equal to .031 (±0.009) and chlorophyll alone is able to explain 84% of the seasonal variation in k. Figure 11 shows this strong relationship as a plot of k vs Chl. in Lake Itasca.

In Bog Lake, seasonal k does not correlate well with either chlorophyll or gilven. It could be that tripton is most important in determining seasonal variation in k in this shallow lake, but the implication that neither chlorophyll nor gilven impact on k is clearly erroneous because both are present at very high concentrations. It is much more likely that their seasonal variance is so small relative to that of gilven, that I do not have the statistical power to detect the impact that they have on k.

An underlying assumption of Equation 5 is that both k_y and k_c are constants over the full range of A_{350} and Chl., and that k is a linear function of their respective concentrations (Kirk, 1983, pg. 215). It is probably true that both gilven and chlorophyll a have an innate capacity to absorb light that is independent of concentration. However, the manner in which these parameters are normally estimated creates an autocorrelation between the specific attenuation coefficient for a substance and its concentration. To use chlorophyll as an example, let k'_c be the innate, specific attenuation coefficient and k''_c be the effective specific attenuation coefficient. k''_c is found by measuring k on several dates when the chlorophyll concentration is at different levels, and then regressing k on Chl. Chlorophyll molecules compete for light. In clear lakes, each molecule of chlorophyll saturates with light, and thus k''_c is close to k'_c. The addition of more chlorophyll has a large impact on k (k'_c*Chl.). At high phytoplankton densities, each chlorophyll molecule experiences lower than saturation levels of light, particularly of the most attenuated wavelengths. Each molecule absorbs only at k''_c because it is light limited. The addition of more chlorophyll has a small impact on k (k''_c*Chl.). A similar argument can be built for gilven, and because gilven and chlorophyll both absorb short wavelengths, they compete, in part, with each other.

These effects are clearly seen in my data. Chlorophyll concentrations are very low in Long Lake, therefore a small increase in Chl. has a relatively large impact on k (high k''_c). In Itasca, Chl. is higher, and the relative impact of adding more chlorophyll on k is much less (each molecule has a lower effective k''_c). Finally, in Bog Lake, Chl. is so high that the statistical power of the regression is not sufficient to measure k''_c; the addition of a lot of chlorophyll is not sufficient to change k. Similar trends are observed for k_y.

This result is important for two reasons. First, lake managers, who are concerned with the transparency of a lake, must realize that the reduction of Chl. by X amount when Chl. is high will increase transparency less than the same reduction when Chl. is low. Secondly, as phytoplankton populations increase, competition for light is expressed as

a lowered k''_c. This allows various ecological predictions to be made about how algae might be expected to compete (e.g. cell buoyancy and Chl. content/cell might increase).

One way to increase the statistical power of regression analysis is to collect data that include a wide range of values of Chl. and A_{350}. This can be done if the data from my three study lakes are pooled. This assumes that the nature of attenuating substances is the same in the three lakes (e.g. both gilven and Chlorophyll a are optically similar in each lake. Recall that the gilven in Long Lake shows some difference in its value of S from the other two, and the species of phytoplankton vary amongst the lakes).

The result of this regression is $k=.282 + .014*Chl. + 1.18*A_{350}$. It is notable that this mean value of k_c, 0.014, is within the range of published values (Kirk, 1983, Table 9.1). 0.014 is the effective specific attenuation coefficient that falls out of data sets that estimate k_c over the range of chlorophyll concentrations found in nature. Variation around 0.014 is a reflection of the range of Chl. used in a particular study, with low values found in turbid waters and high values found in clear waters. The specific attenuation coefficient due to gilven can not be compared to other work because there is not a standard wavelength that is used by all authors.

The best estimate of the specific attenuation coefficient for each constituent is therefore found from a multiple regression that includes the pooled data from all three lakes. Because k_w is a constant, k_t can be found by subtraction. It is then possible to determine the proportional contribution to attenuation by each component by calculating the ratio between each specific attenuation coefficient and the mean seasonal k value in each lake. These results are summarized in Table 3.

This analysis indicates that Long Lake is a freshwater analog of many marine waters in which attenuation is dominated by water itself (64%). The attenuation of light in Bog Lake is dominated by gilven, even though it has a very high chlorophyll concentration. In Lake Itasca, light attenuation is by all four components, but the most important are tripton and chlorophyll.

Spectral distribution of irradiance: It has long been known that the spectral distribution of downwelling irradiance changes with depth until the light becomes monochromatic (Duntley, 1963). The nature and concentration of the attenuating substances determine which wavelength becomes dominant. In clear waters with low gilven and chlorophyll concentrations, shorter wavelengths (e.g. at or slightly below 500nm) dominate. The dominant wavelength shifts towards longer wavelengths in more turbid water. The shift is to about 550nm in chlorophyll dominated lakes, and to 680-700 nm in gilven dominated lakes (Kishino et al., 1984; Kirk, 1979; Dubinsky and Berman, 1979; Jewson, 1977). This same trend is seen in my three study lakes. In Bog Lake and Itasca, red light becomes the dominant wavelength, with the shift particularly pronounced in Bog Lake due to its high gilven concentration. In Long Lake, both chlorophyll and gilven concentrations are low enough so that attenuation by water is significant, and thus the most penetrating wavelength is green light.

Spectral radiation distributions, like Figure 8, were calculated six times in each lake during the summer of 1986, and the shapes of the curves are very stable over the study period. Figure 12 is a plot of the seasonal trends in k for three wavelengths in Long Lake. It can be seen that there is little variation in them over the course of the summer. At certain times, when Long Lake has higher chlorophyll concentrations, the shape of its irradiance spectra is similar to Lake Itasca's.

Role of Secchi disks: The role of the Secchi disk in modern aquatic science is a subject of considerable debate. Arguments about the disk divide into three groups. One group views the Secchi disk as a quaint anachronism that contributes little unique information about the optics of a water body to a study of water clarity. The major contribution of this group has been to explain why a Secchi disk disappears from sight at the depth that it does (Preisendorfer, 1986; Tyler, 1968).

A second group uses Secchi transparency as a relative measure of water clarity, and compiles data to document seasonal and geographical trends in water clarity. This conservative approach is appropriate, but it is somewhat limited in scope. For reasons outlined previously, there are

significant advantages to using k, rather than s, as a measure of water clarity.

The third group has extended the use of Secchi disk transparency, through the use of statistical correlations, to predict various other environmental parameters, such as: k, the depth of the euphotic zone, and in certain cases, even the beam attenuation coefficient, c (Lorenzen, 1980; Megard et al. 1980; Holmes, 1970; see Preisendorfer, 1986, for comments).

The principal reason that biologists study water clarity is to gain an understanding of how much light is available at a given depth for biological processes, such as photosynthesis and vision. k is, therefore, a biologically relevant parameter. The safest and most important extension of Secchi transparency is to use it to predict k by relationships similar to Eq. 3.

Even in this use, however, there are serious limitations. In lakes with limited seasonal variability in water clarity, there may be only a poor correlation between 1/s and k. Figures 1 and 2 illustrate this; although the seasonal trends for k and 1/s show a broad similarity in each lake, there are periods of poor correlation. In Bog Lake, 1/s increases in the late summer but k decreases. In Long Lake, 1/s is constant but k increases in late summer. During the same period in Lake Itasca, both k and 1/s decrease. Attempts to correlate k and 1/s within a lake over a season frequently fail.

A second limitation of using s to predict k is that clear waters, such as oceans and Long Lake, tend to have a lower value of A than do highly turbid waters, such as Bog Lake and Lake Itasca. This implies that A is not a universal constant. If A is defined as $-\ln(E_{(s)}/E_{(0)})$, then A can be calculated independently of s because the depth at which a Secchi disk disappears is dependent on the contrast between the reflected light from the Secchi disk and the background, not on the absolute irradiance (Preisendorfer, 1986). A regression of A (calculated from this definition) on 1/s, using the data in Megard & Berman's Table 3 (in prep) and this study, indicates that A increases as a linear function of 1/s as seen in Figure 13. This means that in highly turbid water, the

Secchi disk disappears at a depth where the ratio of E_s/E_0 is smaller than in clear water. The result that a Secchi disk remains visible to a greater optical depth in turbid water than in clear water is not intuitively obvious. The explanation for this apparent contradiction is that the inherent contrast between a Secchi disk and its background is greater in turbid water than in clear water because the background against which the Secchi disk is viewed is very dark. This greater contrast allows the Secchi disk to be viewed at lower absolute light levels. The intercept, 1.39 (± 0.16) is the value A would have in extremely transparent water (infinite transparency). Oceanic waters are slightly more turbid than this, and the observed values of A range from 1.44 (Holmes, 1970) to 1.7 (Poole & Atkins's, 1929). This regression suggests that Equation 3 should be modified to a more general expression,

$$k = (1.39 + 1.27/s)* 1/s \qquad (6)$$

An alternative model, based on the contrast transmittance theories of Duntley and Preisendorfer (Duntley, 1963), predicts 1/s to be a function of both k and the beam attenuation coefficient, c. This model has a rigorous theoretical basis, but does not allow the extraction of any value except the sum of the two attenuation coefficients. Because k can not be isolated from this sum without a separate measurement of either c or k, this model does not provide a practical application for the Secchi disk.

CONCLUSION

The three study lakes proved to be optically diverse both quantitatively and qualitatively, in spite of the fact that they share a common geology and meteorology. Not only do they differ in absolute transparency, but the factors that control their transparency also differ. Long Lake is a transparent water body that is responsive to changes in both chlorophyll and gilven, but concentrations of both of these components are low enough so that the spectral composition of

downwelling light is primarily affected by water itself. In this sense, Long Lake can be considered to be an analog of many marine systems.

Lake Itasca is strongly responsive to its large fluctuation in chlorophyll concentration, and the spectral composition of downwelling light is largely controlled by chlorophyll and tripton.

Bog Lake is dominated by gilven. This result is not obvious from the regression of k on A_{350}, but the high mean A_{350}, and the spectral distribution of downwelling light in conjunction with the known absorption spectrum for gilven enable this conclusion.

The specific attenuation coefficients for both gilven and chlorophyll are inherent properties of those substances. However, at high concentrations of the substance, this attenuation coefficient is not realized. Instead, due to competition for PAR in general, and to competition for those wavelengths of maximum absorption in particular, each molecule absorbs less than would be predicted on the basis of the inherent specific attenuation coefficient. The effective specific attenuation coefficient is, therefore, concentration dependent. This explains why k is not responsive to the large fluctuations of Chlorophyll in Bog Lake; the effective k_c is too low to impact on k. In general, it is not possible to predict the relative importance of a particular constituent to overall light attenuation based solely on its concentration.

Finally, the controversy surrounding the Secchi disk should be viewed from a practical rather than theoretical frame of reference. It is possible to predict k from s with a reasonable degree of accuracy based solely on statistical correlations. However, the wide availability, ease of use and scientific power of irradiance meters should obviate the need for such a dependence.

REFERENCES

Bricaud, A., A. Morel, and L. Prieur. 1981. Absorption by dissolved organic matter of the sea (yellow substance) in the UV and visible domains. Limnol. Oceanogr. 26(1):43-53.

Davies-Colley, R.J. and W.N. Vant. 1987. Absorption of light by yellow substance in freshwater lakes. Limnol. Oceanogr. 32(2):416-425.

Dubinsky, Z. and T. Berman. 1979. Seasonal changes in the spectral composition of downwelling irradiance in Lake Kinneret (Israel). Limnol. Oceanogr. 24(4):652-663.

Duntley, S.Q. 1963. Light in the Sea. J. of the Optical Soc. of Amer. 53:214-333.

Holm-Hansen, O. and B. Reiman. 1978. Chlorophyll a determination: Improvements in methodology. Oikos 30:438-447.

Holmes, R.W. 1970. The Secchi disk in turbid coastal waters. Limnol. Oceanogr. 15:688-694.

Jewson, D.H. 1977. Light penetration in relation to phytoplankton content of the euphotic zone in Lough Neagh, N. Ireland. Oikos 28:74-83.

Kirk, J.T.O. 1979. Spectral distribution of photosynthetically active radiation in some south-eastern Australian waters. Aust. J. of Mar. Fresh. Res. 30:81-91.

Kirk, J.T.O. 1980. Spectral absorption properties of natural waters: Contribution of the soluble and particulate fractions of light absorption in some inland waters of south-eastern Australia. Aust. J. of Mar. Fresh. Res. 31:287-296.

Kirk, J.T.O. 1983. Light and Photosynthesis in Aquatic Ecosystems. Cambridge Univ. Press. Cambridge.

Kishino, M., C.R. Booth, and N. Okami. 1984. Underwater radiant energy absorbed by phytoplankton, detritus, dissolved organic matter and pure water. Limnol. Oceanogr. 29(2):340-349.

Lorenzen, M.W. 1980. Use of chlorophyll-Secchi disk relations. Limnol. Oceanogr. 25(2):371-372.

McFarland, W.N. and F.W. Munz. 1975. The evolution of photopic visual pigments in fishes. Vision Res. 15:1071-1080.

Megard, R.O., W.S. Combs, Jr., P.D. Smith, and A.S. Knoll. 1979. Attenuation of light and daily integral rates of photosynthesis

attained by planktonic algae. Limnol. Oceanogr. 24(6):1038-1050.

Megard, R.O., J.C. Settles, H.A. Boyer and W.S. Combs Jr. 1980. Light, Secchi disks and trophic states. Limnol. Oceanogr. 25(2):373-377.

Megard, R.O. and T. Berman. (in prep.) Effects of algae on the transparency of the south-eastern Mediterranean Sea.

Plass, G.N. and G.W. Kattawar. 1972. Monte Carlo calculations of radiative transfer in the Earth's atmosphere-ocean system: 1. Flux in the atmosphere and ocean. J. of Phys. Ocean. 2:139-145.

Poole, H.H. and W.R.G. Atkins. 1929. Photoelectric measurements of submarine illumination throughout the year. J. of the Marine Biol. Ass. of the U.K. 16:297-324.

Preisendorfer, R.W. 1986. Secchi disk science: Visual optics of natural waters. Limnol. Oceanogr. 31(5):909-926.

Smith, R.C. and K.S. Baker. 1978. Optical classification of natural waters. Limnol. Oceanogr. 23:260-267.

Smith, R.C. and K.S. Baker. 1981. Optical properties of the clearest natural waters. Applied Optics 20(2):177-184.

Tyler, J.E. 1968. The Secchi disk. Limnol. Oceanogr. 13(1):1-6.

Wright, D.W., W.J. O'Brien, and G.L. Vinyard. 1980. Adaptive value of vertical migration: A simulation model argument for the predation hypothesis. In Evolution & Ecology of Zooplankton Communities. W.C. Kerfoot Ed. New England Press, NH.

TABLE 1

	ITASCA		LONG		BOG	
	1985	1986	1985	1986	1985	1986
Secchi Depth (m)	2.59	2.18	6.98	6.92	1.58	1.46
(±95% CI)	(1.94)	(1.77)	(2.80)	(2.95)	(.42)	(.39)
CV	33.6%	36.9%	18.1%	19.4%	12.1%	11.5%
k (m^{-1})	0.83	0.91	0.26	0.25	1.65	1.53
(±95% CI)	(.45)	(.57)	(.11)	(.08)	(.27)	(.12)
CV	24.2%	29.1%	19.2%	14.4%	7.3%	3.5%
Chl. *a* (mg m^{-3})	12.69	13.87	1.46	1.05	19.41	9.96
(±95% CI)	(12.66)	(16.36)	(1.05)	(2.34)	(29.65)	(9.50)
CV	45.7%	63.5%	31.5%	53.0%	68.6%	42.2%
Gilven (A_{350})	.184	-	.035	-	.952	-
(±95% CI)	(.067)	-	(.013)	-	(.066)	-
CV	16.3%	-	17.9%	-	3.2%	-

Table 1. Summary of optical parameters from the three study lakes. The following are given for each parameter: a seasonal mean value, its 95% confidence interval (±95% CI), and the coefficient of variation (CV).

TABLE 2

LAKE	$k_{(w+t)}$	k_c	k_y	n	R^2
BOG LAKE	2.97*	0.004	-1.45	9	.274
LAKE ITASCA	0.46**	0.031**	-0.02	6	.964
LONG LAKE	0.02	0.088**	3.24*	9	.720
ALL LAKES	0.28**	0.014**	1.18**	24	.937

* Significant at the 0.10 level.
** Significant at the 0.05 level.

Table 2. Results of a multiple regression of k on Chl. and A_{350} in each of the three study lakes during 1985. k_{w+t} is found from the intercept, k_c and k_y are found from the respective slopes.

TABLE 3

LAKE	k_w/k	k_t/k	k_g/k	k_p/k
BOG LAKE	10.0%	5.4%	68.1%	16.5%
LAKE ITASCA	19.8%	32.6%	26.2%	21.4%
LONG LAKE	63.5%	12.7%	15.9%	7.9%

Table 3. Proportion of light attenuated by each constituent in each lake in 1985. In each case, the partial specific attenuation coefficients are derived from the pooled data regression given in Table 2 and the mean seasonal values for Chl. and k_x given in Table 1.

FIGURE CAPTIONS

Fig. 1. Reciprocal transparency in each lake during 1985. 1/s is shown rather than s to facilitate comparison with Fig. 2.

Fig. 2. The vertical attenuation coefficient for diffuse PAR (k) during 1985. Note the reduced seasonal variation in Fig. 2 compared to Fig. 1. Both figures 1 and 2 are similar in broad outline, but there are periods of poor correlation between them, such as late summer.

Fig. 3. Spectrophotometric scan of the beam attenuation coefficient for gilven *vs* wavelength. Gilven is the dominant attenuating component at wavelengths below 550nm. Bog Lake data are from 6/24/85, Itasca data are from 6/10/85 and Long Lake data are from 6/11/85.

Fig. 4. Plot of the beam scattering coefficient due to gilven *vs* wavelength. The beam scattering coefficient is calculated from the Davies-Colley and Vant equation (1987) as outlined in the text. The same data are used as in Fig. 3.

Fig. 5. A semi-log plot of the beam absorption coefficient due to gilven *vs* wavelength in each of the three lakes. The beam absorption coefficient is calculated by subtracting Fig. 4 from Fig. 3.

Fig. 6. Seasonal trends of gilven, as measured by A_{350}, during 1985.

Fig. 7. Seasonal trends of phytoplankton abundance as measured by the concentration of Chl. *a* during 1985.

Fig. 8. Depth profiles of irradiance for eight wavelengths in each lake. The depths represent 100% (0m), 50%, 10% and 1% of surface PAR remaining in each lake.

Fig. 9. Scatter plot of k vs 1/s from data collected in all three lakes over two years. The value A is the slope of a linear regression constrained to pass through the origin. The form of the equation is k = 2.10(1/s), n=55, R^2 = .956.

Fig. 10. Scatter plot of k' vs 1/s. In each case, the wavelength with the lowest k is plotted against 1/s. Five data were not used in computing the regression. The form of the equation is k' = 1.96(1/s), n=42, R^2 = .965.

Fig. 11. Scatter plot of k vs c in Lake Itasca using data collected in both 1985 and 1986. n=18.

Fig. 12. Seasonal trends in k_{400}, k_{560}, and k_{670} in Long Lake during 1986. The curves are very flat, which indicates that there is little change in the spectral composition of downwelling light over the course of the year.

Fig. 13. Scatter plot of values of A (calculated from the slope of k vs 1/s regressions) vs 1/s. n=15.

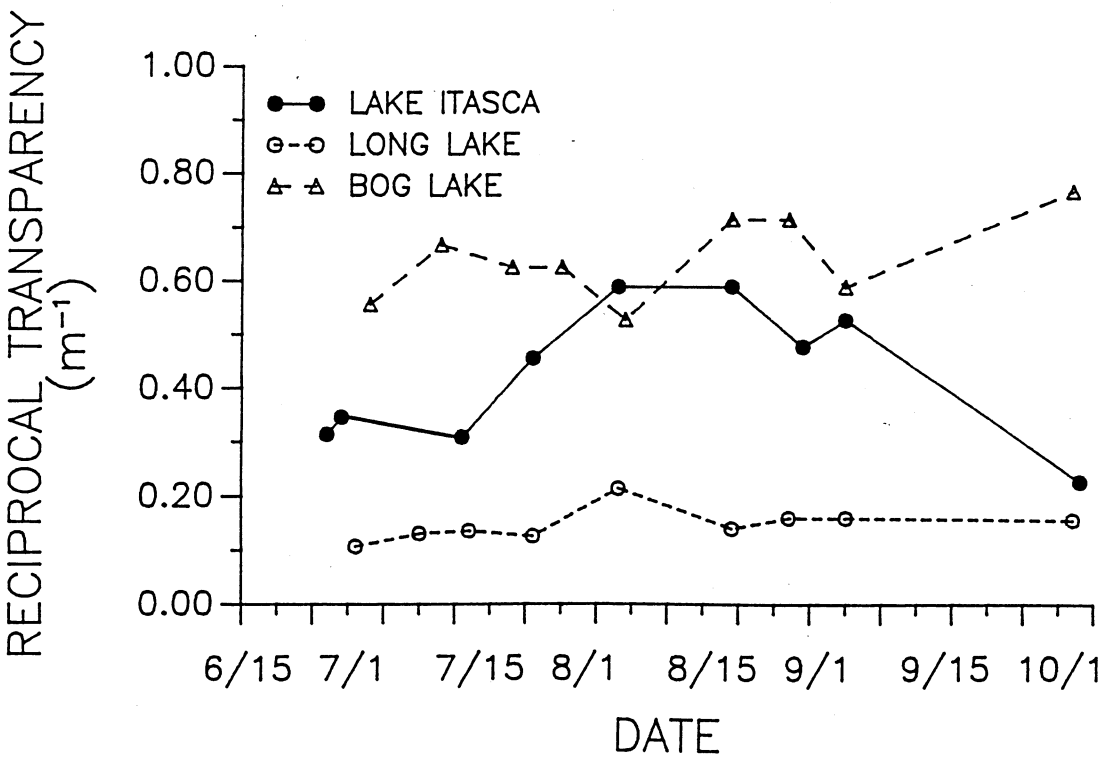
RECIPROCAL TRANSPARENCY (m⁻¹)
1.00
0.80
0.60
0.40
0.20
0.00
LAKE ITASCA
LONG LAKE
BOG LAKE
6/15
7/1
7/15
8/1
8/15
9/1
9/15
10/1
DATE

FIGURE 1

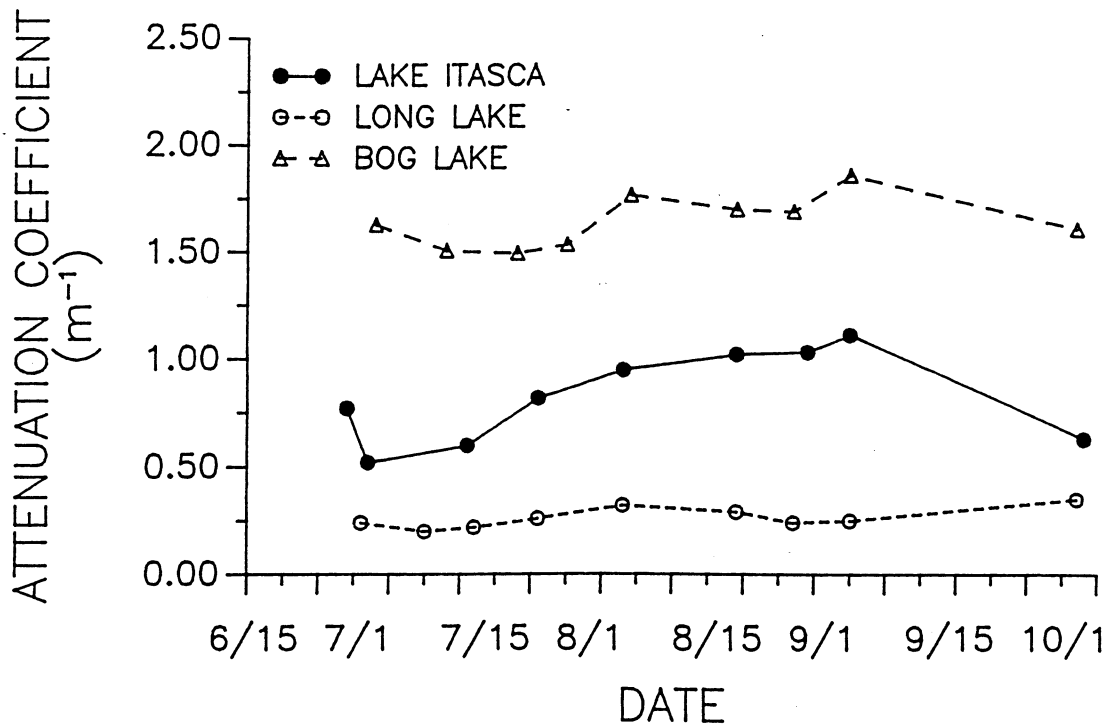
ATTENUATION COEFFICIENT
(m-1)
2.50
2.00
1.50
1.00
0.50
0.00
LAKE ITASCA
LONG LAKE
BOG LAKE
6/15
7/1
7/15
8/1
8/15
9/1
9/15
10/1
DATE

FIGURE 2

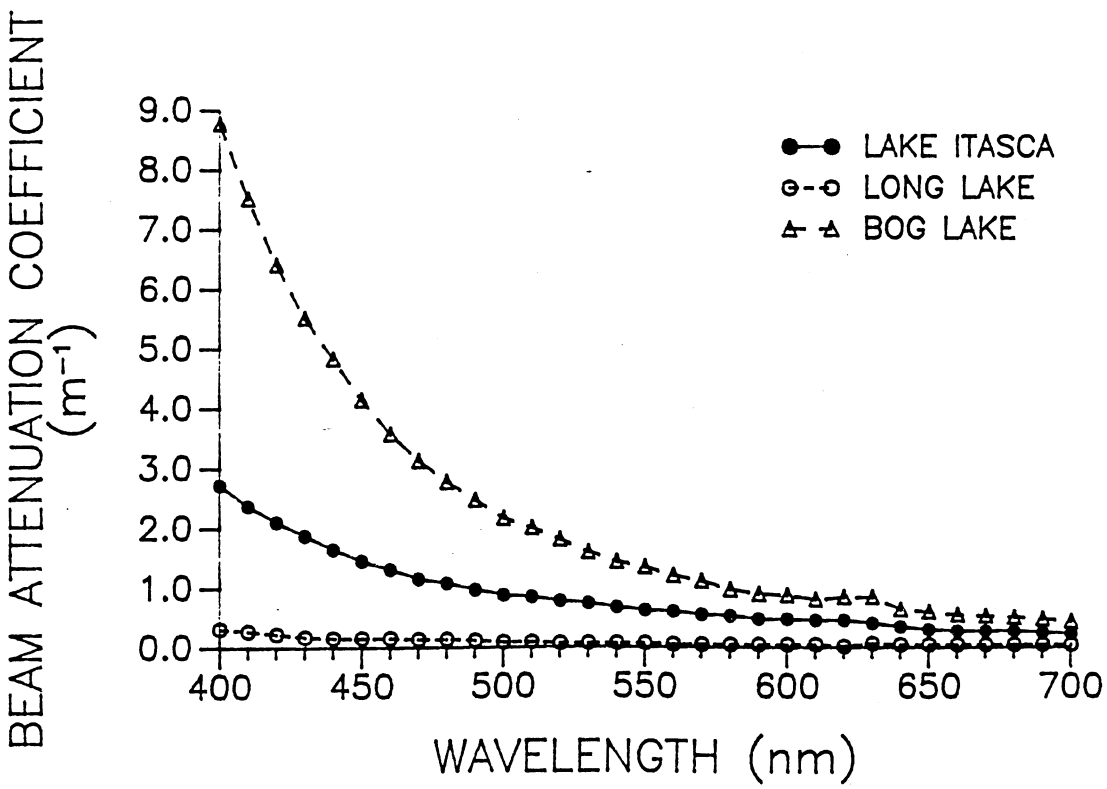
BEAM ATTENUATION COEFFICIENT (m⁻¹)
9.0
8.0
7.0
6.0
5.0
4.0
3.0
2.0
1.0
0.0
400
450
500
550
600
650
700
WAVELENGTH (nm)
LAKE ITASCA
LONG LAKE
BOG LAKE

FIGURE 3

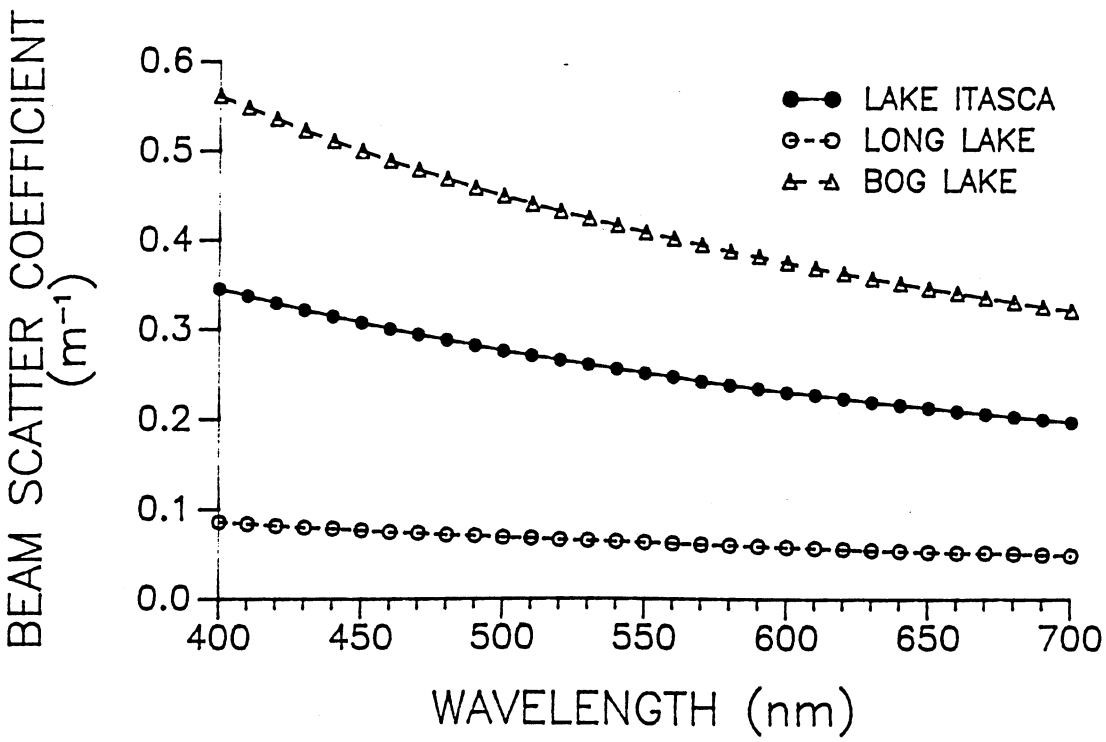
BEAM SCATTER COEFFICIENT
(m⁻¹)
0.6
0.5
0.4
0.3
0.2
0.1
0.0
400
450
500
550
600
650
700
WAVELENGTH (nm)
LAKE ITASCA
LONG LAKE
BOG LAKE

FIGURE 4

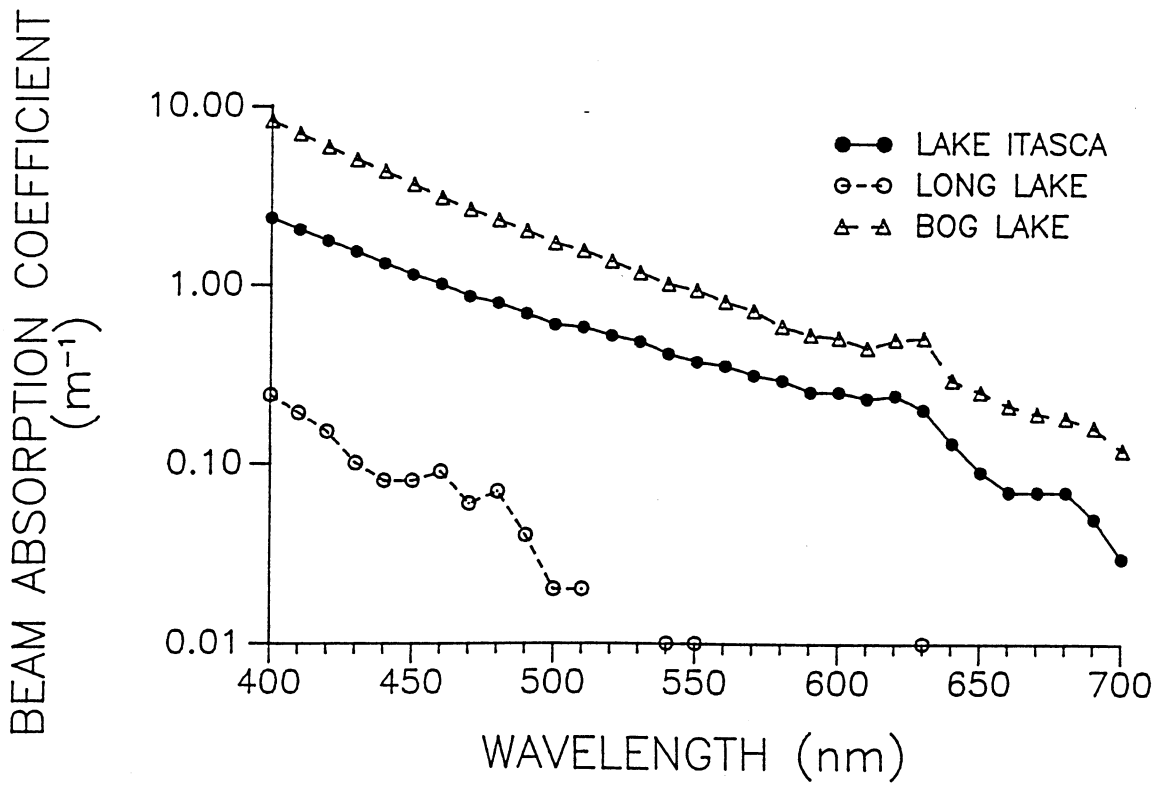
BEAM ABSORPTION COEFFICIENT
(m⁻¹)
10.00
1.00
0.10
0.01
400
450
500
550
600
650
700
WAVELENGTH (nm)
LAKE ITASCA
LONG LAKE
BOG LAKE

FIGURE 5

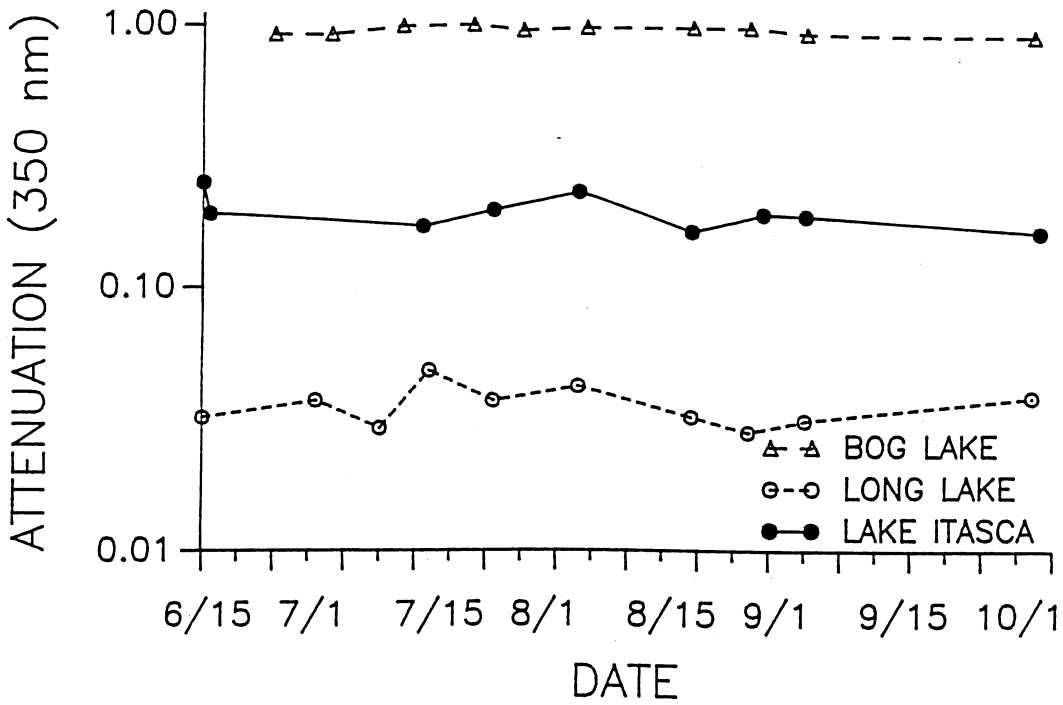
ATTENUATION (350 nm)
1.00
0.10
0.01
6/15
7/1
7/15
8/1
8/15
9/1
9/15
10/1
DATE
BOG LAKE
LONG LAKE
LAKE ITASCA

FIGURE 6

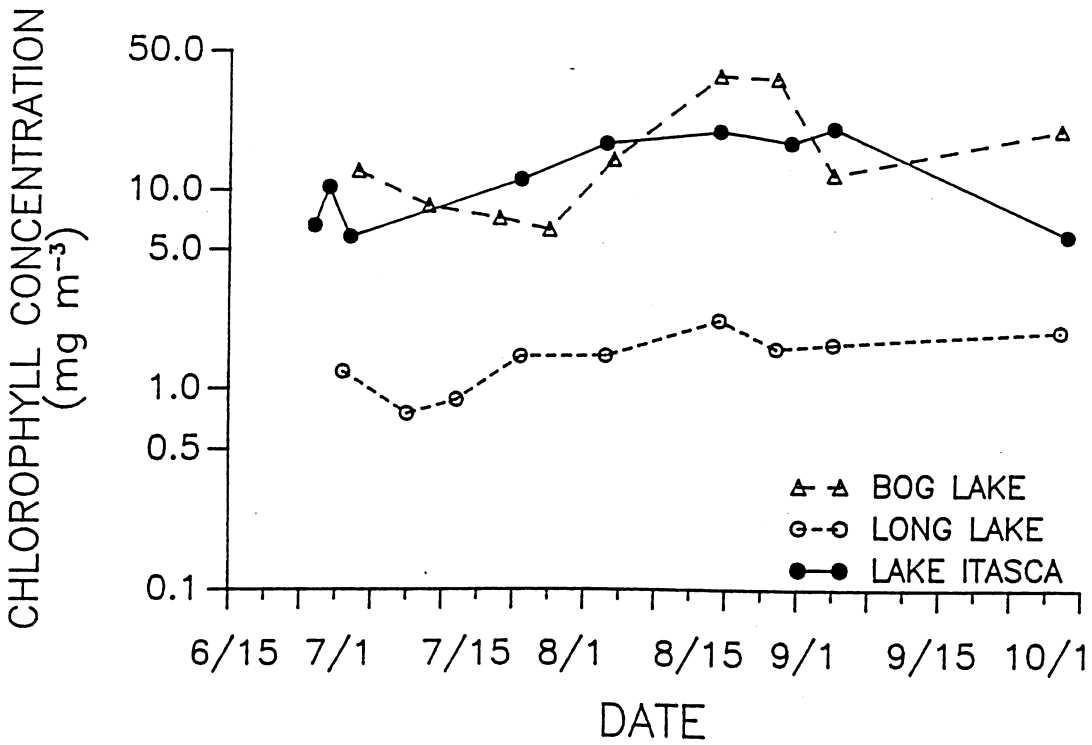
CHLOROPHYLL CONCENTRATION
(mg m-3)
50.0
10.0
5.0
1.0
0.5
0.1
6/15
7/1
7/15
8/1
8/15
9/1
9/15
10/1
DATE
BOG LAKE
LONG LAKE
LAKE ITASCA

FIGURE 7

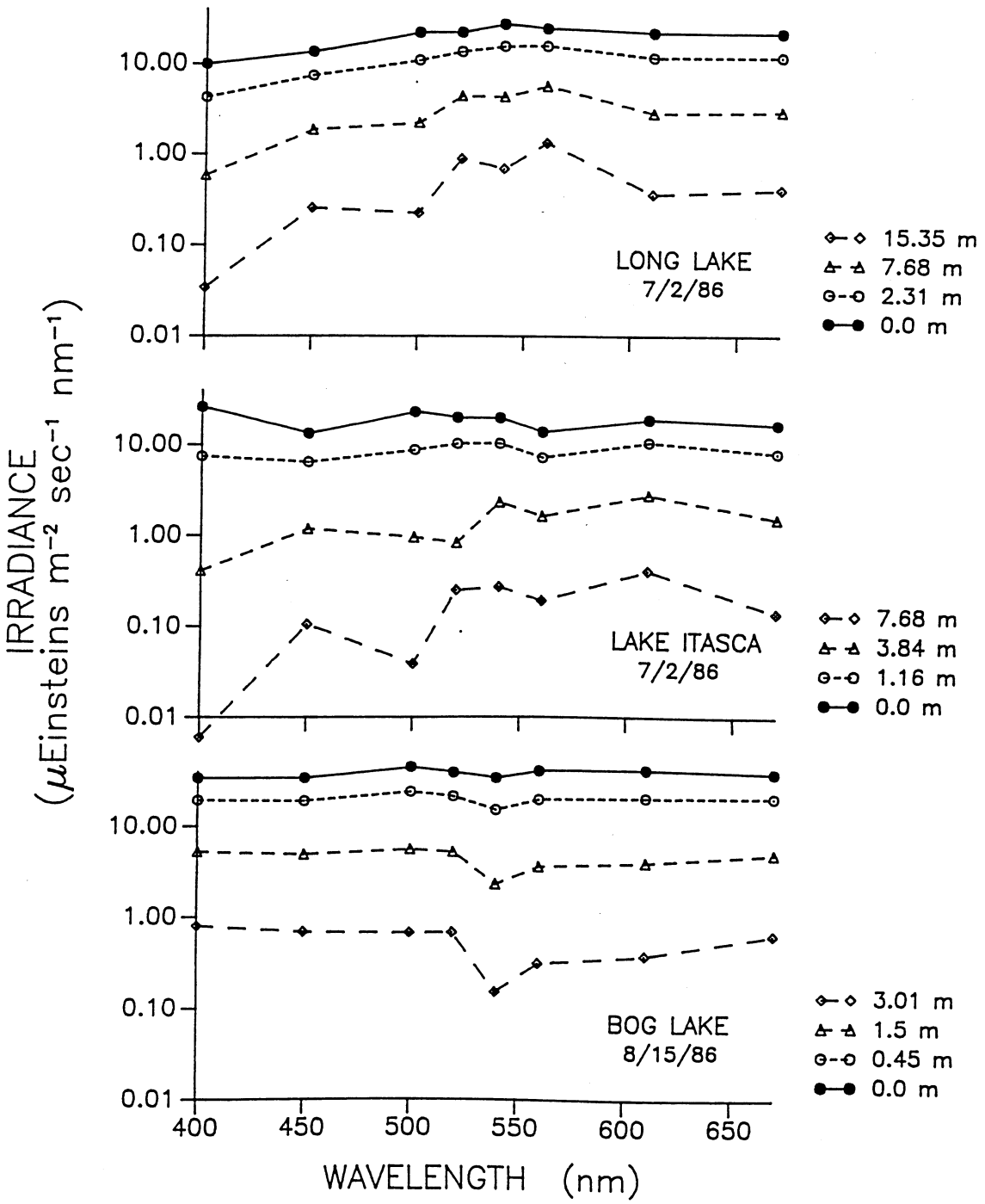
IRRADIANCE
(μEinsteins m⁻² sec⁻¹ nm⁻¹)
10.00
1.00
0.10
0.01
LONG LAKE
7/2/86
15.35 m
7.68 m
2.31 m
0.0 m
LAKE ITASCA
7/2/86
7.68 m
3.84 m
1.16 m
0.0 m
BOG LAKE
8/15/86
3.01 m
1.5 m
0.45 m
0.0 m
400
450
500
550
600
650
WAVELENGTH (nm)

FIGURE 8

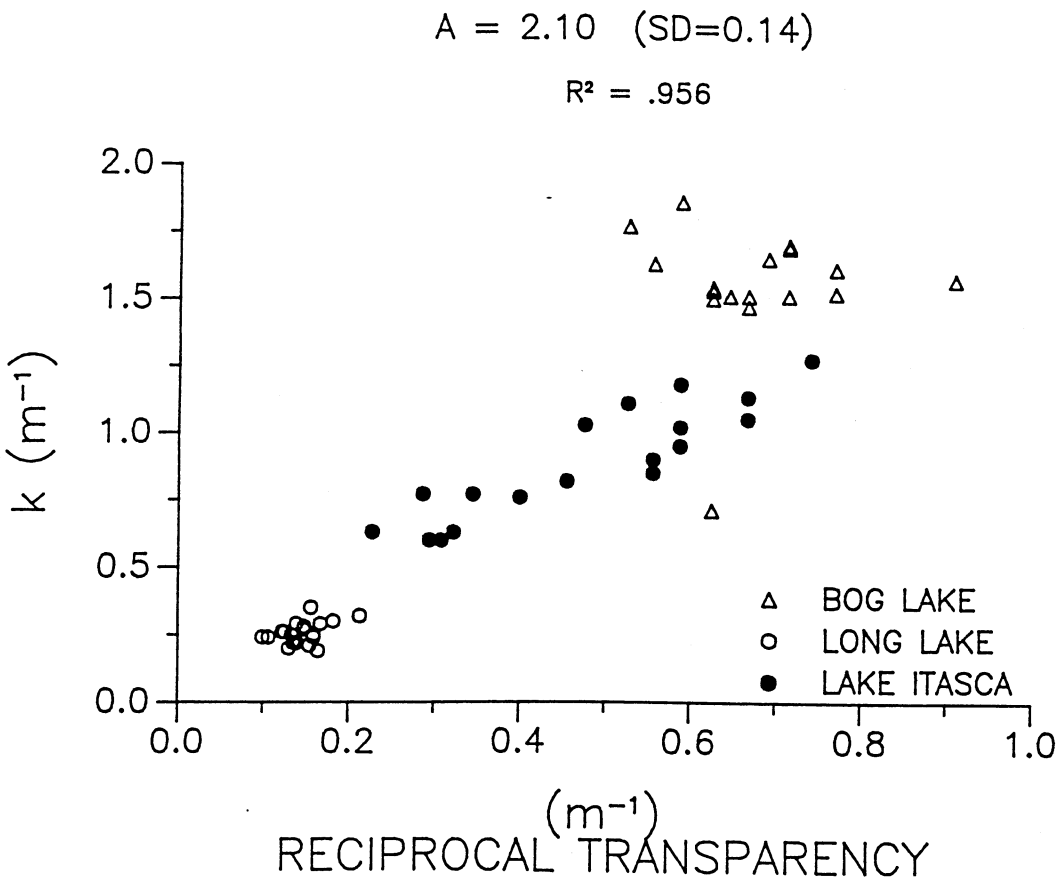
A = 2.10 (SD=0.14)
R² = .956
2.0
1.5
1.0
0.5
0.0
k (m⁻¹)
0.0
0.2
0.4
0.6
0.8
1.0
(m⁻¹)
RECIPROCAL TRANSPARENCY
BOG LAKE
LONG LAKE
LAKE ITASCA

FIGURE 9

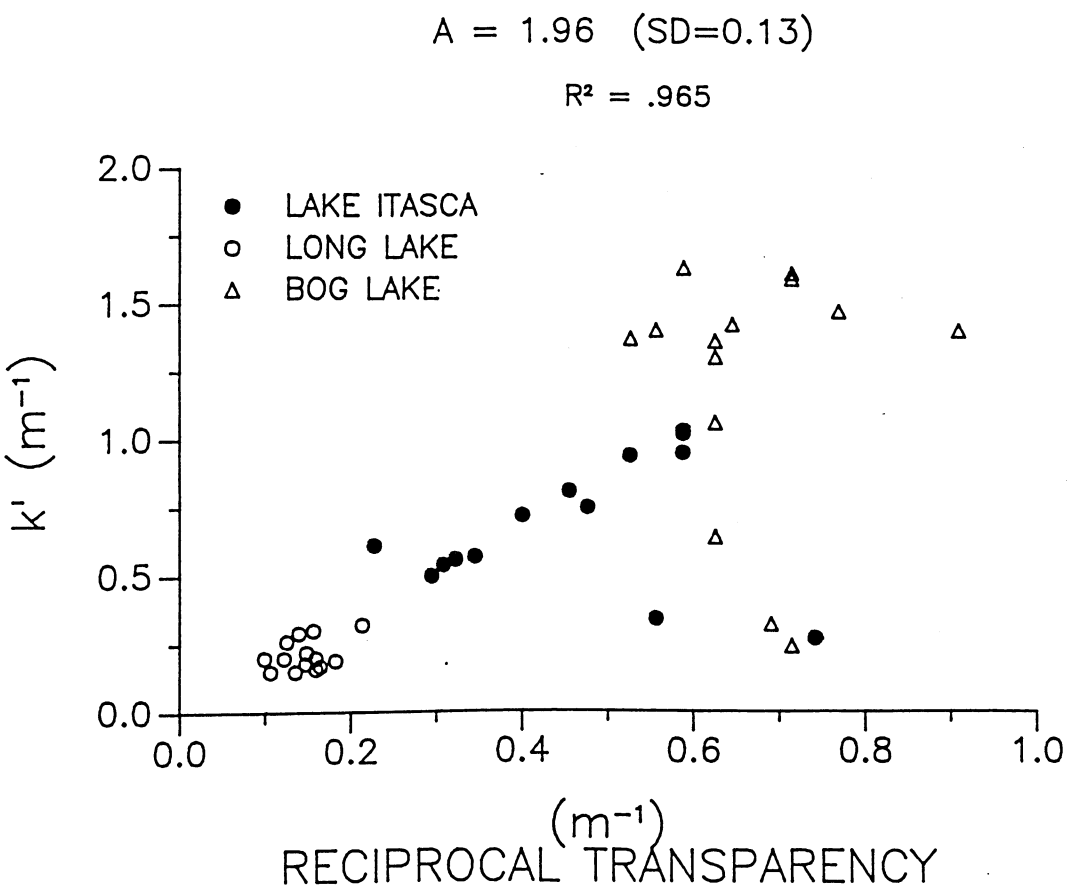
A = 1.96 (SD=0.13)
R² = .965
LAKE ITASCA
LONG LAKE
BOG LAKE
k' (m⁻¹)
2.0
1.5
1.0
0.5
0.0
0.0
0.2
0.4
0.6
0.8
1.0
(m⁻¹)
RECIPROCAL TRANSPARENCY

FIGURE 10

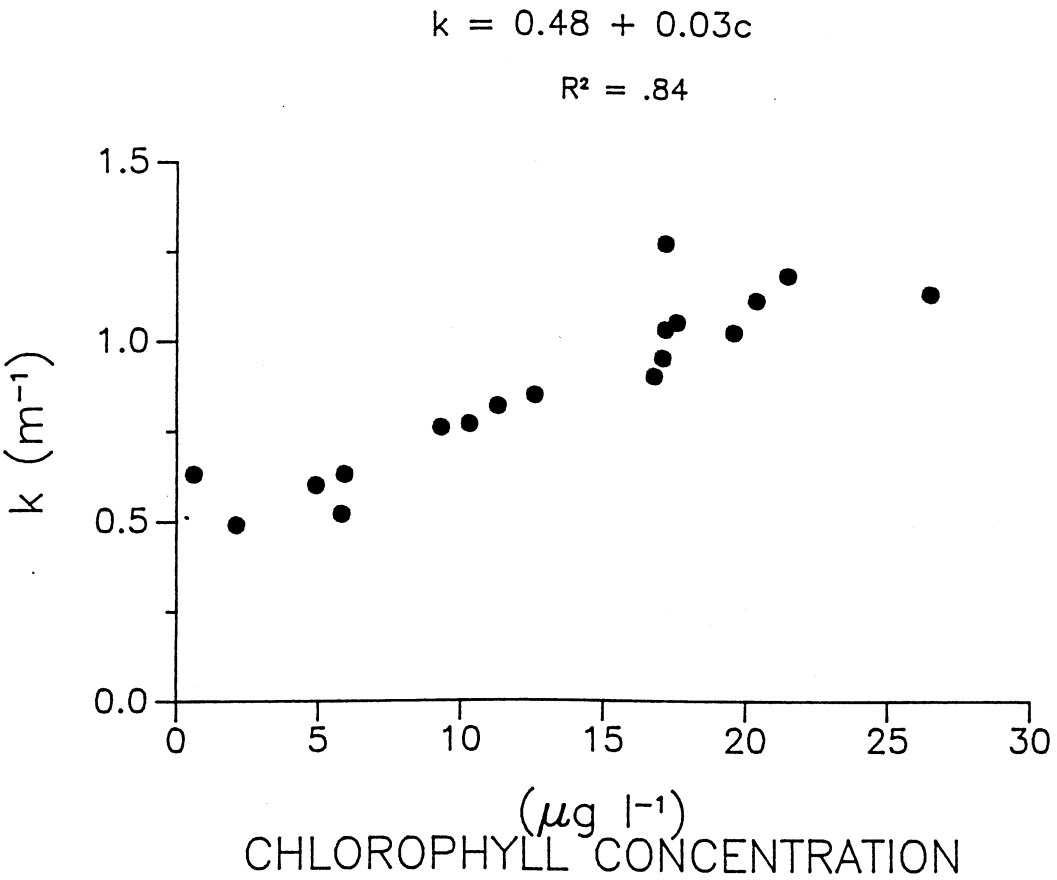
k = 0.48 + 0.03c
R² = .84
1.5
1.0
0.5
0.0
k (m⁻¹)
0
5
10
15
20
25
30
(μg l⁻¹)
CHLOROPHYLL CONCENTRATION

FIGURE 11

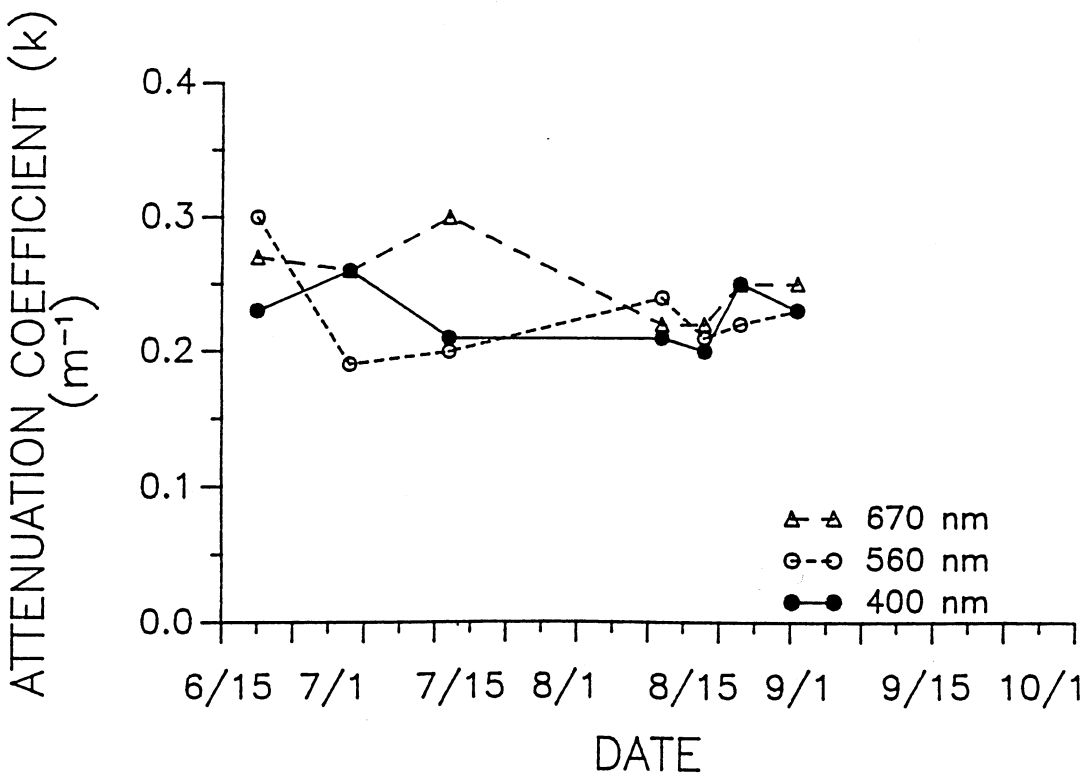
ATTENUATION COEFFICIENT (k)
(m⁻¹)
0.4
0.3
0.2
0.1
0.0
6/15
7/1
7/15
8/1
8/15
9/1
9/15
10/1
DATE
670 nm
560 nm
400 nm

FIGURE 12

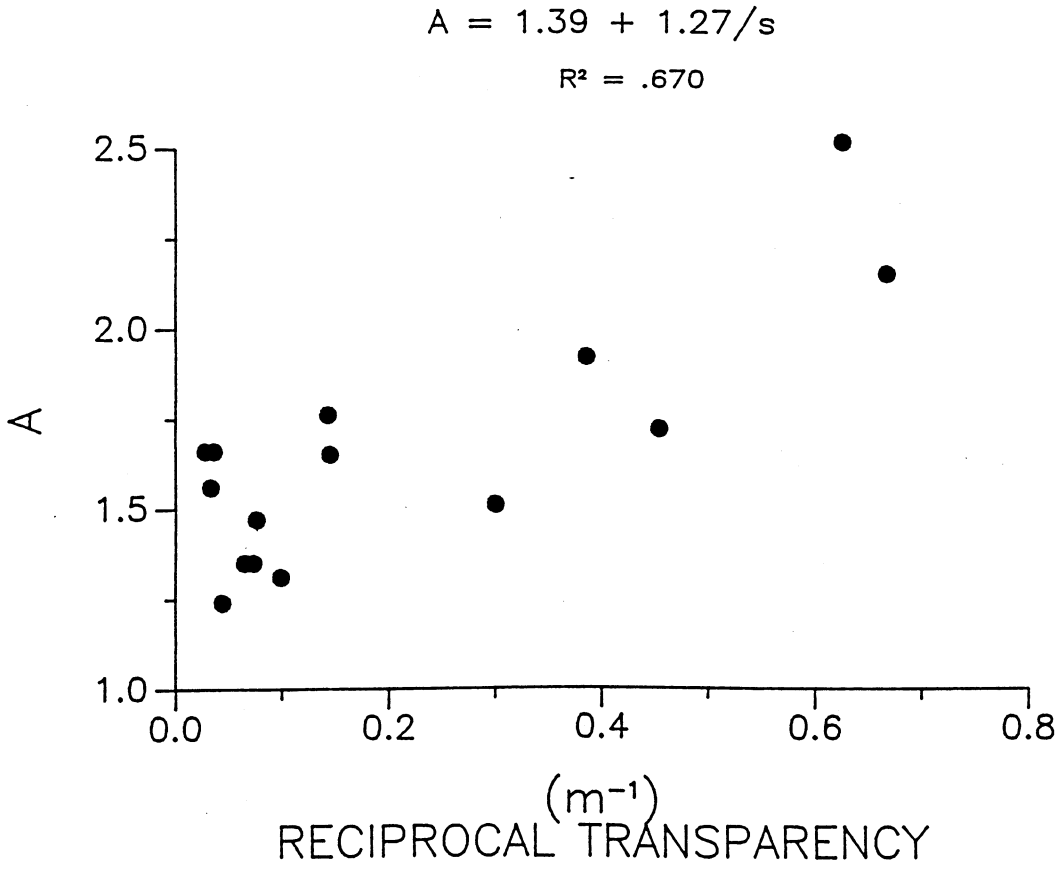
A = 1.39 + 1.27/s
R² = .670
2.5
2.0
1.5
1.0
A
0.0
0.2
0.4
0.6
0.8
(m⁻¹)
RECIPROCAL TRANSPARENCY

FIGURE 13

CHAPTER 4

THE SPATIAL AND TEMPORAL DISTRIBUTION OF ZOOPLANKTON IN LAKE ITASCA: ACTIVE PARTICIPANTS IN A DYNAMIC WORLD

Abstract

Intensive sampling is used to describe the small-scale vertical distribution and large-scale horizontal distribution of zooplankton in Lake Itasca. Patterns in the distribution and mesocosm experiments are used in an attempt to explain the ultimate cause of the observed distributions. It is shown that distribution patterns are population, not community, specific. In addition, there is a close temporal coupling between the vertical and horizontal distributions of many limnetic organisms. This suggests that the observed distributions are the result of biological interactions rather than large-scale physical factors such as, dark/light cycles and water currents.

Introduction

Heterogeneous populations: The assumption that zooplankton are randomly distributed within the epilimnion of a lake is implicit in terminology such as "plankton" (derived from the Greek planktos; to drift aimlessly) and "mixed-layer". This assumption has tremendous heuristic value in that it greatly simplifies sampling routines and permits straightforward calculations of lake-wide population estimates. Unfortunately, many zooplankton populations best fit a superdispersed Poisson, or some closely related, distribution (Ricker, 1937; Cassie, 1959; Hutchinson, 1967; Wiebe, 1970; Stavn, 1971). It is possible to randomize such a distribution by pooling a large number of samples, or by using sampling routines which integrate samples horizontally and vertically (McNaught and Hasler, 1964). These sampling methods assume that enough water volume is sampled so that the various concentrations of zooplankton are sampled in proportion to their abundance, or that the investigator has *a priori* knowledge about the distribution, and samples accordingly.

There are two conditions under which the randomized mean derived from these sampling methods is a suitable statistic of abundance. First, if aggregations of organisms dissipate more rapidly than they can be exploited. Second, if all relevant functional response curves are linear, so that predators show the same behavior regardless of the concentration of prey. Either of these conditions would undermine the ecological significance of aggregations. However, there is ample evidence that these assumptions are frequently violated, and that sampling routines that minimize the importance of heterogeneity may seriously underestimate the ecological significance of the organism's abundance. For example: fish are known to exploit zooplankton patches (McNaught and Hasler, 1961), zooplankton exploit phytoplankton patches (Mullin and Brooks, 1976) and phytoplankton may even exploit zooplankton patches (Lehman and Scavia, 1982; Alldredge and Cohen, 1987). In addition, many functional response curves are non-linear. Fish foraging on *Daphnia* are known to have either a Holling's type II or type III curve depending on the light conditions (Townsend and Risebrow, 1982).

Filtering rates by copepods are a rectilinear or hyperbolic function of phytoplankton density (Mullin et al., 1975) and may show a minimum threshold level below which no feeding occurs (Frost, 1975). Finally, the functional response of Chaoborus predation on nauplii is linear, but curvilinear for all other groups of zooplankton (Fedorenko, 1975b).

These results provide strong support for the contention that the heterogeneity of zooplankton is ecologically significant at the level of individuals. Steele (1974) has suggested that this heterogeneity is important at higher levels of organization as well, and may contribute to community stability. Thus, in many cases it may be inappropriate to use the randomized mean as a measure of "ecological" abundance, and some other statistic, such as the maximum (McNaught, 1978) or the median (Wiebe, 1970) may be appropriate. In any case, a knowledge of the spatial and temporal distribution of zooplankton is fundamental to the understanding of their general ecology.

Two types of non-random distributions are possible. Superdispersed populations are characterized by "patches" of zooplankton which inhabit a discrete volume of water, persist for a discrete time interval and which differ from contiguous regions by the concentration or organisms within the patch (Wiebe, 1970). Zooplankton swarms are an extreme example of superdispersion, and have been described from a variety of organisms. Mysids form shoals of up to 20m in diameter with concentrations of 0.5/liter (Clutter, 1969). Krill have been detected with acoustic equipment at concentrations as high as 1/liter (Greene et al., 1988). Copepods form swarms with concentrations from 500 to 1,500/liter (Hamner and Carleton, 1979; Emery, 1968), and cladocera have been observed in swarms with concentrations of 1,000/liter (Colebrook, 1960). Very little is known about how swarms form or what role they play, but Hamner and Carleton (1979) suggest that they are common enough to question most estimates of copepod abundance and they challenge the established notion (of Odum and Odum, 1955) that copepods are insignificant to the energy dynamics of reef systems. Swarms are typically composed of a single species, and frequently contain only a single size class of individuals.

Infradispersion is a second type of non-random distribution in which the organisms are more evenly spaced than one would expect by chance. These populations show a regular spatial pattern amongst individuals. Infradispersion has only rarely been observed in zooplankton populations, and is usually attributed to chance (Hutchinson, 1967).

Observed distributions of plankton populations have been attributed to both physical and biological forces. The two forces are thought to operate at different scales and along different space and time dimensions. For example, George and Edwards (1973) suggest that the horizontal patchiness of Daphnia is due to concentration in Langmuir cells, whereas the vertical distribution is due to vertical migration (Cushing, 1951). Medium sized patches of phytoplankton (50m to 3km) are thought to be generated by physical processes, but larger patches are attributed to differential reproductive success (Platt & Denman, 1974). It is important to stress that the type of distribution one observes is strongly dependent on the sampling regimen, and any conclusion that an investigator draws is restricted to the time and space scale appropriate to that particular regimen.

Vertical distribution: The vertical distribution of zooplankton has been extensively studied. The primary focus of previous studies has been diel vertical migration, and there is now an enormous literature that: 1) describes vertical migration from a wide variety of organisms (reviewed by Cushing, 1951 and Hutchinson, 1967), 2) explains the proximate stimuli which motivate and direct the migrations (Ringelberg, 1964; McNaught & Hasler, 1964; Enright & Hamner, 1967; Larow, 1968) and 3) which address the adaptive significance, or ultimate cause, of vertical migration (e.g. McLaren, 1963; Zaret & Suffern, 1976; Wright et al.,1980).

A common observation of many studies is that in a population of migrating organisms there is variation in individual behavior. This variation may be in the amplitude, phase or even the presence of migratory behavior (Weider, 1984; McNaught, 1966). This variation has been variously attributed to: age or size (Huntley & Brooks, 1982), sex (Hutchinson, 1967, Magnien & Gilbert, 1983), morph type (Brooks, 1965),

genotype (Weider, 1984) and ecological strategy (Stitch & Lambert, 1981). Of the organisms that do not migrate, but that remain in the epilimnion throughout the day, little is known of their small-scale vertical distribution. Their abundance and distribution are important, however, because it is these organisms that are subject to the putative adverse affects of high light intensity (Hairston, 1980), increased visual predation (Zaret & Suffern, 1976, Wright et al., 1980) and loss to the littoral region via longitudinal currents (Siebeck, 1964) that migrating organisms are thought to be avoiding.

Horizontal distribution: Sampling from longitudinal transects across a lake routinely show that the sublittoral margins are often depauperate of zooplankton that are contemporaneously abundant in the pelagial water. This is true even if the sublittoral zone is not mechanically isolated from the circulating epilimnion. This distribution pattern has been observed in rotifers (Preissler, 1977a, 1977b), copepods and cladocera (Siebeck, 1968) and even in jellyfish (Scyphomedusae) (Hamner and Hauri, 1981). A second type of horizontal distribution is shown by several species of cladocera which inhabit both the sublittoral and the pelagic zones. These species are dimorphic with each morph restricted to only one of the two habitats (Green, 1967; Kerfoot, 1975). A third distribution is described in Lake Lanao by Lewis (1979) in which some pelagic species (mostly herbivores) show an increase from mid-lake toward the shore to the 25m depth contour, and others (mostly invertebrate predators) show a decrease along the same transect.

Three different mechanisms have been invoked to explain the stability of these horizontal distributions. Colebrook (1960) suggested that wind driven epilimnetic currents, an internal seiche, and the vertical migration of zooplankton could interact to concentrate zooplankton on the windward side of a lake, leaving the lee shore relatively depauperate of zooplankton. This complex mechanism depends on the confluence of three independent events that must be in proper phase with respect to each other. This hypothesis predicts that on a calm day there should be no net horizontal transport of zooplankton, and on a windy day the

zooplankton should be removed from the lee side of the lake to the windward side. This displacement should be most pronounced at night when most zooplankton are in the epilimnion, and the distribution should remain stable until the currents change.

Siebeck, (1964, 1968, 1969, 1980) has suggested that limnetic zooplankton actively avoid the shore (uferflucht). He proposes that radiance distributions of sublittoral regions are distinct from those of pelagic regions. The distinctive radiance distribution of the littoral region enables zooplankton to determine their proximity to shore, orient with respect to the shore and then stimulates them to swim away from it. The operative component of the radiance distribution is thought to be a shadow imposed on the radiance distribution by the shore's horizon. Zooplankton are thought to detect the shadow as a deviation from the symmetrical radiance distribution of pelagic regions, orient in a positively phototactic manner and swim away from the shadow and hence avoid the shore. Once in the pelagic zone, the zooplankton are exposed to a symmetric radiance distribution, become negatively phototactic, and then migrate downward.

Siebeck's model (1968, 1980) predicts that zooplankton should be randomly distributed within the epilimnion at night (particularly if it is windy), but at dawn limnetic zooplankton on both shores should leave the lake margins and move back towards the center of the lake. Additionally, the radiance distribution must provide a reliable beacon both for the location and orientation of zooplankton.

Kerfoot (1975) and Green (1967) suggest that fish predation on zooplankton is more intense in the sublittoral than in pelagic regions. They propose that fish consume most of the larger invertebrates in the sublittoral and that the morphs of cladocera which persist there are adapted to heavy visual predation. Visual predation by fish is less intense off-shore, but is replaced by more intense invertebrate predation, and so cladocera are subjected to a different form of selection there. Lewis (1979) invokes a similar scenario which involves the cascading effects of visual predation to explain the complex distribution of zooplankton in Lake Lanao. In both cases, it is habitat-

dependent predation pressure that determines the distribution of species and morphs. Both models predict that limnetic zooplankton will invade the littoral on wind driven currents, but will be removed during daylight by visual predators.

It is the purpose of this study to describe in detail the horizontal and vertical distribution of epilimnetic organisms in Lake Itasca. The sampling and experiments were designed to test the predictions of the three principal hypotheses which have been proposed to explain the large scale horizontal distribution of zooplankton, and to explore any linkage between the vertical and horizontal distributions of epilimnetic zooplankton.

METHODS

Light: Irradiance was measured with a Li-Cor 185 quantum meter (Lambda Instruments) and a submersible cosine collector that responds only to wavelengths between 400 and 700 nm. Measurements were made on the sunny side of the boat at 0.5m depth increments. Radiance distribution measurements were made following the procedure described in Chapter 2. Radiance measurements made in the sublittoral (within a few meters of the shore or emergent macrophyte bed) are compared to contemporaneous radiance distributions measured in the middle of the lake.

Vertical distribution of zooplankton: Three buoys were anchored in a linear transect across the north arm of Lake Itasca. One was at the edge of the emergent vegetation on the east shore in 2.0m of water, one at the deep point of the north basin in 10m of water, and one at the edge of the emergent vegetation on the west shore in 2.0m of water. Because of the morphometry of the lake basin, the mid-lake station was only 150m from the west station and about 450m from the east station. On 9/3/86, zooplankton were collected at 1.25, 2.0, 3.0, 4.0 and 5.0m at the mid-lake station. Five meters is at the bottom of the epilimnion. Three replicate samples were collected at each depth from different positions in the boat with a 27 liter Schindler trap (Schindler, 1969) to minimize

small scale horizontal variation. The samples were combined and preserved in methanol and a sucrose/formalin solution (Haney and Hall, 1973). In the lab, subsamples were obtained with a Henson-Stemple pipette and the animals were counted under a dissecting microscope in a zooplankton wheel (Wildco). Between 100 and 500 organisms were counted in each sample.

Horizontal distribution of zooplankton: On two dates (8/27/86 and 9/3/86) the zooplankton were sampled at each station at a depth of 1.25m (mid-depth of a 45-cm high trap) every two hours over a 24 hour period. Sampling began at 20:00 hours on 8/27 and at 21:00 hours on 9/3. The stations were always sampled in the order: east, mid, west; and about 45 minutes were required for the sampling process. Wind speed and direction were measured with a hand-held vane type meter. Wind speed and meteorological conditions were recorded at the mid-lake buoy every sampling period. The zooplankton sampling and sample processing procedures were the same as described above.

Mesocosms: Twelve experimental mesocosms were constructed that were 1.0m in diameter and 1.5m deep (volume = $1.2m^3$). The bags were closed at the bottom. The top opening was covered with 0.5mm nitex mesh that was attached by strips of velcro to the bags to permit daily access for sampling. The bags were anchored just inside the margin of the emergent vegetation (mostly Zizania aquatica) along the east shore of the north arm of Lake Itasca. Winds in this area are predominately from the west. The tops of the bags were submerged just beneath the surface of the lake to permit colonization of the bags by zooplankton.

Each bag was randomly assigned to one of four groups. All bags received an initial aliquot of limnetic zooplankton captured by net during the day in the epilimnion of Lake Itasca. Only these zooplankton were added to the bags in group one. Approximately 1kg of rinsed macrophyte (Ceratophyllum sp.). A bluegill sunfish (Lepomis machrochirus) of about 10-cm standard length (a stocking rate of $21.8gm/m^3$). Both macrophytes and fish were added to group four.

Experiments were run twice; once for six days and once for seven days. Each bag was sampled daily for chlorophyll and zooplankton concentration. To sample, the bags were pulled to the surface, the top opened and the bag was stirred with a canoe paddle. Algae were collected by inverting a 1 liter bottle at about 0.5m depth and the concentration of chlorophyll was measured using the procedure of Holm-Hansen and Reimann (1978). Zooplankton were sampled by making two vertical hauls within the bag with a net from the bottom to the top. This sampling removed about 8% of the zooplankton daily. Zooplankton were preserved and counted as above.

RESULTS

Lake Itasca: Lake Itasca lies at 47° 14' N, 95° 10' W in northwestern Minnesota. The north basin of the lake has a surface area of 117 ha, a maximum depth of 11m and a mean depth of 5.0m (Megard, 1968). The west station (Fig. 1) lies at the base of Hill Point (8m elevation). The littoral margin is very narrow (10m), and the bottom slope is quite steep. The mid-lake station is at the maximum depth of the transect (8m) about 150m from the west station. The east station is just south of the biological station and there is a very shallow bottom slope and a 75m wide littoral zone between the east sampling station and the shore. There is no significant elevation on the east shore other than trees.

Figure 2a is a plot of temperature and irradiance vs depth at 14:30 on 9/3/86. The epilimnion extends from the surface to 5m, and is thermally isolated from the deeper water. The attenuation coefficient for downwelling irradiance is $1.05m^{-1}$, and 99.5% of the surface irradiance is attenuated within the epilimnion.

Figure 2b is a plot of wind speed vs time on the two dates on which horizontal sampling was conducted. 8/27 was a relatively calm day, with moderate winds only in the afternoon. 9/3 was a very windy day with modest winds in the morning which built into very strong winds in the early afternoon.

Vertical migration: Twelve groups of zooplankton were sufficiently abundant in the epilimnion to enumerate. These included six cladocera (Daphnia galeata, D. retrocurva, Chydorus sphaericus, Diaphanosoma leuchtenbergianum, Ceriodaphnia reticulata, and Leptodora kindti), one calanoid copepod (Diaptomus pallidus), one cyclopoid copepod (Cyclops bicuspidatus thomasi), one rotifer (Asplanchna sp.), one free swimming ostracod, and one larval insect (Chaoborus americanus).

Figures 3a-d show the average concentration of each species in the epilimnion over the course of the 24 hour period on 9/3/86. Changes in the epilimnetic average are most likely due to vertical migration of the organisms across the metalimnion. Given this assumption, five different migration strategies are employed by the zooplankton in Lake Itasca:

1) Nocturnal Ascent (NA): Four species demonstrate a classical vertical migration. Ostracods (3d) and Leptodora (3c) are the only species which show all of Cushing's (1951) four-phase scheme (evening ascent, midnight sinking, dawn rise, and descent to day-depth). They enter the epilimnion just after sunset and swim almost to the surface, as indicated by temporal changes of the mean depth of the population (Figures 4d and 4c). Both their numbers and their mean depth gradually decline over the course of the night, but in the early morning there is a resurgence of both concentration and mean depth until about sunrise, and then there is a final decline, and they leave the epilimnion by 10:00.

Chaoborus larvae enter the epilimnion about two hours later than ostracods, and swim up slowly until they reach a mean depth of 3m (Figs. 3d and 4d). After reaching their peak abundance a few hours after sunset, Chaoborus leave the epilimnion at a constant rate throughout the night. There is no indication of either a midnight sinking or of a dawn rise phase because their mean depth does not change at the appropriate times. This is consistent with patterns observed in other Chaoborus populations (Swift, 1976).

Daphnia retrocurva shows a third variation on the classical migratory pattern. Their numbers in the epilimnion (3b) increase gradually from 13:00 until midnight and then decrease gradually until 13:00 again. The

unique aspects of their migration are that the cycle is continuous and that some of the Daphnia never leave the epilimnion. The percentage of the population that participates in the migration can be calculated from the expression (peak - background)/peak, in which peak and background are the maximum and minimum epilimnetic mean concentrations respectively. 70% of the D.retrocurva take part in the migration.

In general, NA species are characterized by at least one peak abundance in the epilimnion between 21:00 and 5:00 hours, a high participation (in three out of four species, 100% of the population migrates), and fairly long migratory durations (the time during which the epilimnetic concentration is equal to or greater than the average of the maximum and the minimum concentrations). This information is summarized in Table 1.

2) Evening Ascent (EA): Five groups show some variation on the strategy of being most abundant in the epilimnion in the late afternoon or early evening. All of the copepods (Fig. 3a) show a behavior in which their abundance gradually increases from sunrise until a few hours before sunset, and then gradually decreases to their minimum values by midnight. 63% of the calanoids, 76% of the nauplii, and only 36% of the cyclopoids participate in the migration.

Diaphanosoma is never very abundant in the epilimnion, but it does increase about three-fold around sunset (Fig. 3c). They do not penetrate very far into the epilimnion, as their mean depth at the time of their maximum abundance is about 4m, compared to a high value of 1.5m at 9:00 (Fig. 4d).

The most dramatic EA is seen in Chydorus (Fig. 3b). Background epilimnetic concentrations are very constant at about 8 org./liter, but at 14:00 there is an influx of organisms that increases the epilimnetic population to 40 org./liter. This migration has a very short duration (240 min.), and the migrating organisms leave the epilimnion by sunset.

In general, evening ascent migrations are characterized by a peak abundance between 15:00 and 19:00, and less strong participation in the migration than NA populations. The two species with the highest participation (Chydorus and Diaphanosoma) also have very short durations, whereas the other groups have durations similar in length to NA species.

3) Morning Ascent (MA): Only Ceriodaphnia (Fig. 3c) is maximally abundant in the early morning. It has a broad peak from 5:00 to 9:00, and is present at very low concentrations during the rest of the day. A high percentage of the population is migratory, and the duration of the migration is comparable to the NA species.

4) Diurnal Ascent (DA): This pattern is commonly known as a "reverse" migration and is most common amongst the rotifers (Dumont, 1972). Only Asplanchna (Fig. 3d) showed this pattern in Lake Itasca. The rotifers are most abundant in the epilimnion between 9:00 and 15:00, but only 47% of the population participates in the migration. Thus, there is a fairly high concentration of Asplanchna in the epilimnion at all times.

5) No Migration (NM): Only Daphnia galeata (Fig. 3b) showed no strong migration, but they do have a very slight tendency to be more abundant in the morning and the evening. On 8/27/86 sampling at 1.25m strongly suggests that D. galeata exhibits a MA vertical migration pattern, similar to Ceriodaphnia. In general, however, D. galeata are present in the epilimnion in more or less equal numbers throughout the day.

Vertical distribution: Figures 5 to 8 are contour plots of zooplankton concentrations that summarize their diel vertical distribution in the epilimnion. One common statistic that is used to express the vertical distribution of zooplankton at any given time is their mean depth (Figs. 4a-4d). Except for ostracods, Leptodora and Diaphanosoma, however, there are no significant variations in mean depth in the epilimnion over the course of the day. Most of the organisms studied show a mean depth of about 3m (mean depth of the sampling interval). September 3, 1986 was a very windy day (Fig. 2b), and turbulent mixing was likely a significant factor in the organisms' vertical distribution. However, in several

cases, there are strong vertical concentration gradients between one and five meters. The appropriate statistic to estimate the departure from a random Poisson distribution is the coefficient of dispersion (CD = Variance/Mean) (Sokal & Rohlf, 1981). A value of CD greater than 1 indicates superdispersion, and a value of CD less than one indicates infradispersion. Six organisms show a tendency towards superdispersion at some time, but only three of these are significant at the 0.05 level (Chi Square test for a significant departure from a CD of 1.0). These are cyclopoid copepods (Fig. 9a) at 17:00, Chydorus (Fig. 9b) at 17:00 and Ceriodaphnia (Fig. 9c) at 19:00. Cyclopoids are concentrated at the surface, and Chydorus has aggregations at 1m and 3m. Ceriodaphnia is so rare at 19:00 that this may be an artifact of its rarity. The CD for D. retrocurva (Fig. 9b) at 15:00 and for calanoid copepods (Fig. 9a) are significant at the 0.10 level, and are attributable to a high concentration above 2m and a concentration above 3m, respectively.

All of the remaining organisms show no significant tendency towards clustering, and there is some indication that there is vertical infradispersion for most of them during most of the day.

Horizontal distribution: Twelve of the zooplankton were sufficiently abundant to enumerate in the horizontal transects. They are the same organisms that were studied in the vertical studies with the exception of ostracods, which are omitted because they appear sporadically in the 1.25m samples. Bosmina longirostris was included in the study because it is consistently found in the sublittoral samples.

Figures 10 to 21 present the data on horizontal distribution of zooplankton in Lake Itasca on a calm day (8/27/86) and a very windy day (9/3/86) (see Fig. 2). The distribution of microorganisms is clearly non-uniform. Six species are more abundant in the middle of the lake, two species are more abundant in the sublittoral regions, and four species are more or less evenly distributed across the epilimnion. One index of this distribution is the ratio calculated by dividing the population size on the east shore by the population size at mid-lake at each time period. Mean ratios of less than 0.5 are considered to indicate a

limnetic distribution. Large ratios indicate a sublittoral distribution, and ratios around one indicate and indiscriminate distribution. These results are summarized in Table 2. In only a few instances are there any major discrepancies between the windy and the calm days, which suggests that wind-driven currents are less important than biological factors in determining the horizontal distribution. In general, the horizontal distributions that are seen are much more complex than a simple partitioning between limnetic and sublittoral populations.

limnetic organisms: Calanoid copepods (Fig. 10) are abundant at the west shore and the mid-lake stations, and are much less abundant at the east shore. Although the overall abundances on the west shore and mid-lake are comparable, they do not show the same temporal distribution pattern. On the west shore, their numbers decrease from the early morning through the late morning and then increase from noon until past sunset. This contrasts with the mid-lake population which slowly increases from early morning until about sunset. There are no obvious population trends on the east shore.

D. galeata (Fig. 11) is most abundant in mid-lake, but there are two prominent peaks in the shore regions: one on 8/27 on the west shore at 10:00 which is about the same concentration as mid-lake populations, and one at 17:00 on 9/3 on the east shore which is about 15-times mid-lake populations. This extreme concentration suggests that this is a swarm, and not just an infusion of mid-lake water. Again, there is a contemporaneous decline during the morning on the west bank and an increase at the mid-lake station.

D. retrocurva (Fig. 12) shows a very similar pattern to calanoid copepods in that they are much more abundant in mid-lake and the west shore than on the east shore. They also show the inverse temporal pattern described above, in that they have a progressive decline during the morning on the west shore with a contemporaneous increase (at least on 8/27) in mid-lake. There are large peaks at 17:00 on 9/3 on the east shore and at 16:00 on 8/27 on the west shore that dissipate before the subsequent sampling period. Both of these peaks are about the concentration that is present at mid-lake at the same time.

Chaoborus (Fig. 13) has a straightforward distribution. Only one specimen in one sample was observed on the east shore. Otherwise, it is present on the west shore and at slightly higher concentrations in the mid-lake throughout the night. It is absent from all locations during the day.

Cyclopoid copepods (Fig. 14) are found throughout Lake Itasca, but the mean numbers are about 50% lower on the east shore than at the other two sampling locations. This is particularly noticeable in the evening when the mid-lake and west shore populations are augmented by migratory individuals, which do not appear to penetrate to the east shore. The one exception to this is the 7:00 sample on 9/3/86 which is three times as great as any other sample from the east shore on that date, but which is the same concentration present in the mid-lake 7:00 sample.

Chydorus (Fig. 15) shows a similar pattern to the above species, but there is a significant population at all times on the east shore. Chydorus on both the east and west shore tend to decrease during the early morning, while the mid-lake population is increasing. The late afternoon influx of Chydorus during vertical migration is seen on the west shore and, to a lesser extent, on the east shore.

Sublittoral organisms: Bosmina (Fig. 16) is rarely observed at the mid-lake station and is most abundant on the two shores. It is most abundant at 15:00 on 9/3 on the east shore, which corresponds to the time of maximum winds (23mph average with gusts to 38mph). There is a strong correlation between wind speed and Bosmina concentration (Pearson correlation coefficient of .74), which suggests that strong turbulence suspended an otherwise benthic or epiphytic population. Bosmina shows some sign of an NA vertical migration on 8/27/86.

Leptodora (Fig. 17) is much more predominant on the two shores than it is in mid-lake, and in both shore locations it shows evidence of a NA vertical migration pattern. In the mid-lake region, Leptodora is most abundant at dawn and dusk.

Indiscriminate organisms: Nauplii (Fig. 18) are found throughout the lake, but the greatest numbers are found on the east shore. On 8/27, the east shore population shows a very systematic increase to a peak at

16:00, which is very similar to the vertical migration described in the mid-lake region on 9/3 (Fig. 3a). The pattern is apparently suppressed on 9/3 on the east shore.

Diaphanosoma (Fig. 19) is more or less evenly distributed across the lake, but shows several interesting behaviors. First, it is generally more abundant on 8/27 than it is on 9/3. Both shore populations undergo a systematic increase on 8/27, but it occurs six hours later on the west shore than on the east shore, while the mid-lake population shows a slight increase at both times. It is as if half of the mid-lake population behaved like the east shore population and the other half displays a west shore behavior.

Asplanchna (Fig. 20) is found throughout the lake, but the west shore population exhibits a systematic increase in the evening that is seen only weakly in the mid-lake area on 8/27 and not at all on the east shore. This suggests an EA vertical migration from the littoral into the sublittoral open water.

Ceriodaphnia (Fig. 21) shows two examples of swarming. Background concentrations are very low throughout the lake, but two samples are 5 to 15 times background levels. The first is at 10:00 on the west shore on 8/27 and the second is at 17:00 at the east shore on 9/3.

Mesocosm experiments: The mesocosm experiments were designed to answer four questions. First, the mesocosms act as zooplankton traps to see if limnetic zooplankton colonize the sublittoral zone on the east shore of Lake Itasca. Second, if zooplankton do colonize the sublittoral zone, can they persist there? Third, can fish exclude limnetic zooplankton from the mesocosms, and thus also from the sublittoral zone? Fourth, can limnetic zooplankton take advantage of macrophytes to reduce the impact of fish predation?

Chlorophyll was measured in each mesocosm throughout the experiments as an indicator of food availability for the herbivores. Food probably was not limiting in any of the mesocosms in either experiment because chlorophyll concentrations increased in all mesocosms. During the first experiment the concentration of chlorophyll increased from a mean of

5.5μg/liter to 7.5μg/liter, and in the second experiment it increased from 9.7μg/liter to 12.9μg/l. There were no significant differences among any of the treatments.

In no case in either experiment did the presence of macrophytes have a significant effect. These data are not presented, and the macrophyte treatments are considered together with the no macrophyte treatments.

Ten zooplankton species were followed in the mesocosm experiments. The behavior of each species can be described as belonging to one of three outcomes.

1: No fish effect. Six species showed no effect of the presence of fish. These include all of the copepods (Figs. 22, 23, 24), Ceriodaphnia (Fig. 25), Diaphanosoma (Fig. 26) and Asplanchna (Fig. 27). In nine out of twelve of these results, the organisms increased during the experiment, and all six species increased in at least one of the experiments. This suggests that these organisms can live in the sublittoral zone even in the presence of fish.

2: Negative fish effect. Two groups show a negative effect of fish on their numbers. Daphnia (Fig. 28) (D. retrocurva and D. galeata combined) colonize the mesocosm on day 3 of the first experiment. Mesocosms with fish lose their Daphnia population in two days whereas mesocosms without fish still have some Daphnia at day 7. Daphnia never colonize the second experiment in significant numbers, and the populations in both treatments stay constant at the level they were inoculated with.

Chaoborus (Fig. 29) never colonized the first experiment, but did colonize the second experiment on day 4 and then again on day 8. Chaoborus colonized all six of the "no fish" mesocosms and persisted in five of them until the end of the experiment. It colonized five of the six "fish" mesocosms, but persisted until the end of the experiment in only one of these.

3: Positive fish effect. In the second experiment, two species showed a positive fish effect (Fig. 30). Bosmina shows this most clearly. In both "fish" and "no fish" mesocosms Bosmina declines throughout the second experiment, but it does so much more rapidly in the "no fish" mesocosms. At the end of the experiment there are only about 30% as many

Bosmina in the "no fish" mesocosms as in the "fish" mesocosms. A similar trend is seen in Chydorus (Fig. 31) where in the first experiment there is no difference between treatments, but in the second experiment the population grows more rapidly in the presence of fish.

One explanation for this is that the fish may be acting as a keystone predator by eliminating an invertebrate predator that preys on Bosmina and Chydorus. If the mesocosms are regrouped into Chaoborus and no Chaoborus "treatments" (the c panel in each figure, and Figure 32a and 32b), it can be seen that only Bosmina and Chydorus show significant negative effects in the presence of Chaoborus. This is consistent with the known diet of Chaoborus (Fedorenko,1975a), and it is also consistent with other enclosure studies (Lynch, 1979).

Radiance Distributions: The central assumption of Siebeck's mechanistic hypothesis to explain "uferflucht" is that the radiance distribution (RD) within Snell's Window is symmetric in limnetic regions and asymmetric in sublittoral regions (Siebeck, 1968; 1980). The asymmetry is attributed to a shadow imposed on the RD by the shore's horizon. Siebeck (1968) presents both supporting and detracting evidence for the existence of a shadow, but the circumstances under which a shore shadow might be expected are not described.

The results presented here are the relevant findings of an extensive study of radiance distributions in four lakes that are presented in Chapter 2. Figure 33a shows two radiance distributions made in Lake Itasca, one near the west shore and one near mid-lake. According to Siebeck's hypothesis, the two distributions should be symmetrical and identical except for that portion of Snell's Window that points towards the west (310 to 360°). The radiance distribution made on the west shore should be slightly depressed, but is in fact slightly greater than the mid-lake RD. None of the radiance distributions are symmetrical.

Figure 33b shows three radiance distributions made on the east shore, west shore and at the mid-lake location of Bush Lake (optically similar to Lake Itasca). Again, a shore shadow is not detected on either shore, and in both cases the shore-ward direction appears slightly brighter than the same region at the mid-lake station.

At least two factors have been identified that are much more important in determining the RD than proximity to the shore. The first is the solar position. This is shown in Figure 34a. These measurements were made only 3m from the southeast shore at 10:30 on a clear morning. The RD is heavily skewed towards the sun. Zooplankton following Siebeck's hypothesis would be expected to swim towards the shore in this situation. In fact, this mechanism suggests that they should swim towards the southeast shore at dawn and towards the southwest shore at dusk. Moonlight poses a very similar set of problems.

Figure 34b shows the importance of cloud cover in determining the RD. These measurements were made in the middle of the lake on a day that was solidly overcast except in the north. The RD is more symmetrical than Figure 34a, but note that the blue sky to the north creates a slight asymmetry. Partly cloudy days create a mosaic of changing, asymmetrical radiance distributions.

Figure 34c is a comparison of radiance distributions made under complete cloud cover in a clear water lake (Long Lake) near a very tall shore horizon. These are the most favorable conditions for the detection of a shore shadow. The mid-lake distribution is very symmetrical, and there is a detectable shore shadow between 310° and 350°. These are the only conditions, however, under which I was able to detect a shore shadow.

DISCUSSION

Vertical distribution: Vertical migration is clearly important in the determination of the abundance of zooplankton in the epilimnion at any given time. All organisms, with the exception of D. galeata, show a diel

flux across the metalimnion. However, each species migrates in a unique pattern. The patterns vary in their timing of ascent, the duration of the migration and the percent of the population that participates in the migration. The timing of the ascent has long been thought to hold ecological significance (e.g. Wright et al., 1980; Enright, 1977), but has generally been treated as a community, rather than as a population character. The complexity of patterns that are described here suggests that no single ultimate cause is sufficient to explain the observed behavior of all species.

The NA species comprise that group which most closely conforms to the expectations of the visual predation hypothesis (Zaret & Suffern, 1976; Wright et al., 1980). Chaoborus, Ostracods and Leptodora are all large and therefore are expected to be selected by visually foraging fish (Brooks & Dodson, 1965). Their high participation in the migration suggests that selection for migration is very strong. The timing of their ascent and descent suggests that they avoid lighted regions of the lake. Tactile predators, such as Chaoborus and Leptodora are able to forage in complete darkness (Swift, 1976). Ostracods are filter-feeding herbivores which are too large to be consumed by these invertebrate predators.

D. retrocurva appears to be anomalous when compared to the other NA species. It is a smaller herbivore and a lesser proportion of the population migrates. D. retrocurva is a potential prey item for Chaoborus (Fedorenko, 1975b), but the individuals at the time of this sampling had well developed helmets. Helmet growth in cyclomorphic species is induced by the presence of Chaoborus and other predators (Grant & Bayly, 1981; Krueger & Dodson, 1981; Hebert & Grewe, 1985) and have been shown to be effective in reducing Chaoborus predation (Havel & Dodson, 1984). Because Daphnia are also favored food items of planktivorous fish (O'Brien, 1976), helmets may enable D. retrocurva to have a NA migration. Thus, helmets directly reduce the risk of Chaoborus predation and indirectly reduce the risk of fish predation. D. galeata have poorly developed helmets, and are ambiguous in their migratory

strategy. They are also less successful than D. retrocurva in that they are less abundant at this time.

All of the EA, MA and DA migrating species are potential prey for Chaoborus (Fedorenko, 1975a, 1975b). Chaoborus predation may explain why these species do not migrate at night, but it can't explain why there are three temporal strategies. Enright (1977) also observed EA migration strategies in marine copepods and attributed it to a strategy to maximize their foraging efficiency on the day's algal production. Algae should be both more abundant and more nutritious at the end of the day than at the beginning. This may explain the predominance of EA as opposed to MA or DA migration strategies.

Rotifers are not reported as a major component of most fish diets. They are small, highly transparent and their smooth swimming movements probably would not attract fish. These characteristics reduce their visibility and thus their susceptibility to fish predation. They are, however, consumed by many invertebrate predators (Anderson, 1970), thus, their DA strategy might be explained in terms of the avoidance of invertebrate predators.

The percent participation and the duration of the migrations are also likely to hold ecological significance. Migrations incur costs in that they result in organisms being exposed to food-poor environments for a period each day. In a predator-free world, it is always metabolically advantageous for an herbivore to stay in the epilimnion (Orcutt & Porter, 1983). Predators also induce costs, however, and herbivores are forced to make trade-offs between predation risk and starvation risk (Gliwicz, 1986). The proportion of the population that migrates may be a measure of the relative importance of these two risks. Thus, all of the cladocera and the herbivorous copepods have a percent participation between 65% and 90%, whereas the predacious cyclopoid copepods have only 30% participation.

Similarly, the duration of the migration may also be related to food abundance. All organisms, except Chydorus and Diaphanosoma, spend about 450 minutes in the epilimnion. It is not known whether these two species are more efficient grazers, or whether they are just more susceptible to

visual or tactile predators, and are therefore confined into a narrow window of opportunity between the two groups of predators.

Aggregations: Within the epilimnion, several species show a tendency to aggregate at about sunset. This includes all of the organisms that show an EA vertical migration except Diaphanosoma. This clumping might be an artifact of vertical migration, but two factors argue against this. First, four migratory species do not show this tendency to aggregate when they migrate. Second, D. retrocurva and Ceriodaphnia aggregate at times when they are not migrating. This suggests that these aggregations have a biological rather than a mechanical origin, and that the organisms that aggregate do so actively rather than passively.

Aggregations appear to be even more common and pronounced in sublittoral areas. D. retrocurva, D. galeata, Ceriodaphnia and cyclopoid copepods all show at least one sublittoral sample which is more than twice the concentration of other samples before and after it. Of four such aggregations, two occur just before sunset and two just after sunrise. They appear to be equally likely to occur on both shores, and on both windy and calm days. Most aggregations are comprised of more than one species, but never more than three species. There is no consistent pattern in the species composition of the aggregations. In three cases, the concentration of a species in the sublittoral aggregation is very similar to that species' concentration in mid-lake. This might suggest that the aggregation is merely an intrusion of mid-lake water. Three facts argue against this. The aggregations do not correlate with wind speed and occur on both the calm and windy days. Thus, the aggregations are neither dependent on nor dissipated by wind currents. Second, only a few of the mid-lake species are represented in any given aggregation, whereas a wind-driven current should bring in all species. Third, in five instances, the aggregated species are at far higher concentrations than the mid-lake concentration.

Several authors have reported zooplankton swarms and have suggested that they are formed biologically and are ecologically significant (Colebrook, 1960; Clutter, 1969; Hamner & Carleton, 1979). Swarms in

Lake Itasca appear to be unique in that they frequently contain two or three species, are largely restricted to the period around sunset in mid-lake and both sunrise and sunset near shore. Sublittoral swarms tend to be much more sharply defined in both time and concentration than are mid-lake aggregations.

Many hypotheses as to the ecological significance of these swarms are possible: swamping of predators which have hyperbolic functional response curves, reinforcement of directional orientation for both vertical and horizontal migration, and aggregations at a concentrated food source are three possibilities. The data presented here do not allow the elimination of any of these hypotheses.

Horizontal distribution: Horizontal sampling clearly permits the designation of all organisms as being primarily limnetic, sublittoral or indiscriminate in their distribution. However, all organisms are found in all habitats at least occasionally, and even Chaoborus, which was never sampled on the east shore colonized the mesocosms that were placed there. There is no known physical barrier between the zones, and so it is presumed that the barrier is biological. There are three lines of evidence which support the hypothesis that limnetic zooplankton actively avoid the sublittoral region. First, there is a much stronger coupling in the limnetic zooplankton's behavior between the west shore and mid-lake than there is between the two shores or mid-lake and the east shore. If organisms were being passively distributed by wind currents, one might expect a stronger cohesion between the east shore (wind-ward) and mid-lake, at least on windy days. This is not seen, and there is little difference in the behavior of any zooplankton species between windy and calm days.

Second, if wind driven currents were responsible for an organisms's distribution, one would expect increases near shore to correlate with wind speed. Instead, systematic increases near shore are better correlated with the time when mid-lake populations are also increasing. This implies that inshore intrusions are a secondary result of vertical migration, and that there is a horizontal component to the migration as

well as a vertical component. Fewer organisms penetrate to the east shore simply because it is further from the mid-lake region than the west shore is.

Figure 35 shows the ratio between west shore populations and mid-lake populations for the four EA species that are also considered to be limnetic. A ratio of less than one indicates the population is more concentrated in the mid-lake region, and a ratio of more than one indicates that the west shore population is more concentrated. In all four species, the ratio is at or below one from mid-morning until early afternoon. At the period of migration the ratio rises to about one, and then following migration the ratio is above one for several hours. This increase in the ratio is caused by a decrease in the concentration of mid-lake organisms as they migrate down to day depth. The ratio falls below one after there is light between 6:00 and 10:00 in the morning. This same pattern is seen on both days. It is also observed on both shores, but on the east shore the ratio does not rise above one in most cases. This suggests that zooplankton move throughout the epilimnion at the time of migration, but those that find themselves in shallow water can not leave until morning.

Shore avoidance: This study provides support for the hypothesis that some zooplankton are able to detect shores and then actively avoid them. This support is derived from three arguments.

First, intensive sampling along horizontal transects on both windy and calm days indicates that six species are much more abundant in pelagial than in sublittoral waters. This is true even though there are no known physical boundaries to dispersal from the limnetic to the sublittoral. In the absence of active shore avoidance, epilimnetic zooplankton would be expected to be more abundant in the sublittoral at times when wind-driven currents exist. Such was not the case, however.

Second, three cladocera species and both copepods have a tendency to decrease in abundance near shore at about sunrise but to contemporaneously increase at mid-lake. The predation hypothesis can explain the decrease near shore, but not the increase at mid-lake. In

addition, the mesocosm experiments suggest that only Chaoborus and Daphnia sp. are excluded from the sublittoral area by Centrarchid fishes. It is also known that the predominant minnows in Lake Itasca migrate horizontally to forage off-shore (Hanych et al. 1987). Avoidance of littoral predators may remain the ultimate cause for shore-avoidance, but the best interpretation of these data is that zooplankton can detect the shore when there is light and then they actively leave it. This exodus results in the early morning decline in population near shore and a simultaneous increase in the mid-lake population.

The third argument is derived from the strong coupling between vertical migration and the observed horizontal distributions. There appears to be a small horizontal component to the ascent during vertical migration. This horizontal motion is sufficient to bring organisms into the west shore sublittoral region in numbers about equal to mid-lake. Smaller numbers penetrate to the east shore. This horizontal motion is logical because the lake's area always increases towards the surface, thus there is more habitat near the surface than there is at depth. Zooplankton that invade the lake's margins as they ascend increase the resource base that is available to them during their feeding period. However, for this strategy to be effective, they must have some mechanism for locating their deep water refuge during the day.

Although this study supports the hypothesis of "uferflucht", there is little support for Siebeck's proposed mechanism of how zooplankton avoid the shore. Radiance distributions are typically asymmetrical, and the proximity to shore has only a weak influence on the radiance distribution. Although shore shadows can be detected under certain restrictive conditions, they are at best an unreliable beacon for zooplankton. The timing of when zooplankton leave the shore suggests that the mechanism is light dependent, but some other aspect of the light environment must be the cue. Other possibilities include the polarization of light, radiance reflectance and light color. Zooplankton are known to be able to detect and respond to all of these (Baylor & Smith, 1953; Ringelberg, 1964; Smith & Baylor, 1953).

Predator-prey interactions: Ecologists have long studied the significance of vertebrate predation in structuring zooplankton communities. Important predators are known to have both direct effects on their prey populations (Brooks & Dodson. 1965) and also indirect effects on competitors of their prey (Lynch, 1979). Centrarchid predation in Lake Itasca appears to have been very selective. In accordance with documented bluegill diets and with size-selective foraging theory, bluegill predation directly influenced only two groups, Chaoborus and Daphnia spp. In addition, bluegills appear to have indirectly affected two other species that were prey for Chaoborus. A modification of the Keystone Predator Hypothesis suggests a mechanism to explain the horizontal distribution of Bosmina. Bluegills enable Bosmina to persist in the littoral region because fish predation excludes their major predator, Chaoborus. Chaoborus, however, excludes Bosmina from the limnetic zone.

CONCLUSION

The pattern of horizontal and vertical distribution of zooplankton are complex and indicate that each species is unique in this regard. This complexity strongly suggests that biological factors are important in the determination of these distributions. Large scale physical forces, such as wind-driven currents and light/dark cycles may play a lesser role than has generally been assumed.

There is a strong temporal linkage between the vertical and horizontal distributions and movements of zooplankton. Organisms that are primarily limnetic occur in sublittoral areas during the period of vertical migration. This is best explained by a horizontal component to the migration that would enable them to exploit all of the food resources of the epilimnion.

To return to the deep-water refugia, zooplankton must be able to leave the shore region. They apparently require light to do this, but it is unlikely that the radiance distribution is the beacon that they use.

The ultimate cause of active shore avoidance may be related to the avoidance of fish predation, at least for a few species. But fish predation may enable some species (e.g. Bosmina) to persist in sublittoral areas by eliminating their invertebrate predators. Invertebrate predation in Lake Itasca may play a major role both in structuring the distribution of herbivores and in regulating their vertical migration.

REFERENCES

Alldredge, A.L. & Y. Cohen. 1987. Can microscale chemical patches persist in the sea? Microelectrode study of marine snow, fecal pellets. Science 235:689-691.

Anderson, R.S. 1970. Predator-prey relationships and predation rates for crustacean zooplankters from some lakes in western Canada. Can. J. of Zoo. 48:1229-1240.

Baylor, E.R. and F.E. Smith. 1953. The orientation of cladocera to polarized light. American Naturalist 87(833):97-101.

Brooks, J.L. 1965. Predation and relative helmet size in cyclomorphic Daphnia. Proc. N.A.S. 53:119-126.

Brooks, J.L. and S.I. Dodson. 1965. Predation, body size, and the composition of the plankton. Science, 150:28-35.

Cassie, R.M. 1959. Microdistribution of plankton. New. Zealand J. Sci. 2:398-409.

Clutter, R.I. 1969. The microdistribution and social behavior of some pelagic Mysid shrimps. J. Exp. Mar. Biol. Ecol. 3:125-155.

Colebrook, J.M. 1960. Some observations of zooplankton swarms in Windemere. J. Animal Ecol. 29:241-242.

Cushing, D.H. 1951. The vertical migration of planktonic crustacea. Biol. Rev. 26:158-192.

Dumont, H.J. 1972. A competition-based approach of the reverse vertical migration in zooplankton and its implications, chiefly based on a study of the interactions of the rotifer Asplanchna priodonta (Gosse) with several crustacea Entomostraca. Int. Revue ges. Hydrobiol. 57(1):1-38.

Enright, J.T. 1977. Diurnal vertical migration: adaptive significance and timing. Part 1. Selective advantage: A metabolic model. Limnol. Oceanogr. 22:856-872.

Enright, J.T. & W.M. Hamner. 1967. Vertical diurnal migration and endogenous rhythmicity. Science 157:937-941.

Emery, A.R. 1968. Preliminary observations on coral reef plankton. Limnol. Oceanogr. 13(2):293-303.

Fedorenko, A.Y. 1975a. Instar and species specific diets in two species of Chaoborus. Limnol. Oceanogr. 20(2):238-249.

Fedorenko, A.Y. 1975b. Feeding characteristics and predation impact of

Chaoborus (Diptera, Chaoboridae) larvae in a small lake. Limnol. Oceanogr. 20(2):250-258.

Frost, B.W. 1975. A threshold feeding behavior in Calanus pacificus. Limnol. Oceanogr. 20(2):263-266.

George, D.G. & R.W. Edwards. 1973. Daphnia distribution within Langmuir circulation. Limnol. Oceanogr. 18(5):798-800.

Gliwicz, M.Z. 1986. Predation and the evolution of vertical migration in zooplankton. Nature 320:746-748.

Grant, J.W.G. and I.A.E. Bayly. 1981. predator induction of crests in morphs of the Daphnia carinata King complex. Limnol. Oceanogr. 26(2):201-218.

Green, J. 1967. The distribution and variation of Daphnia lumholtzi (Crustacea: Cladocera) in relation to fish predation in Lake Albert, East Africa. J. Zool. Lond. 151:181-197.

Greene, C.H., P.H. Wiebe, J. Burczynski, and M.J. Youngbluth. 1988. Acoustical detection of high-density krill demersal layers in the submarine canyons off Georges Bank. Science 241:359-361.

Hairston, N.G. Jr. 1980. The vertical distribution of diaptomid copepods in relation to body pigmentation. In: Evolution and Ecology of Zooplankton Communities, W.C. Kerfoot Ed. New England Press.

Hamner, W.M. & J.H. Carleton. 1979. Copepod swarms: Attributes and role in coral reef ecosystems. Limnol. Oceanogr. 24(1):1-14.

Hamner, W.M. and I.R. Hauri. 1981. Long-distance horizontal migrations of zooplankton (Scyphomedusae: Mastigias) Limnol. Oceanogr. 26(3):414-423.

Hanych, D.A., M.R. Ross, R.E. Magnien and A.L. Suggars. 1983. Nocturnal inshore movement of the mimic shiner (Notropis volucellus): a possible predator avoidance behavior. Can. J. Fish. Aquat. Sci. 40:888-894.

Havel, J.E. and S.I. Dodson. 1984. Chaoborus predation on typical and spined morphs of Daphnia pulex. Behavioral observations. Limnol. Oceanogr. 29(3): 487-494.

Hebert, P.D.N. and P.M. Grewe. 1985. Chaoborus-induced shifts in the morphology of Daphnia ambigua. Limnol. Oceanogr. 30(6):1291-1297.

Holm-Hansen, O. & B. Reimann. 1978. Chlorophyll a determination: improvements in methodology. Oikos 30:438-447.

Huntley, M. & E.R. Brooks. 1982. Effects of age and food availability on diel vertical migration of Calanus pacificus. Mar. Bio. 71:23-31.

Hutchinson, G.E. 1967. A Treatise on Limnology. V. 2 Willey. 1115 p.

Kerfoot, C.W. 1975. The divergence of adjacent populations. Ecology 56:1298-1313.

Krueger, D.A. & S.I. Dodson. 1981. Embryological induction and predation ecology in Daphnia pulex. Limnol. Oceanogr. 26(2):219-223.

Larow, E.J. 1968. A persistent diurnal rhythm in Chaoborus larvae I. The nature of the rhythmicity. Limnol. Oceanogr. 13:250-256.

Lehman, J.T. & D. Scavia. 1982. Microscale patchiness of nutrients in plankton communities. Science 216:729-730.

Lewis, W.M. Jr. 1979. Zooplankton Community Analysis. Springer-Verlag, New York. 163 p.

Lynch, M. 1979. Predation, competition and zooplankton community structure: An experimental study. Limnol. Oceanogr. 24(2):253-272.

Magnien, R.E. & J.J. Gilbert. 1983. Diel cycles of reproduction and vertical migration in the rotifer Keratella crassa and their influence on the estimation of population dynamics. Limnol. Oceanogr. 28(5):957-969.

McLaren, I. 1963. Effects of temperature on the growth of zooplankton and the adaptive value of vertical migration. J. Fish. Res. Bd. Canada 20:685-727.

McNaught, D.C. 1966. Depth control by planktonic cladocerans in Lake Michigan. Univ. Mich. Great Lakes Res. Div. Publ. 15:98-108.

McNaught, D.C. 1978. Considerations of scale in modeling large aquatic ecosystems. In: Perspectives in Modeling Aquatic Ecosystems. A. Robertson and D. Scavia Eds. Ann Arbor Science pub. Ann Arbor.

McNaught, D.C. & A.D. Hasler. 1961. Surface schooling and feeding behavior in the white bass Roccus chrysops (Rafinesque) in lake Mendota. Limnol. Oceanogr. 6(1):53-60.

McNaught, D.C. & A.D. Hasler, 1964. Rate of movement of populations of Daphnia in relation to changes in light intensity. J. Fish. Res. Bd. Canada 21(2):291-318.

Mullin, M.M., E.F. Stewart & F.J. Fuglister. 1975. Ingestion by planktonic grazers as a function of concentration of food. Limnol.

Oceanogr. 20(2):259-262.

Mullin, M.M. & E.R. Brooks. 1976. Some consequences of distributional heterogeneity of phytoplankton. Limnol. Oceanogr. 21(6):784-796.

O'Brien, J.W. 1979. The predator-prey interactions of planktivorous fish and zooplankton. Am. Scientist. 67:572-581.

Odum, H.T. & E.P. Odum. 1955. Trophic structure and productivity of a windward coral reef community on Eniwetok. Ecol. Monogr. 25:291-320.

Orcutt, J.D. Jr. and K.G. Porter. 1983. Diel vertical migration by zooplankton: constant and fluctuating temperature affects on life history parameters of Daphnia. Limnol. Oceanogr. 28(4):720-730.

Platt, T. and K.L. Denman. 1974. A general equation for the mesoscale distribution of phytoplankton in the sea. Sixth Liege colloquium on ocean hydrodynamics, Ed. J. Nihoul, 8:31-42.

Preissler, K. 1977a. Horizontal distribution and "avoidance of shore" by rotifers. Arch. Hydrobiol. Beih. 8:43-46.

Preissler, K. 1977b. Do rotifers show avoidance of the shore? Oecologia (Berl) 27:253-260.

Ricker, W.G. 1937. Statistical treatment of sampling processes useful in the enumeration of planktonic organisms. Arch. Hydrobiol. 31:68-84.

Ringelberg, J. 1964. The positively phototactic reaction of Daphnia magna (Strauss), a contribution to the understanding of diurnal vertical migration. Neth. J. Sea Res. 2:319-406.

Schindler, D.W. 1969. Two useful devices for vertical plankton and water sampling. J. Fish. Res. Brd. Can. 26:1948-1955.

Siebeck, O. 1964. Researches on the behavior of planktonic crustaceans in the littoral. Verh. Internat. Limnol. 15:746-751.

Siebeck, O. 1968. "Uferflucht" und optische orientierung pelagischer Crustaceen. Arch. Hydrobiol. Suppl. 1:1-118.

Siebeck, O. 1969. Spatial orientation of planktonic crustaceans. Verh. Internat. Verein. Limnol. 17:831-840.

Siebeck, O. 1980. Optical orientation of pelagic crustaceans and its consequences in the pelagic and littoral zones. In Evolution and Ecology of Zooplankton Communities. W.C. Kerfoot Ed. New England.

Smith, F.E. and E.R. Baylor, 1953. Color responses in the cladocera and

their ecological significance. American Naturalist. 87(832):49-55.

Sokal, R.R. & F.J. Rohlf. 1981. Biometry. 2nd Ed. W.H. Freeman & Co. New York.

Stavn, R.H. 1971. The horizontal-vertical distribution hypothesis: Langmuir circulations and Daphnia distributions. Limnol. Oceanogr. 16(2):453-466.

Steele, J.H. 1974. Spatial heterogeneity and population stability. Nature 248:83.

Stitch, H. & W. Lambert. 1981. Predator evasion as an explanation of diurnal vertical migration by zooplankton. Nature 293:396-398.

Swift, M.C. 1976. Energetics of vertical migration in Chaoborus trivittatus larvae. Ecology 57:900-914.

Townsend, C.R. & A.J. Risebrow. 1982. The influence of light level on the functional response of zooplanktivorous fish. Oecologia 53:293-295.

Weider, L.J. 1984. Spatial heterogeneity of Daphnia genotypes: vertical migration and habitat partitioning. Limnol. Oceanogr. 29(2)225-235.

Wiebe, P.H. 1970. Small scale spatial distributions in oceanic zooplankton. Limnol. Oceanogr. 15(2):205-217.

Wright, D., W.J. O'Brien, and G.L. Vinyard. 1980. Adaptive value of vertical migration: A simulation model argument for the predation hypothesis. In: Evolution and Ecology of Zooplankton communities, W.C. Kerfoot, Ed. New England Press.

Zaret, T.M. & J.S. Suffern. 1976. Vertical migration in zooplankton as a predator avoidance mechanism. Limnol. Oceanogr. 21:804-813.

TABLE 1

	Backgr. Conc. (org./l)	Peak Conc. (org./l)	% mig.	Peak Time	Duration (Min.)
NOCTURNAL ASCENT:					
Ostracods.	0.0	3.5, 2.4	100.0	5:00,21:00	142, 142
Leptodora.	0.0	0.5, 0.9	100.0	3:00,21:00	164, 185
Chaoborus.	0.0	1.3	100.0	21:00	436
D. retrocurva.	8.5	26.8	68.3	23:00	469
EVENING ASCENT:					
Calanoid Cop.	12.2	33.2	63.3	15:00	469
Cyclopoid Cop.	18.0	28.2	36.2	17:00	436
Nauplii.	1.5	6.3	76.2	17:00	436
Diaphanosoma.	0.3	1.6	81.3	17:00	295
Chydorus.	7.2	39.0	81.5	19:00	240
MORNING ASCENT:					
Ceriodaphnia. D. galeata (?)	0.1	1.3	90.8	5:00	404
DIURNAL ASCENT:					
Asplanchna.	2.2	4.2	46.7	13:00	338
NO MIGRATION:					
D. galeata (?)	4.1	11.9	-	-	-

Table 1. Summary of vertical migration statistics. Background concentration is the minimum observed value for the mean concentration of organisms during the day. Peak concentration is the maximum concentration observed during the day. % migrating is found according to the formula (peak-background)/peak. Duration is the length of time that the observed concentration is greater than the value (peak + background)/2.

TABLE 2

	EAST/MID-LAKE (SD)
Limnetic organisms:	
Daphnia galeata*	0.02 (.04)
calanoid copepods	0.06 (.04)
Daphnia retrocurva	0.24 (.45)
Chaoborus*	0.28 (.04)
cyclopoid copepods	0.30 (.12)
Chydorus	0.52 (.24)
Sublittoral organisms:	
Bosmina	∞ (-)
Leptodora	∞ (-)
Indiscriminate:	
nauplii	1.24 (.52)
Diaphanosoma	0.85 (.51)
Asplanchna	0.80 (.62)
Ceriodaphnia	- (-)

Table 2. Summary of the horizontal distribution of zooplankton in Lake Itasca. Ratios were calculated at each sampling period by dividing the east shore concentration by the mid-lake concentration. The ratios given are daily mean values and the standard deviation. N = 12 except for those species marked by *, where N = 4. Values are not given for Ceriodaphnia because it occurs at such low concentrations that the ratio is unreliable. It is listed as being indiscriminate because it is found in all habitats much of the time.

FIGURE CAPTIONS

Figure 1: a) Contour map of Lake Itasca showing the transect (A--B) along which all sampling was done. Mesocosm experiments were done at point B. b) Echogram showing the bottom topography along the transect (A--B).

Figure 2: a) Depth profiles of irradiance (PAR--open circles) and temperature (closed circles) in Lake Itasca on 9/3/86. b) Wind speed at the mid-lake station on Lake Itasca on 8/27 and 9/3/86. The wind is primarily from the northwest on both days.

Figure 3: Concentration of the twelve predominant organisms at the mid-lake station on 9/3/86. Values given are the mean of five depths in the epilimnion, and the bars are one standard error.

Figure 4: Mean depth in the epilimnion of the twelve predominant organisms at the mid-lake station on 9/3/86. Standard errors are not given because they are very large.

Figure 5: Concentration contour plots for three groups of copepods on 9/3/86.

Figure 6: Concentration contour plots for three species of cladocera on 9/3/86.

Figure 7: concentration contour plots for three species of cladocera on 9/3/86.

Figure 8: Concentration contour plots for three species of zooplankton on 9/3/86.

Figure 9: Coefficient of dispersion (CD = variance/mean) vs time for the twelve predominant zooplankton in Lake Itasca.

Figure 10: Time-dependent changes in concentration of Daphnia galeata at 1.25m at three locations along transect (A--B) on two days in 1986.

Figure 11: Time-dependent changes in concentration of calanoid copepods at 1.25m at three locations along transect (A--B) on two days in 1986.

Figure 12: Time-dependent changes in concentration of Daphnia retrocurva at 1.25m at three locations along transect (A--B) on two days in 1986.

Figure 13: Time-dependent changes in concentration of Chaoborus at 1.25m at three locations along transect (A--B) on two days in 1986.

Figure 14: Time-dependent changes in concentration of cyclopoid copepods at 1.25m at three locations along transect (A--B) on two days in 1986.

Figure 15: Time-dependent changes in concentration of Chydorus at 1.25m at three locations along transect (A--B) on two days in 1986.

Figure 16: Time-dependent changes in concentration of Bosmina at 1.25m at three locations along transect (A--B) on two days in 1986.

Figure 17: Time-dependent changes in concentration of Leptodora at 1.25m at three locations along transect (A--B) on two days in 1986.

Figure 18: Time-dependent changes in concentration of nauplii at 1.25m at three locations along transect (A--B) on two days in 1986.

Figure 19: Time-dependent changes in concentration of Diaphanosoma at 1.25m at three locations along transect (A--B) on two days in 1986.

Figure 20: Time-dependent changes in concentration of Asplanchna at 1.25m at three locations along transect (A--B) on two days in 1986.

Figure 21: Time-dependent changes in concentration of Ceriodaphnia at 1.25m at three locations along transect (A--B) on two days in 1986.

Figure 22: a) Results of the first mesocosm experiment for calanoid copepods. Values given are means and one standard error. The two treatments are mesocosms with fish (N=6) and mesocosms with no fish (N=6). b) Results of the second mesocosm experiment, treatments as in a. c) Results of the second mesocosm experiment with the results grouped into mesocosms that Chaoborus invaded (N=6) and mesocosm that Chaoborus did not invade (N=6).

Figure 23: Same as Fig. 22 for cyclopoid copepods.

Figure 24: Same as Fig. 22 for nauplii.

Figure 25: Same as Fig. 22 for Ceriodaphnia.

Figure 26: Same as Fig. 22 for Diaphanosoma.

Figure 27: Same as Fig. 22 for Asplanchna.

Figure 28: Same as Fig. 22 for Daphnia spp.

Figure 29: Same as Fig. 22 for Chaoborus.

Figure 30: Same as Fig. 22 for Bosmina. See Fig. 32 for panel c.

Figure 31: Same as Fig. 22 for Chydorus. See Fig 32 for panel c.

Figure 32: a) Bosmina concentration in the second mesocosm experiment with the results partitioned into mesocosms with Chaoborus and mesocosms without Chaoborus. b) Same as Fig. 32a for Chydorus.

Figure 33: a) Two radiance distributions measured at 0.5m in Lake Itasca at 14:30 on 9/2/85. Zenith angles 0°-180° point towards the east, zenith angles 180°-360° point towards the west. Snell's angle is always at 48° from the zenith. No shore shadow is seen in the west direction when the mid-lake and west shore RDs are compared. Cloud cover was 100% and there was a slight drizzle. The west shore measurements were made 30m from the shore. b) Three radiance distributions measured at 0.5m in Bush Lake at 14:30 on 8/15/84. The sky was clear and there was a slight breeze. Measurements were made 11m from the east shore, 20m from the west shore and in the middle of the lake. Elapsed time during the measurements was 50 minutes.

Figure 34: a) Radiance distribution at 0.5m in Bush Lake on 8/24/84 at 10:25 only 3m from the southeast shore. b) Radiance distribution in Bush Lake on 8/17/84 at 13:10 at 1.0m. This shows both a north-south arc and an east-west arc. There was dense cloud cover except for a clear patch of sky to the north. c) Two radiance distributions in Long Lake on 8/29/85 at 13:00 at 1.0m. There was 100% overcast sky and a slight drizzle. A shore shadow is seen as a depression of the west shore RD between 300° and 340°.

Figure 35: The time dependence of the ratio between the west shore population concentration and the mid-lake population concentration for four zooplankton species on 9/3/86. The ratio is high at night and decreases between 6:00 and 10:00 to low values during the day. The values rise to about 1 at the time of vertical migration (18:00) and then increase after migration.

A

LAKE ITASCA

30 JULY, 1987

1530 – 1600 h

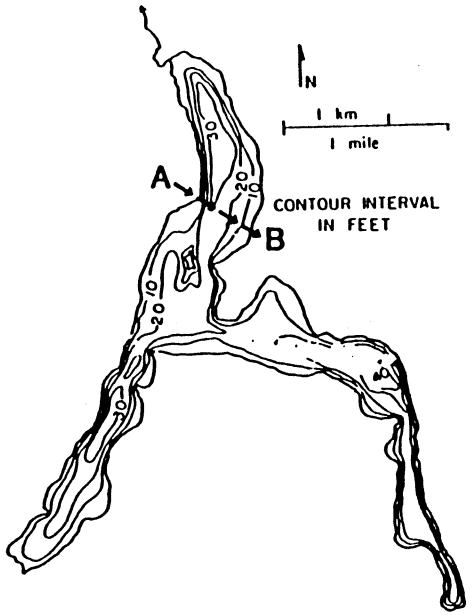

B

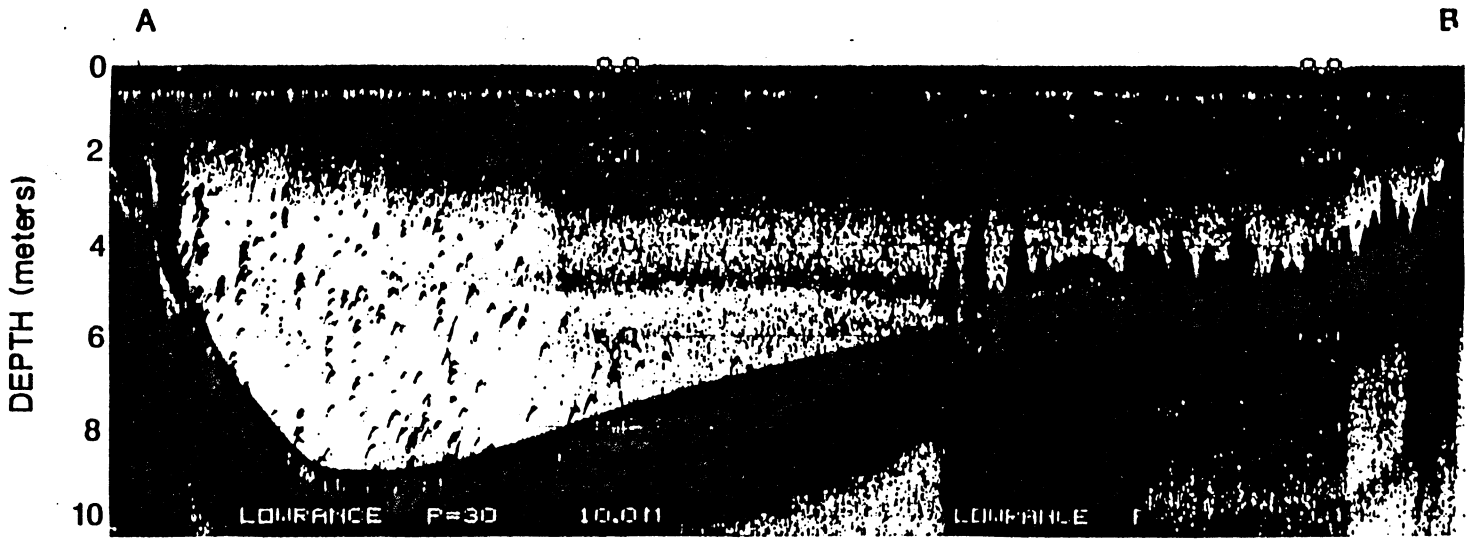

FIGURE 1

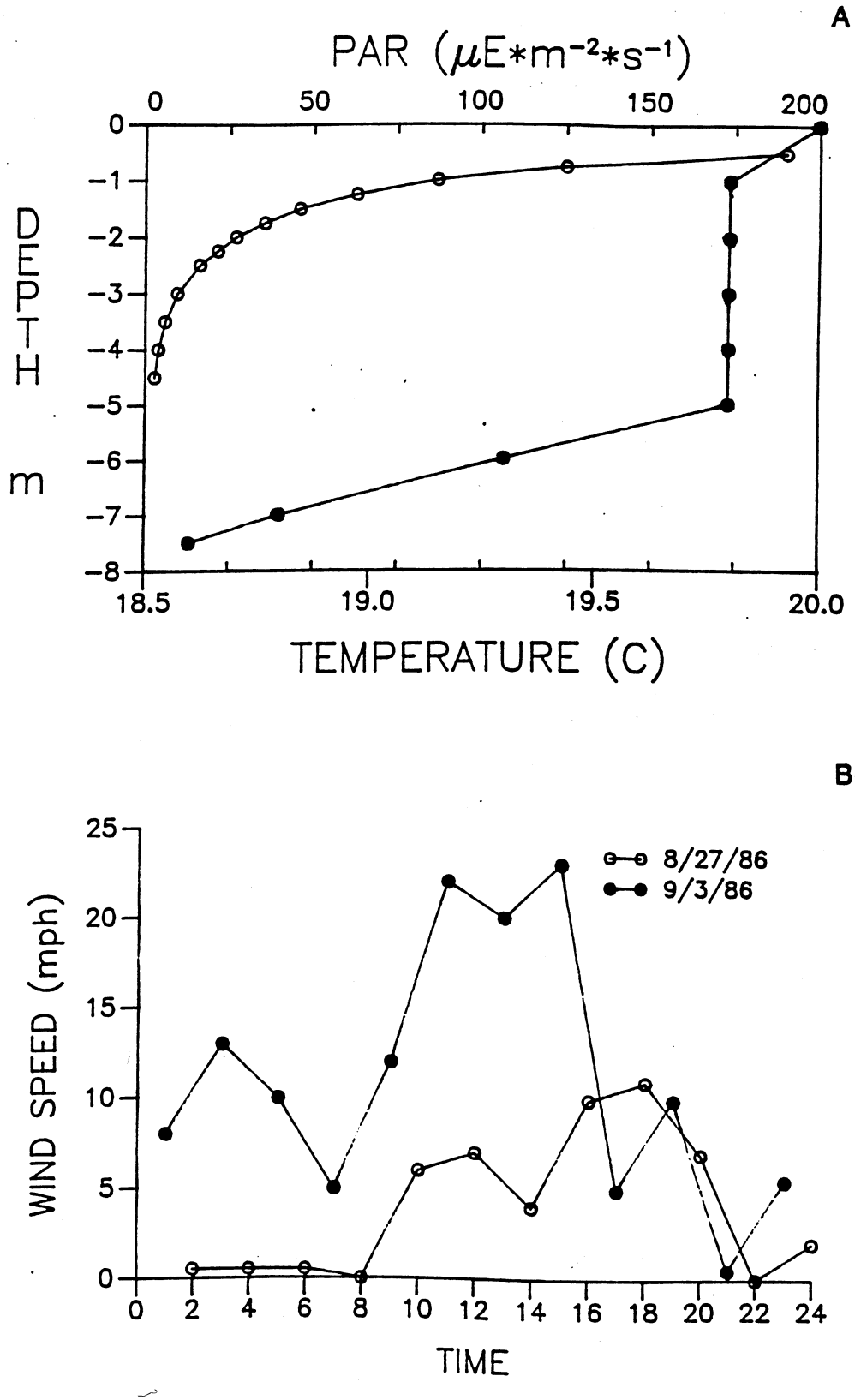
A
PAR (μE*m⁻²*s⁻¹)
0
50
100
150
200
0
-1
-2
-3
-4
-5
-6
-7
-8
DEPTH
m
18.5
19.0
19.5
20.0
TEMPERATURE (C)
B
25
20
15
10
5
0
WIND SPEED (mph)
8/27/86
9/3/86
0
2
4
6
8
10
12
14
16
18
20
22
24
TIME

FIGURE 2

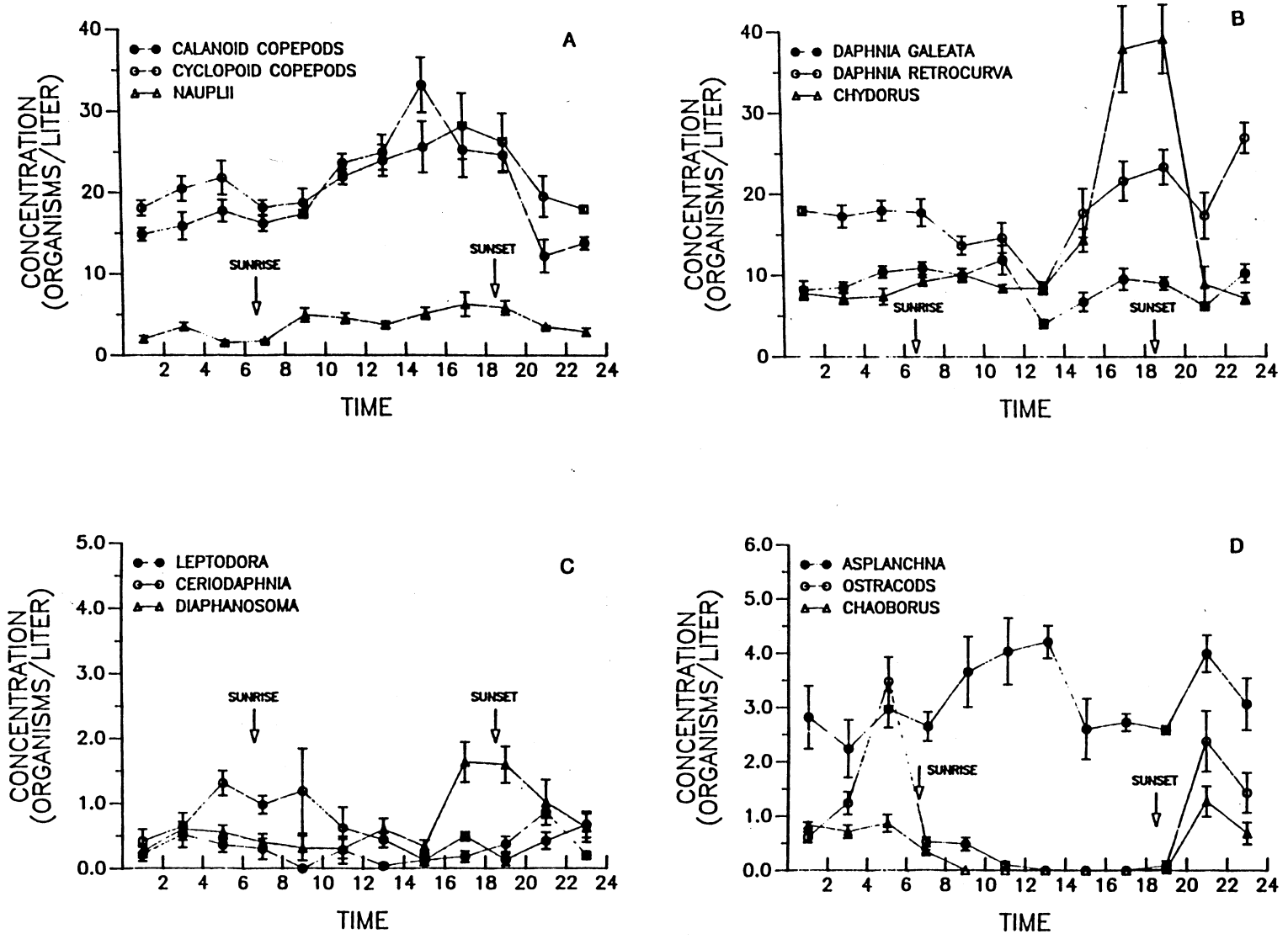
A
CALANOID COPEPODS
CYCLOPOID COPEPODS
NAUPLII
SUNRISE
SUNSET
CONCENTRATION (ORGANISMS/LITER)
TIME
B
DAPHNIA GALEATA
DAPHNIA RETROCURVA
CHYDORUS
SUNRISE
SUNSET
CONCENTRATION (ORGANISMS/LITER)
TIME
C
LEPTODORA
CERIODAPHNIA
DIAPHANOSOMA
SUNRISE
SUNSET
CONCENTRATION (ORGANISMS/LITER)
TIME
D
ASPLANCHNA
OSTRACODS
CHAOBORUS
SUNRISE
SUNSET
CONCENTRATION (ORGANISMS/LITER)
TIME

FIGURE 3

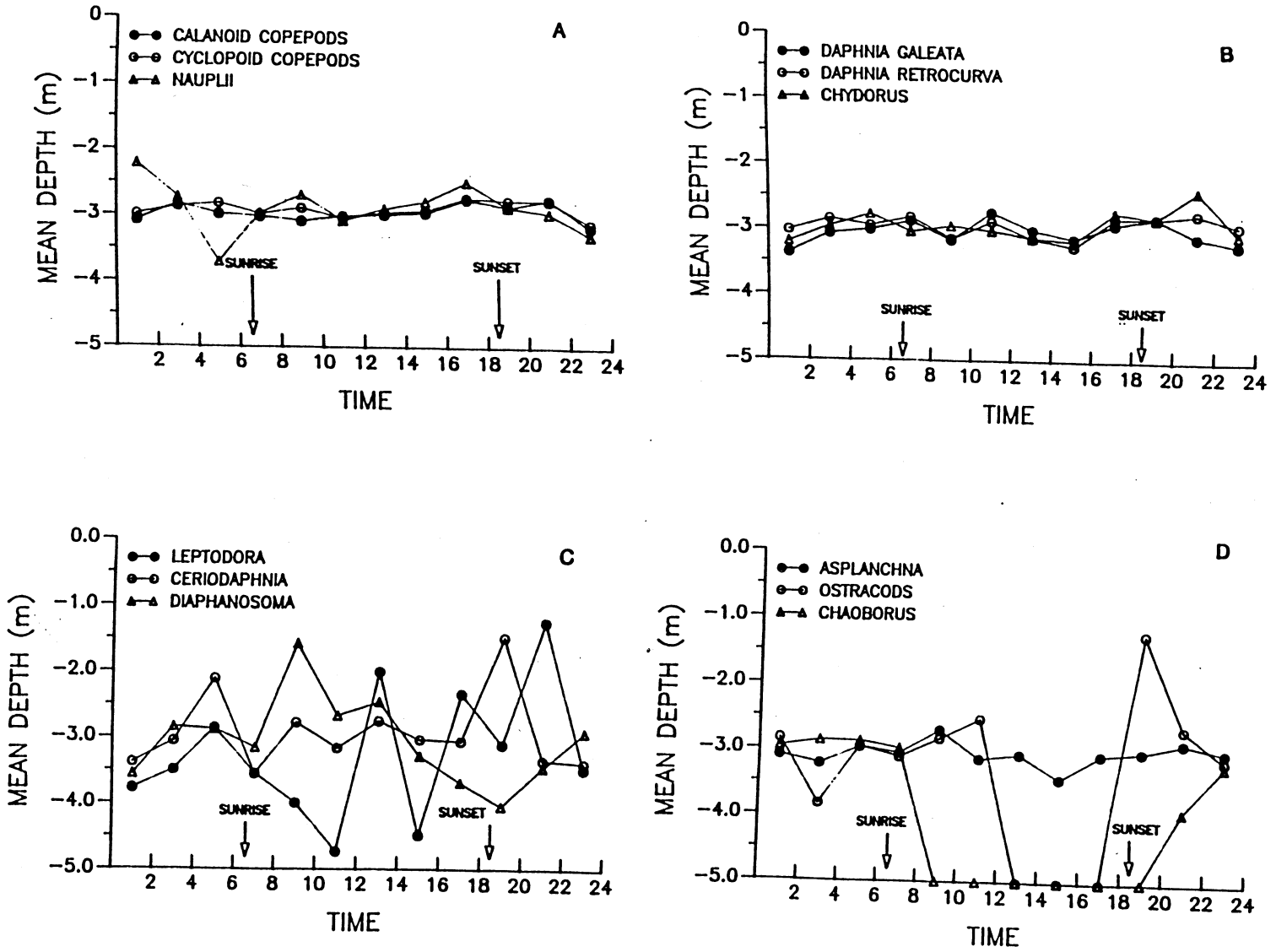
A
CALANOID COPEPODS
CYCLOPOID COPEPODS
NAUPLII
MEAN DEPTH (m)
0
-1
-2
-3
-4
-5
SUNRISE
SUNSET
2 4 6 8 10 12 14 16 18 20 22 24
TIME
B
DAPHNIA GALEATA
DAPHNIA RETROCURVA
CHYDORUS
MEAN DEPTH (m)
0
-1
-2
-3
-4
-5
SUNRISE
SUNSET
2 4 6 8 10 12 14 16 18 20 22 24
TIME
C
LEPTODORA
CERIODAPHNIA
DIAPHANOSOMA
MEAN DEPTH (m)
0.0
-1.0
-2.0
-3.0
-4.0
-5.0
SUNRISE
SUNSET
2 4 6 8 10 12 14 16 18 20 22 24
TIME
D
ASPLANCHNA
OSTRACODS
CHAOBORUS
MEAN DEPTH (m)
0.0
-1.0
-2.0
-3.0
-4.0
-5.0
SUNRISE
SUNSET
2 4 6 8 10 12 14 16 18 20 22 24
TIME

FIGURE 4

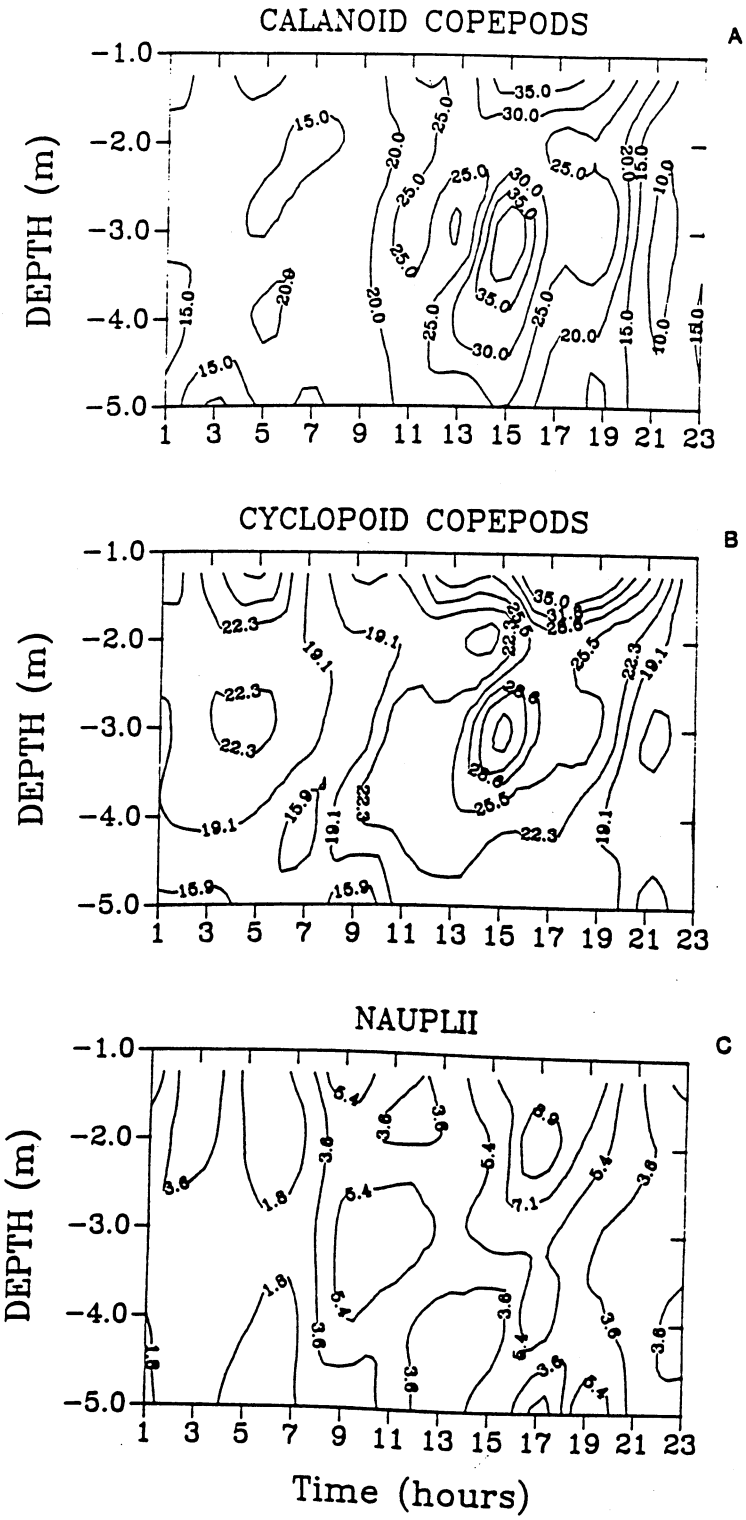
CALANOID COPEPODS
A
DEPTH (m)
-1.0
-2.0
-3.0
-4.0
-5.0
1 3 5 7 9 11 13 15 17 19 21 23
CYCLOPOID COPEPODS
B
NAUPLII
C
Time (hours)

FIGURE 5

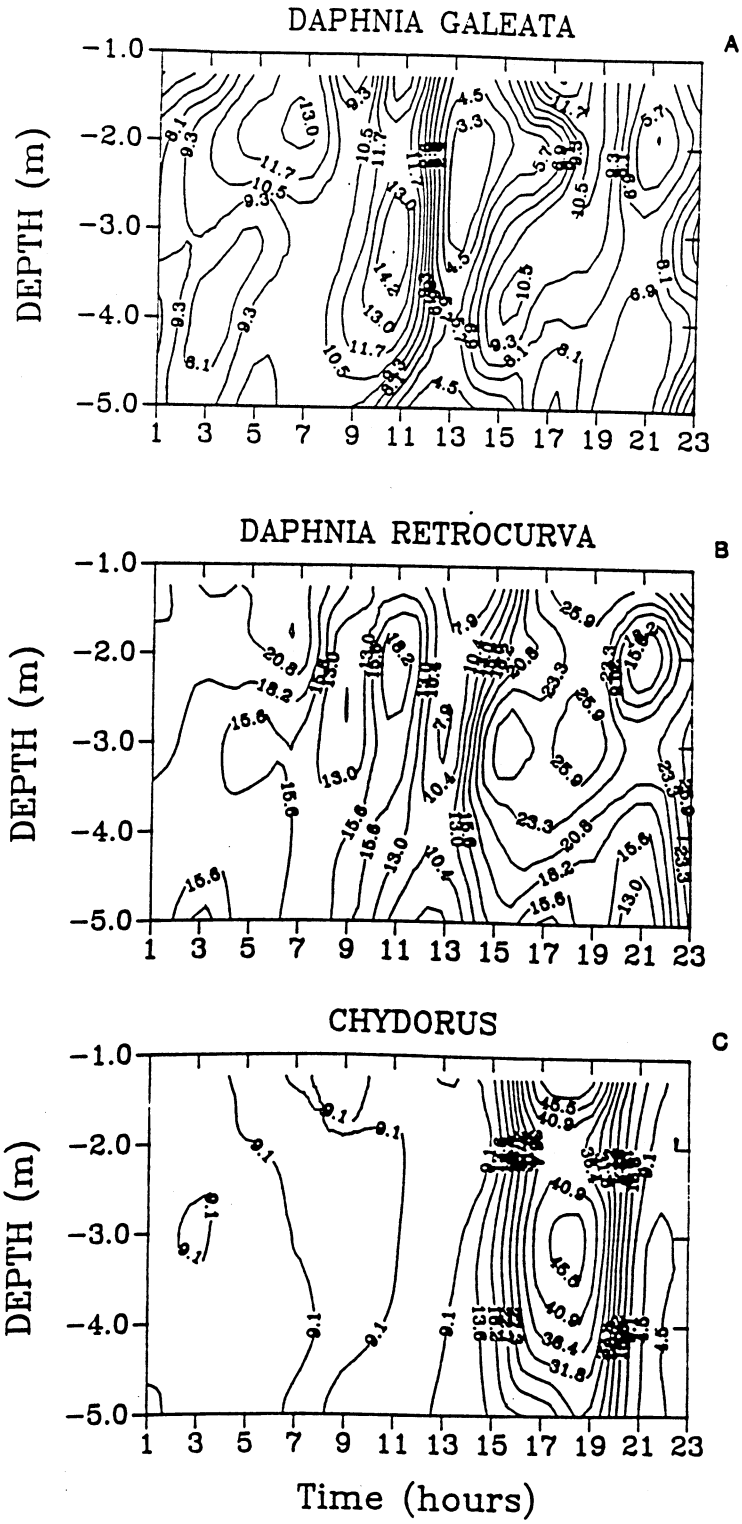
DAPHNIA GALEATA
A
DEPTH (m)
-1.0
-2.0
-3.0
-4.0
-5.0
1 3 5 7 9 11 13 15 17 19 21 23
DAPHNIA RETROCURVA
B
DEPTH (m)
-1.0
-2.0
-3.0
-4.0
-5.0
1 3 5 7 9 11 13 15 17 19 21 23
CHYDORUS
C
DEPTH (m)
-1.0
-2.0
-3.0
-4.0
-5.0
1 3 5 7 9 11 13 15 17 19 21 23
Time (hours)

FIGURE 6

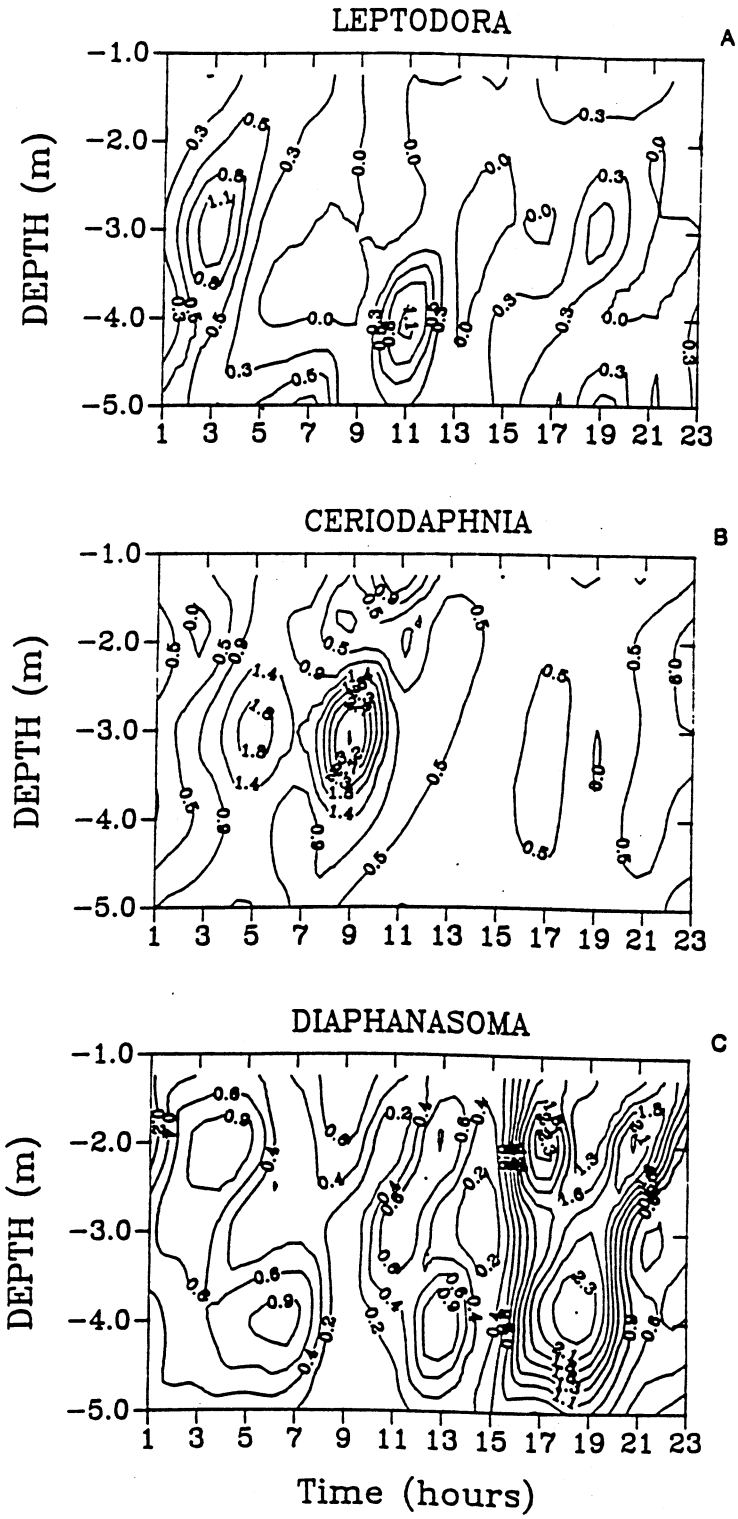
LEPTODORA
A
CERIODAPHNIA
B
DIAPHANASOMA
C
DEPTH (m)
-1.0
-2.0
-3.0
-4.0
-5.0
1 3 5 7 9 11 13 15 17 19 21 23
Time (hours)

FIGURE 7

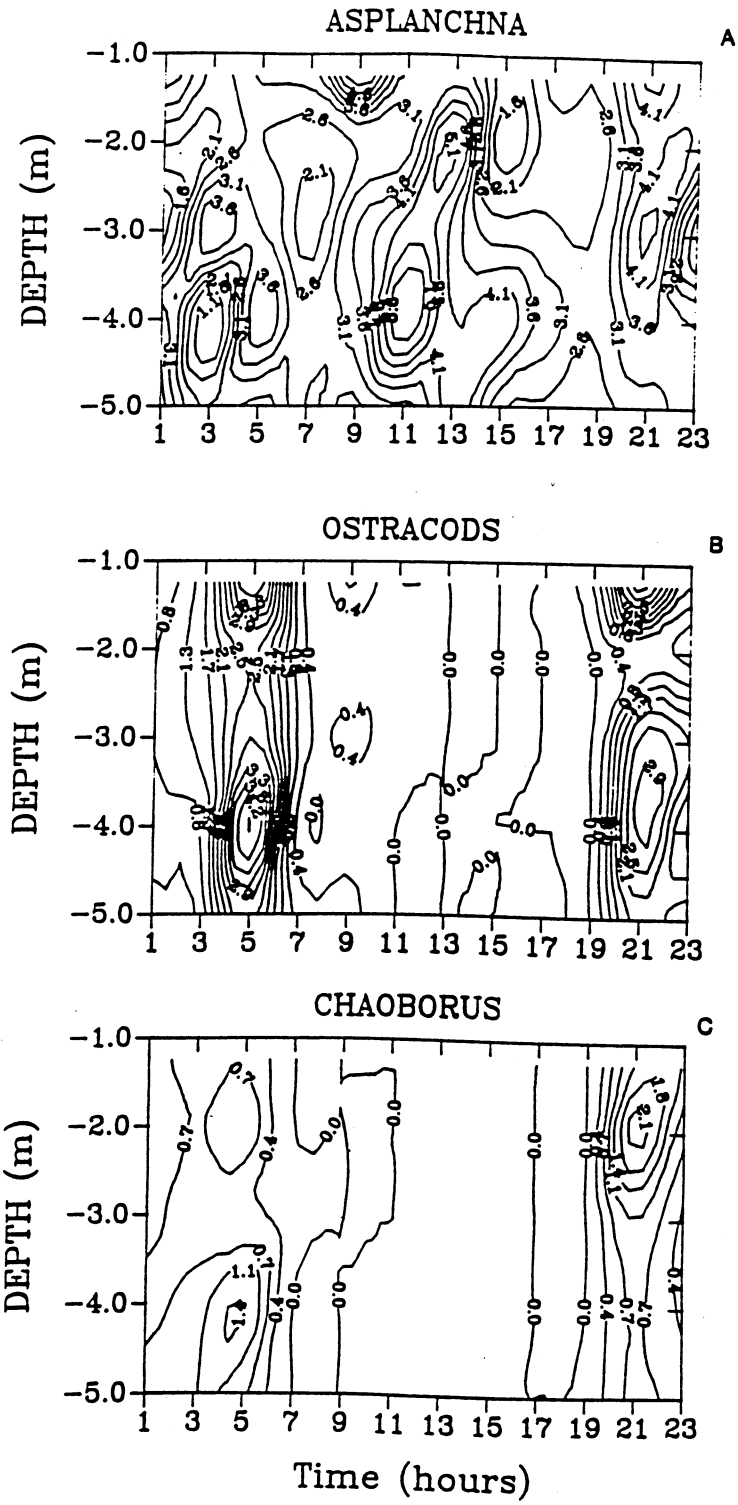
ASPLANCHNA
A
OSTRACODS
B
CHAOBORUS
C
DEPTH (m)
-1.0
-2.0
-3.0
-4.0
-5.0
1 3 5 7 9 11 13 15 17 19 21 23
Time (hours)

FIGURE 8

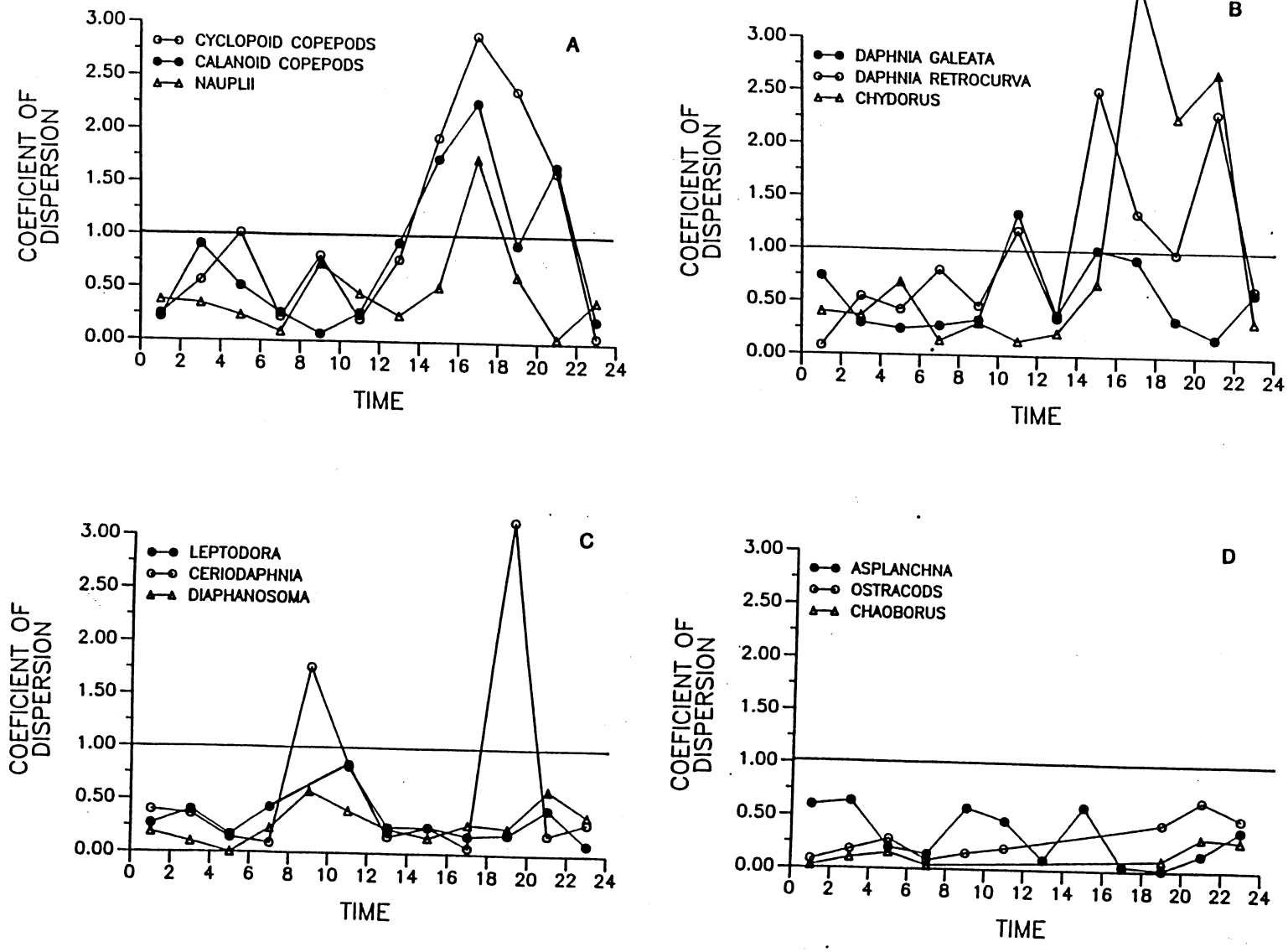
A
CYCLOPOID COPEPODS
CALANOID COPEPODS
NAUPLII
COEFICIENT OF DISPERSION
TIME
B
DAPHNIA GALEATA
DAPHNIA RETROCURVA
CHYDORUS
COEFICIENT OF DISPERSION
TIME
C
LEPTODORA
CERIODAPHNIA
DIAPHANOSOMA
COEFICIENT OF DISPERSION
TIME
D
ASPLANCHNA
OSTRACODS
CHAOBORUS
COEFICIENT OF DISPERSION
TIME

FIGURE 9

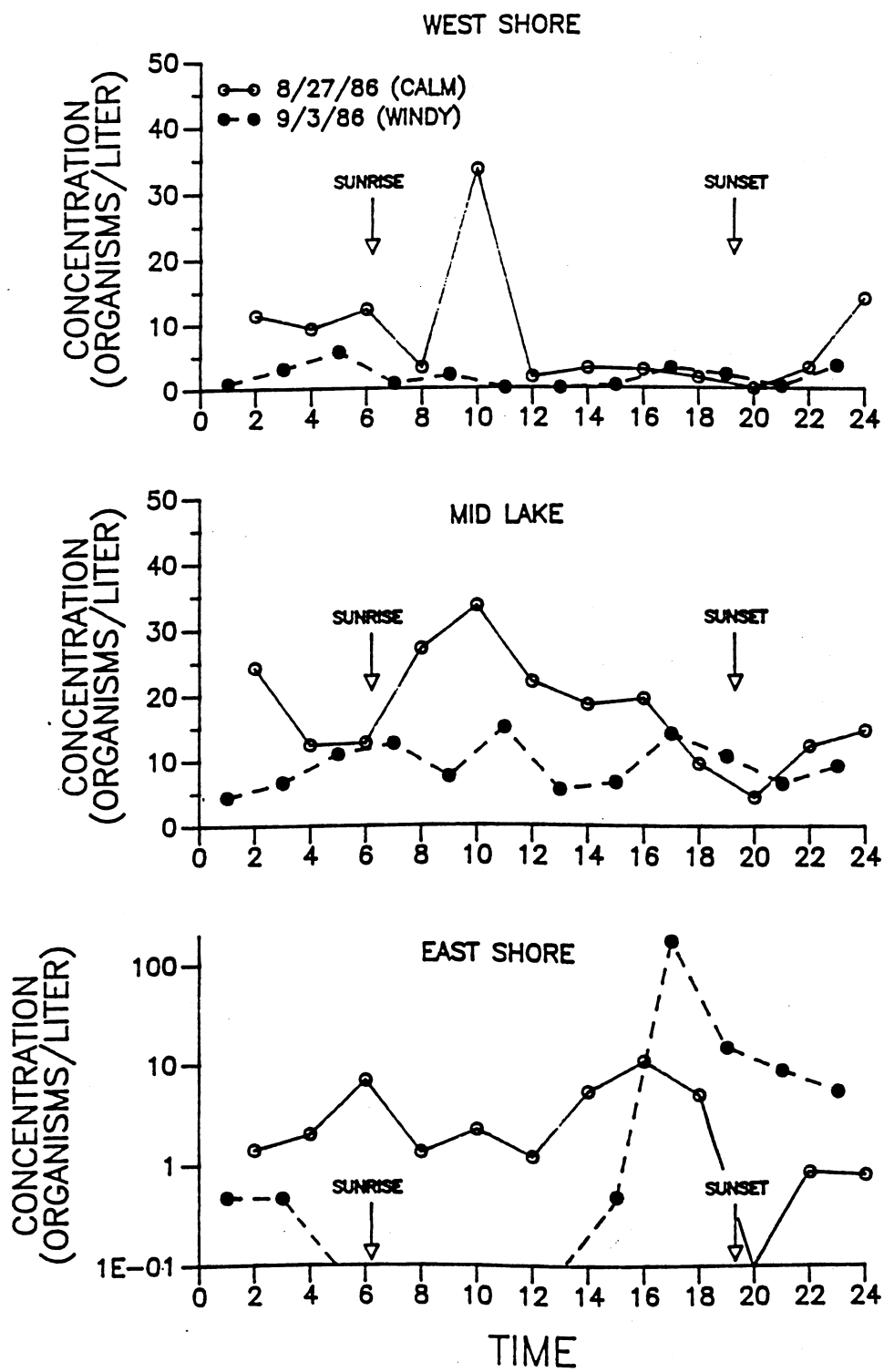
DAPHNIA GALEATA
WEST SHORE
8/27/86 (CALM)
9/3/86 (WINDY)
SUNRISE
SUNSET
CONCENTRATION (ORGANISMS/LITER)
MID LAKE
EAST SHORE
TIME

FIGURE 10

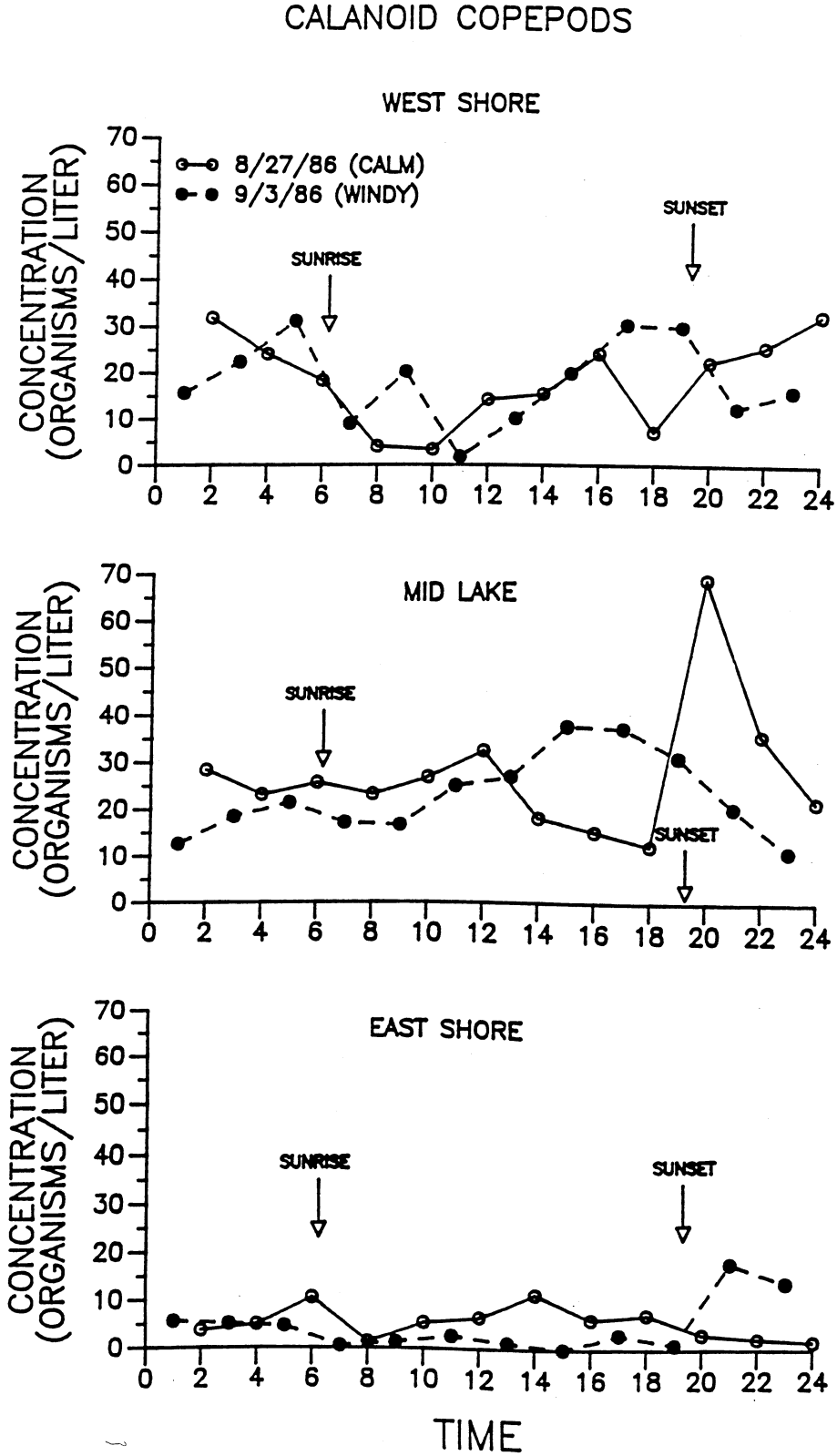
CALANOID COPEPODS
WEST SHORE
8/27/86 (CALM)
9/3/86 (WINDY)
SUNRISE
SUNSET
CONCENTRATION (ORGANISMS/LITER)
MID LAKE
EAST SHORE
TIME

FIGURE 11

DAPHNIA RETROCURVA

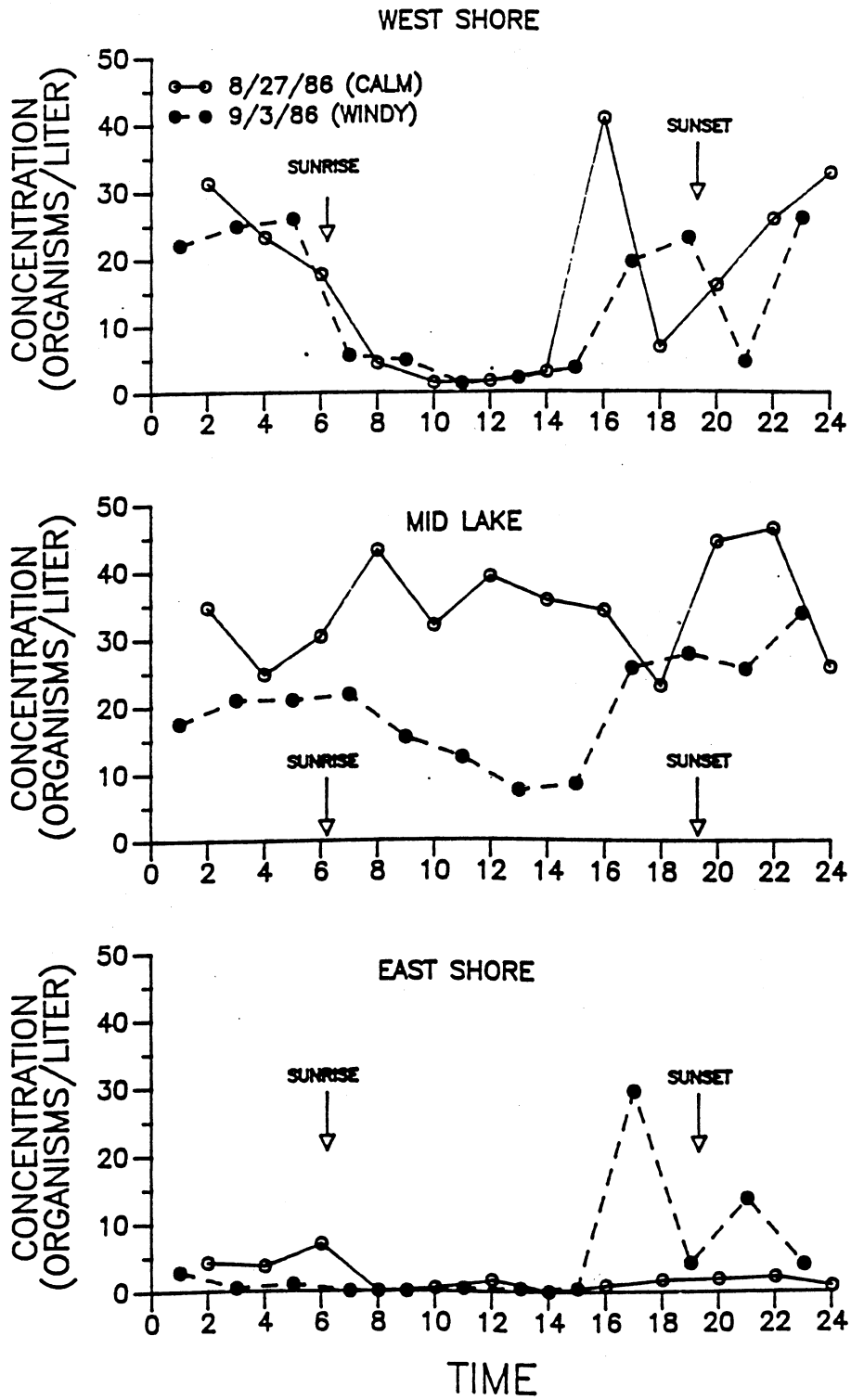

FIGURE 12

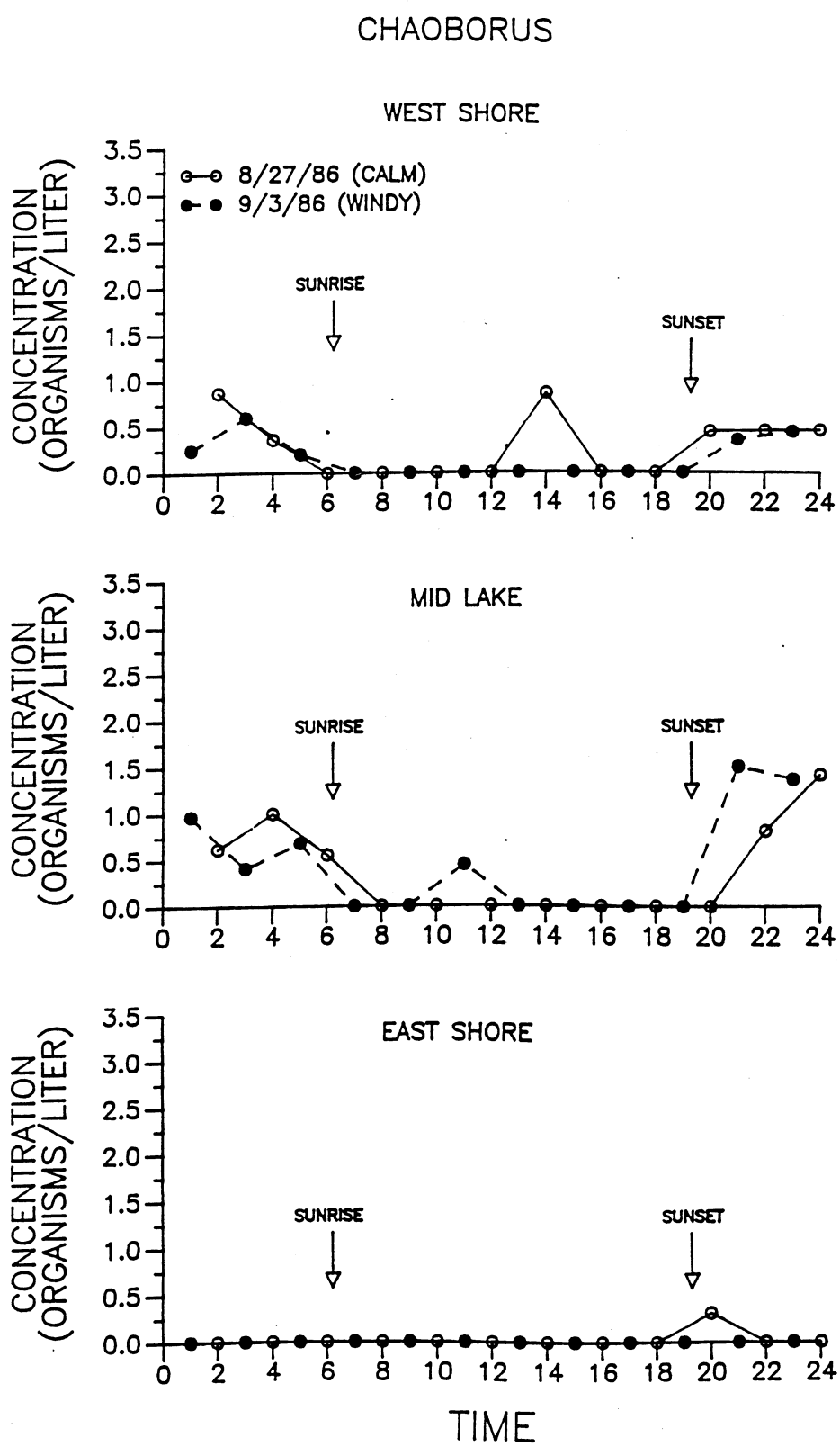
CHAOBORUS
WEST SHORE
8/27/86 (CALM)
9/3/86 (WINDY)
SUNRISE
SUNSET
MID LAKE
EAST SHORE
CONCENTRATION (ORGANISMS/LITER)
TIME
0.0
0.5
1.0
1.5
2.0
2.5
3.0
3.5
0
2
4
6
8
10
12
14
16
18
20
22
24

FIGURE 13

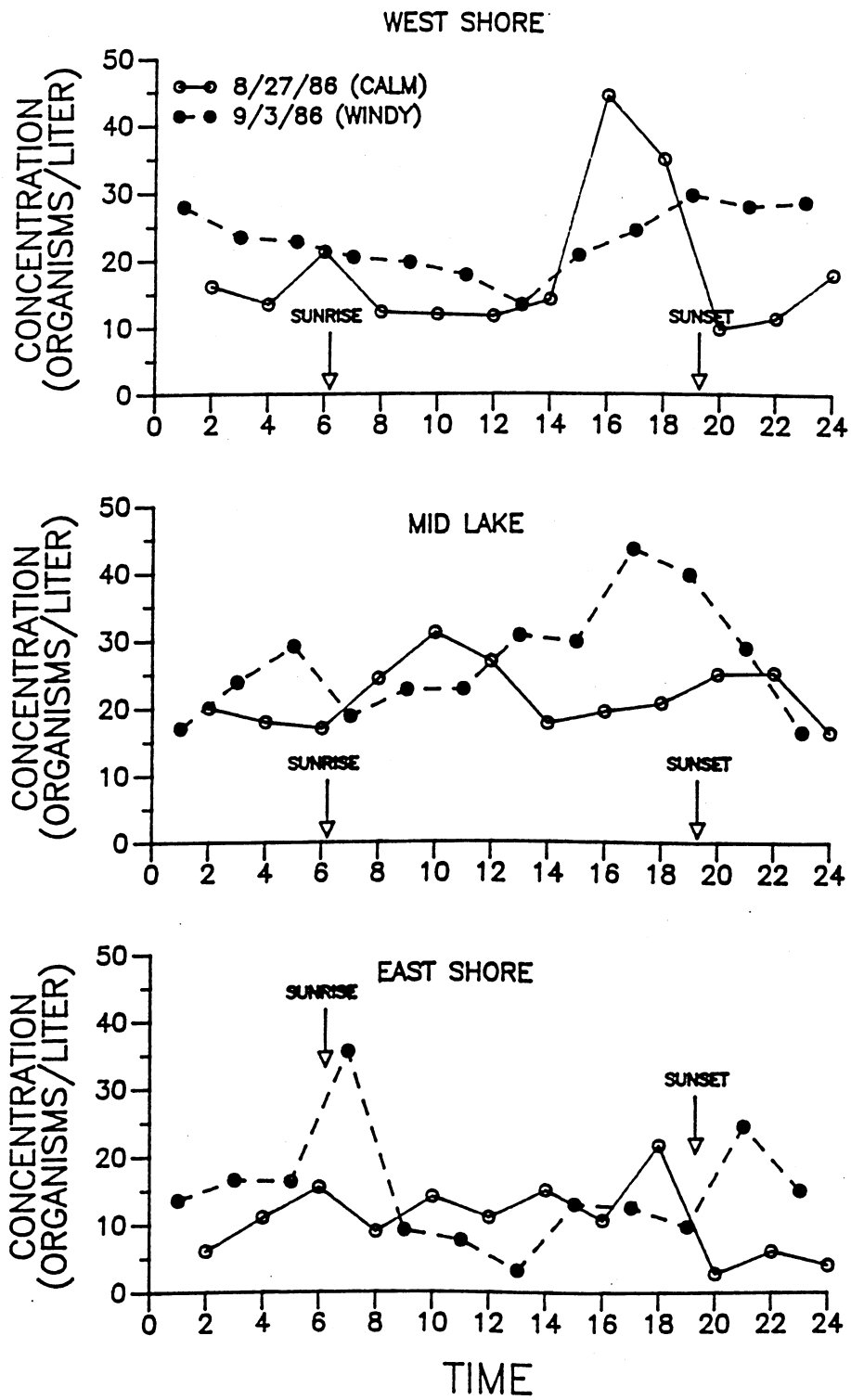
CYCLOPOID COPEPODS
WEST SHORE
8/27/86 (CALM)
9/3/86 (WINDY)
CONCENTRATION (ORGANISMS/LITER)
SUNRISE
SUNSET
MID LAKE
EAST SHORE
TIME

FIGURE 14

CHYDORUS

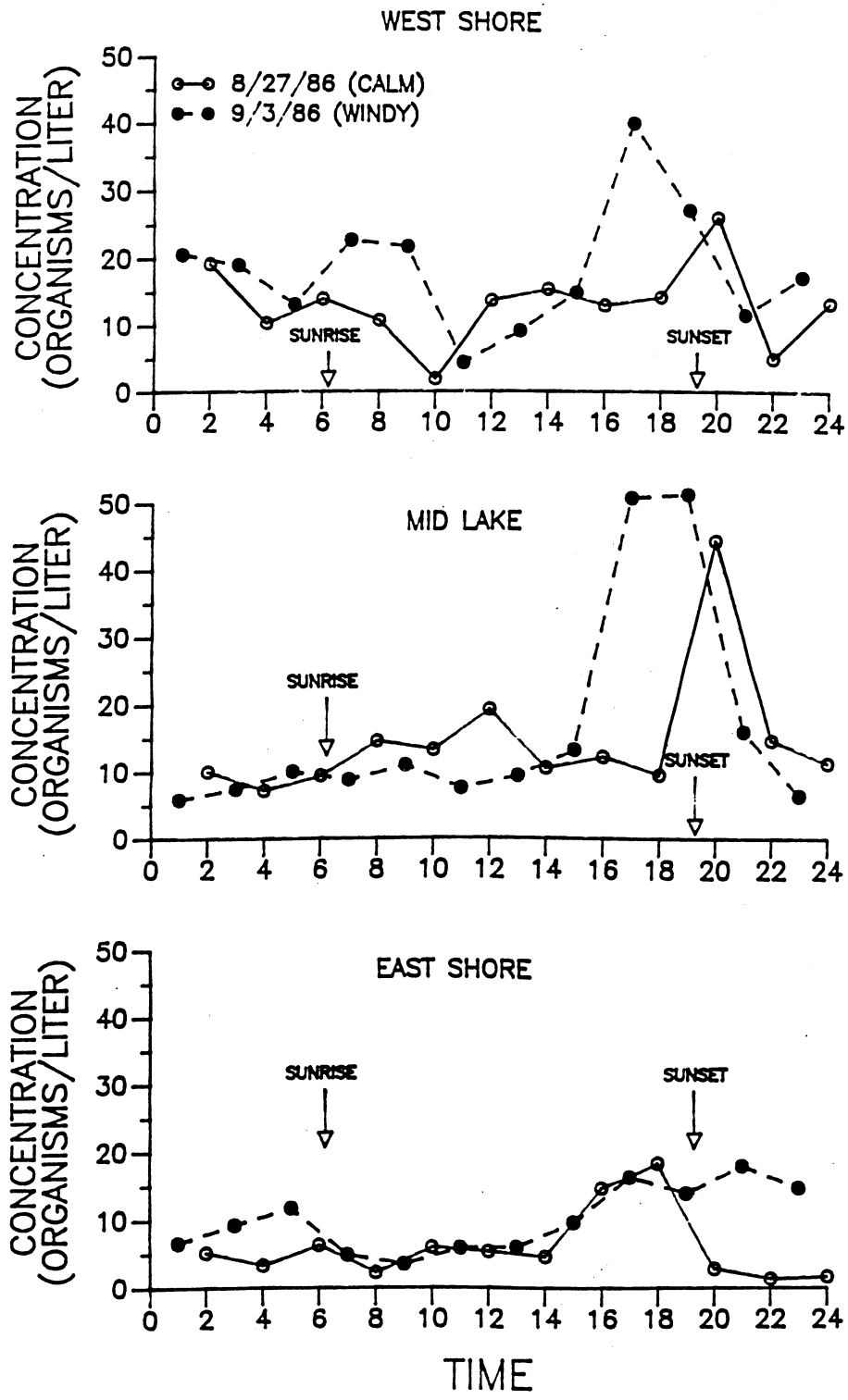

FIGURE 15

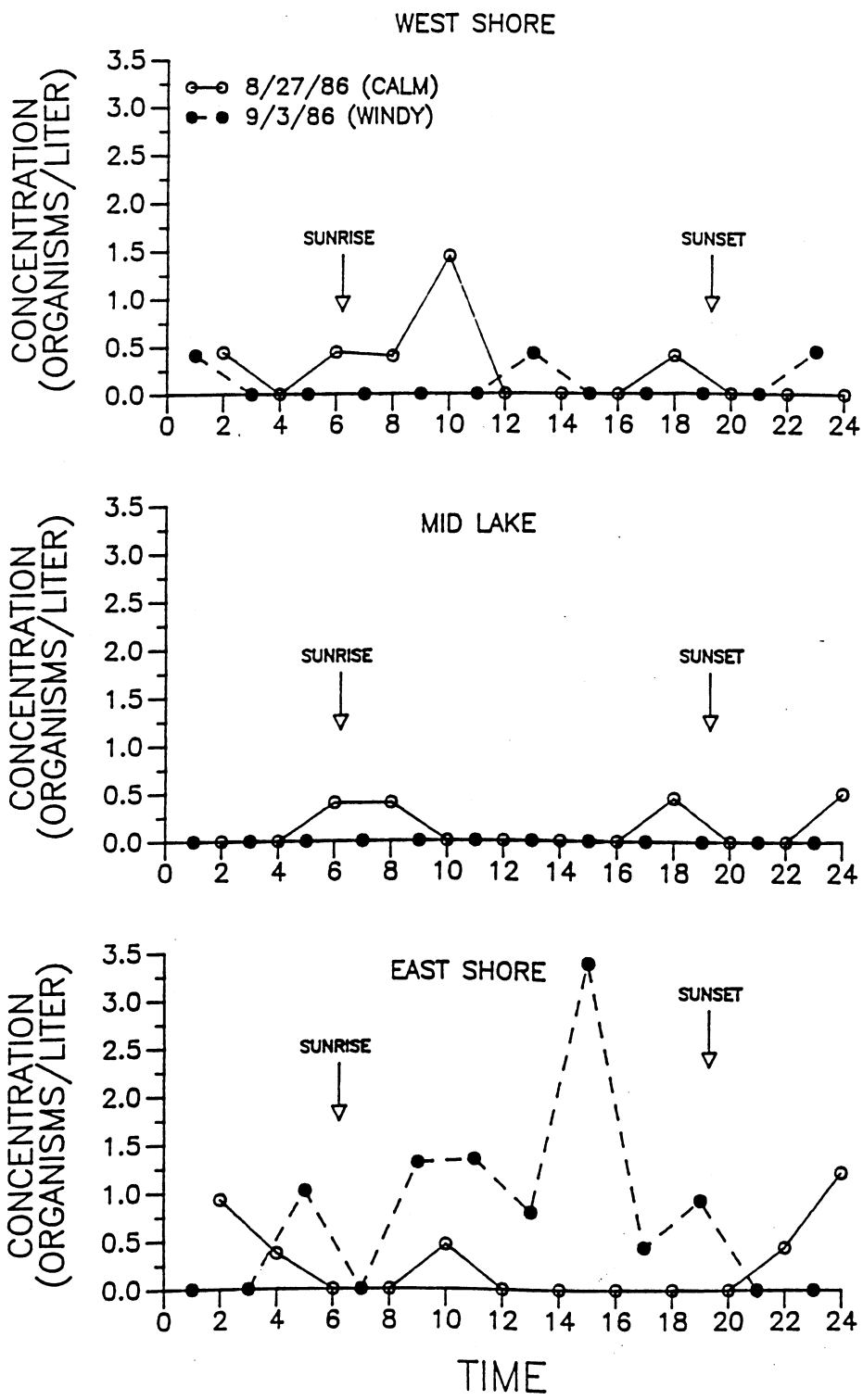
BOSMINA
WEST SHORE
8/27/86 (CALM)
9/3/86 (WINDY)
SUNRISE
SUNSET
MID LAKE
EAST SHORE
CONCENTRATION (ORGANISMS/LITER)
TIME
0.0
0.5
1.0
1.5
2.0
2.5
3.0
3.5
0 2 4 6 8 10 12 14 16 18 20 22 24

FIGURE 16

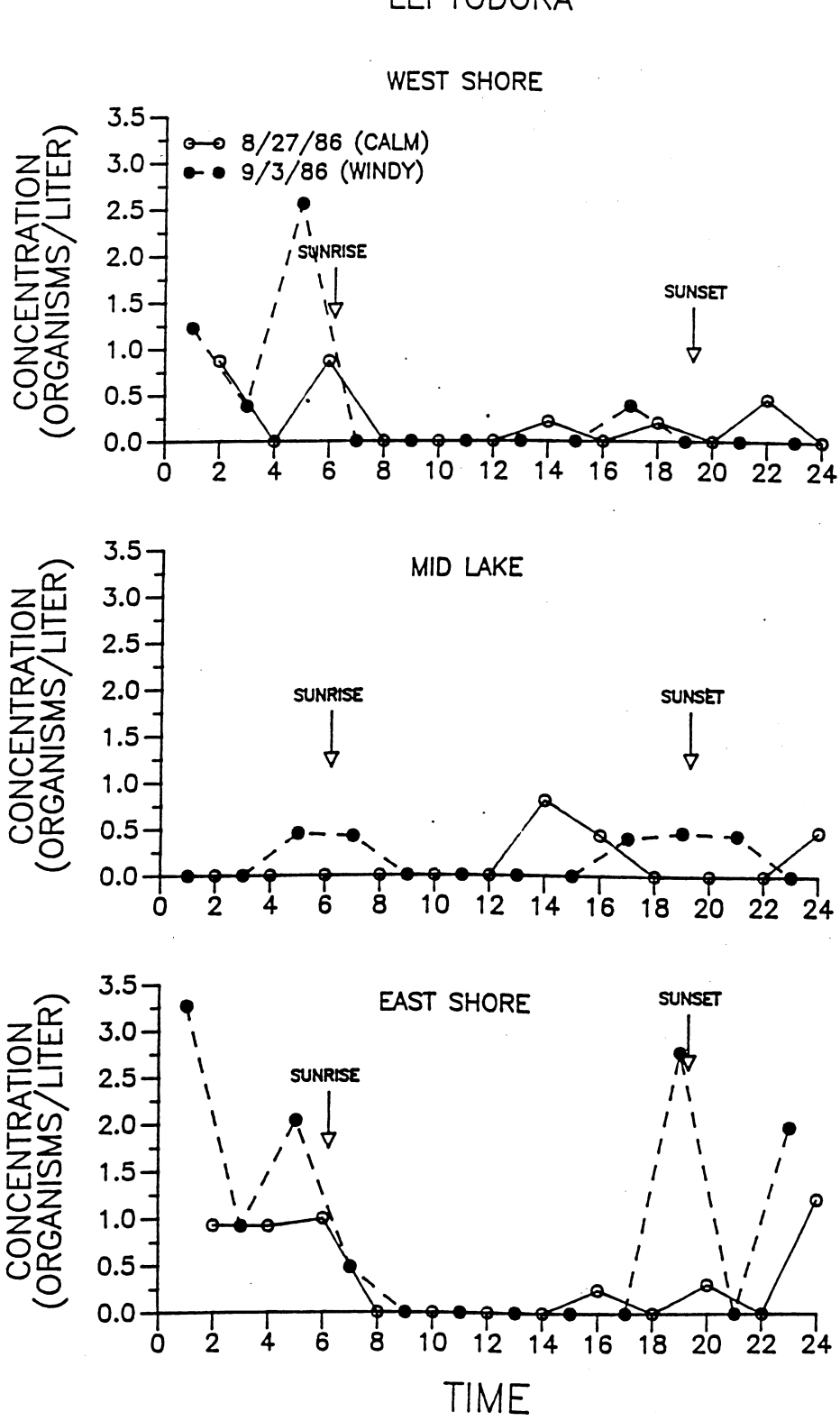
LEPTODORA
WEST SHORE
8/27/86 (CALM)
9/3/86 (WINDY)
SUNRISE
SUNSET
CONCENTRATION (ORGANISMS/LITER)
MID LAKE
SUNRISE
SUNSET
CONCENTRATION (ORGANISMS/LITER)
EAST SHORE
SUNRISE
SUNSET
CONCENTRATION (ORGANISMS/LITER)
0.0 0.5 1.0 1.5 2.0 2.5 3.0 3.5
0 2 4 6 8 10 12 14 16 18 20 22 24
TIME

FIGURE 17

NAUPLII

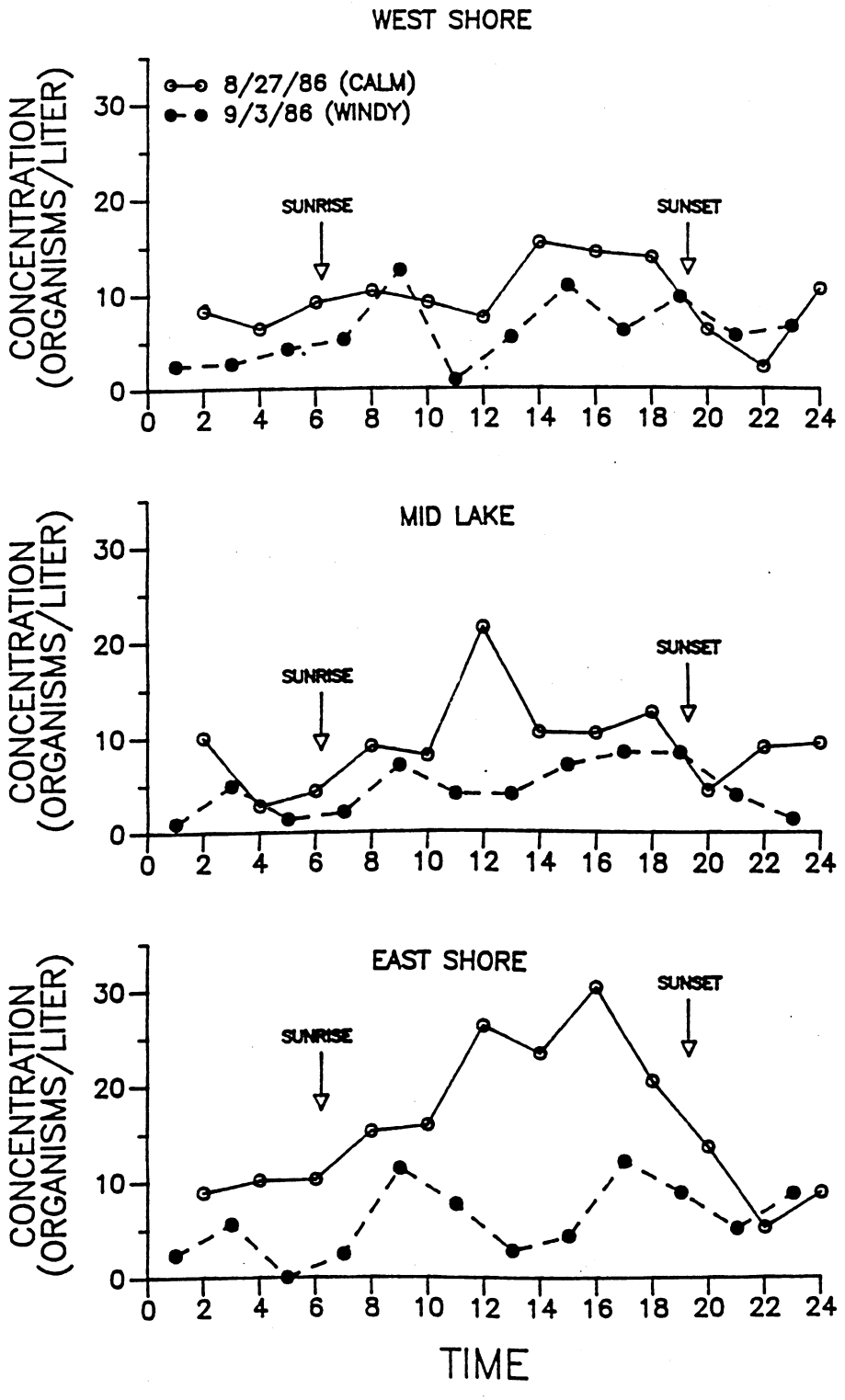

FIGURE 18

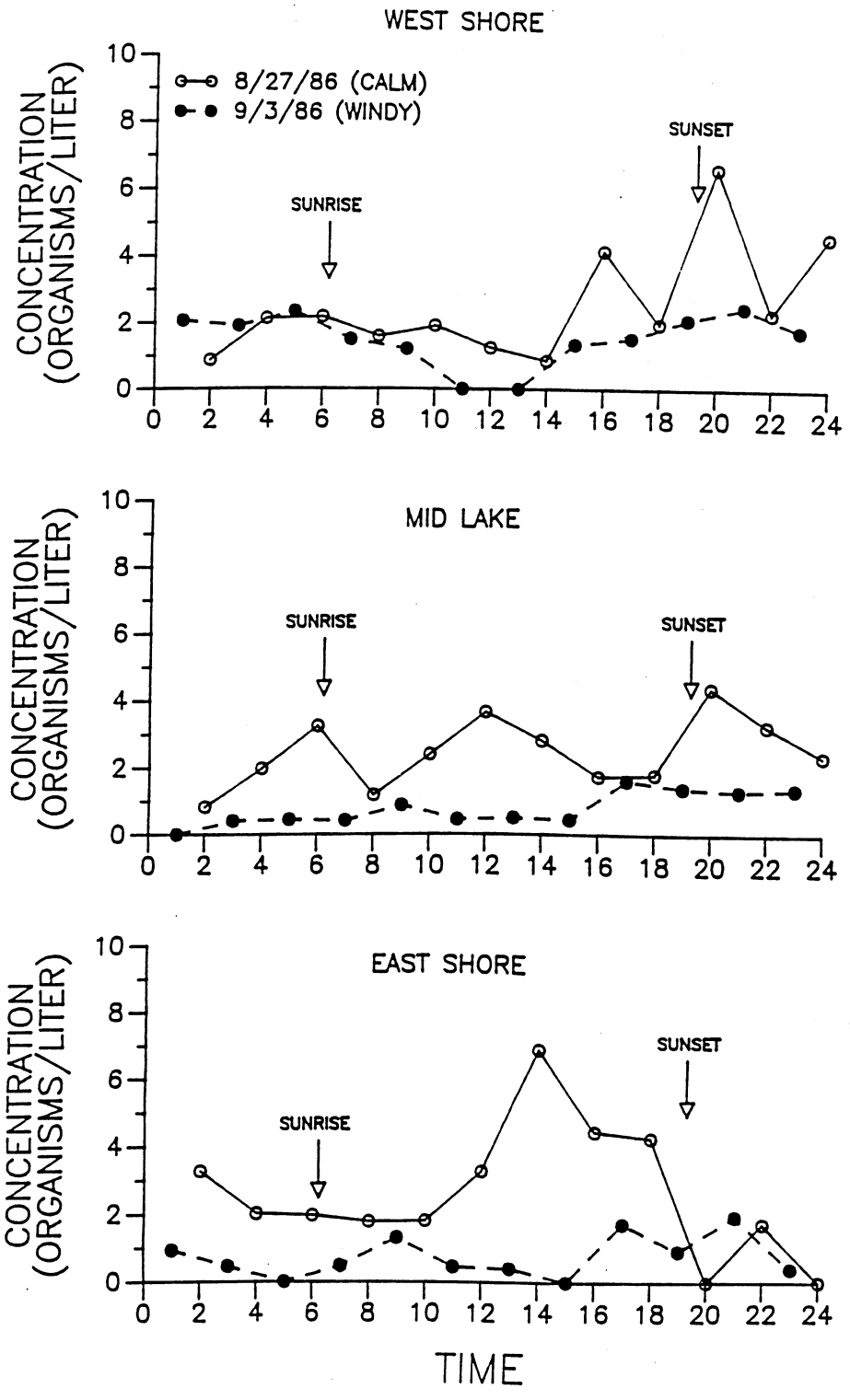
DIAPHANOSOMA
WEST SHORE
8/27/86 (CALM)
9/3/86 (WINDY)
SUNRISE
SUNSET
CONCENTRATION (ORGANISMS/LITER)
MID LAKE
SUNRISE
SUNSET
CONCENTRATION (ORGANISMS/LITER)
EAST SHORE
SUNRISE
SUNSET
CONCENTRATION (ORGANISMS/LITER)
0 2 4 6 8 10 12 14 16 18 20 22 24
TIME

FIGURE 19

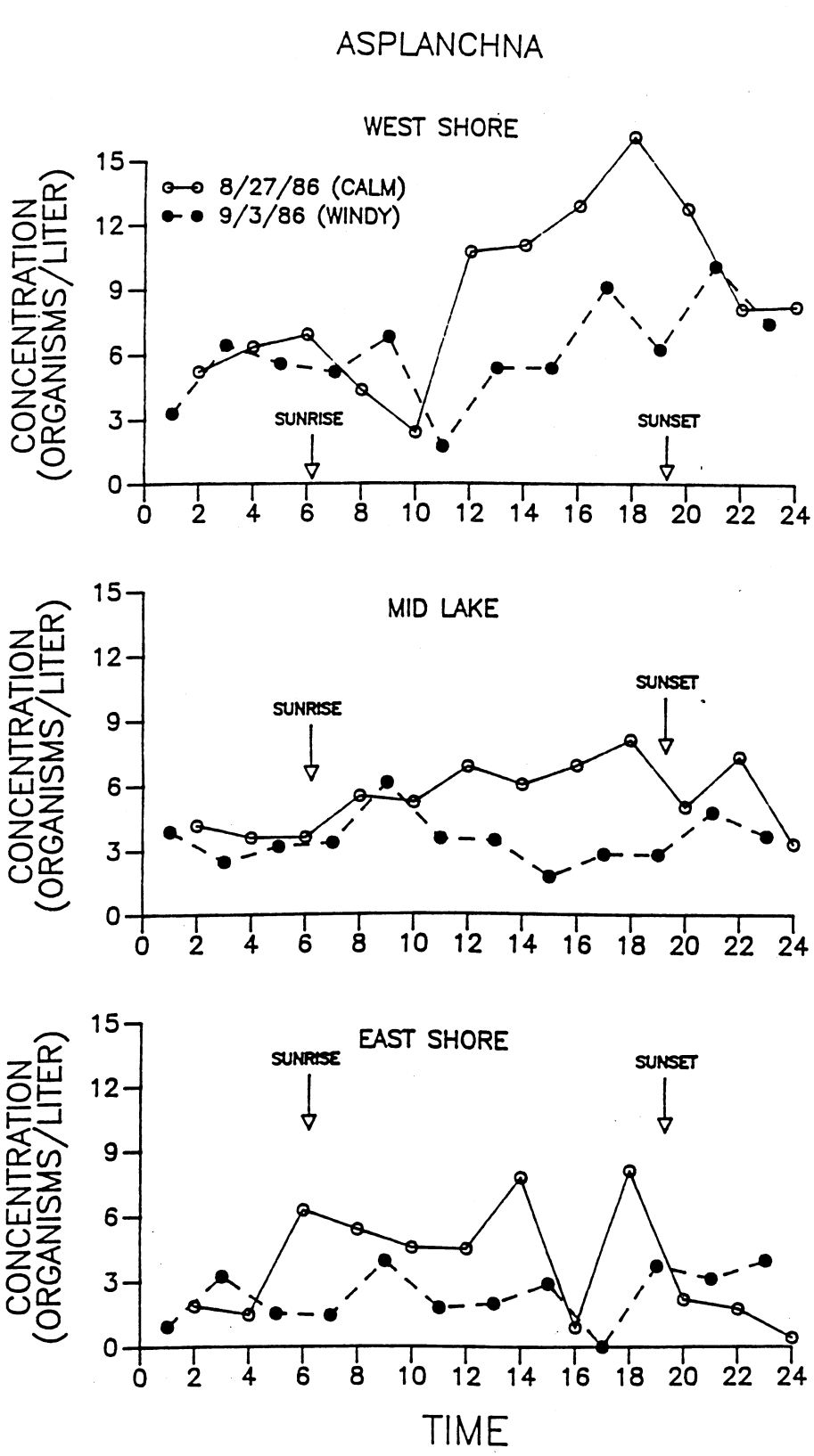
ASPLANCHNA
WEST SHORE
8/27/86 (CALM)
9/3/86 (WINDY)
CONCENTRATION (ORGANISMS/LITER)
SUNRISE
SUNSET
MID LAKE
EAST SHORE
TIME

FIGURE 20

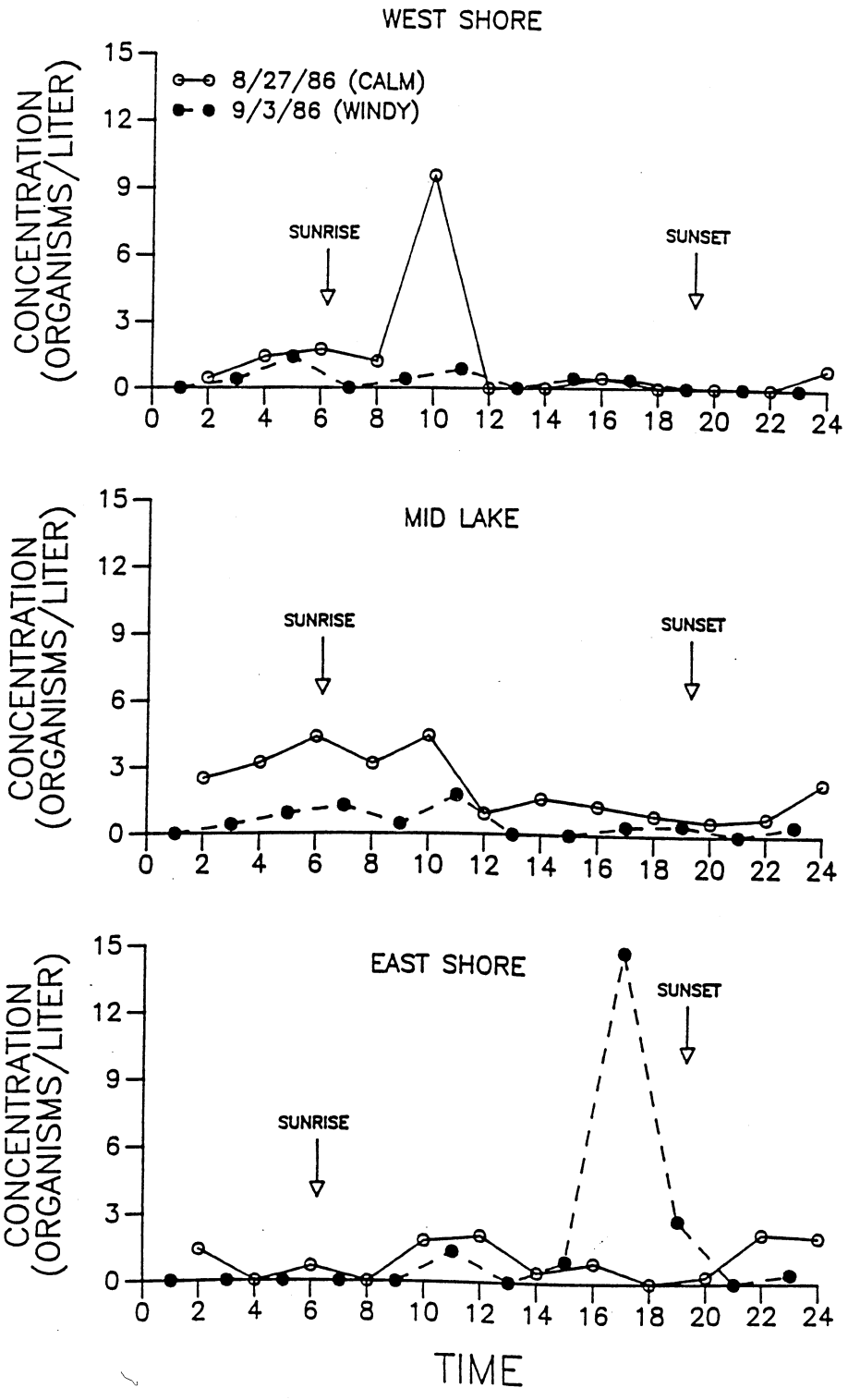
CERIODAPHNIA
WEST SHORE
8/27/86 (CALM)
9/3/86 (WINDY)
SUNRISE
SUNSET
MID LAKE
EAST SHORE
CONCENTRATION (ORGANISMS/LITER)
TIME
0 2 4 6 8 10 12 14 16 18 20 22 24
0 3 6 9 12 15

FIGURE 21

CALANOID COPEPODS

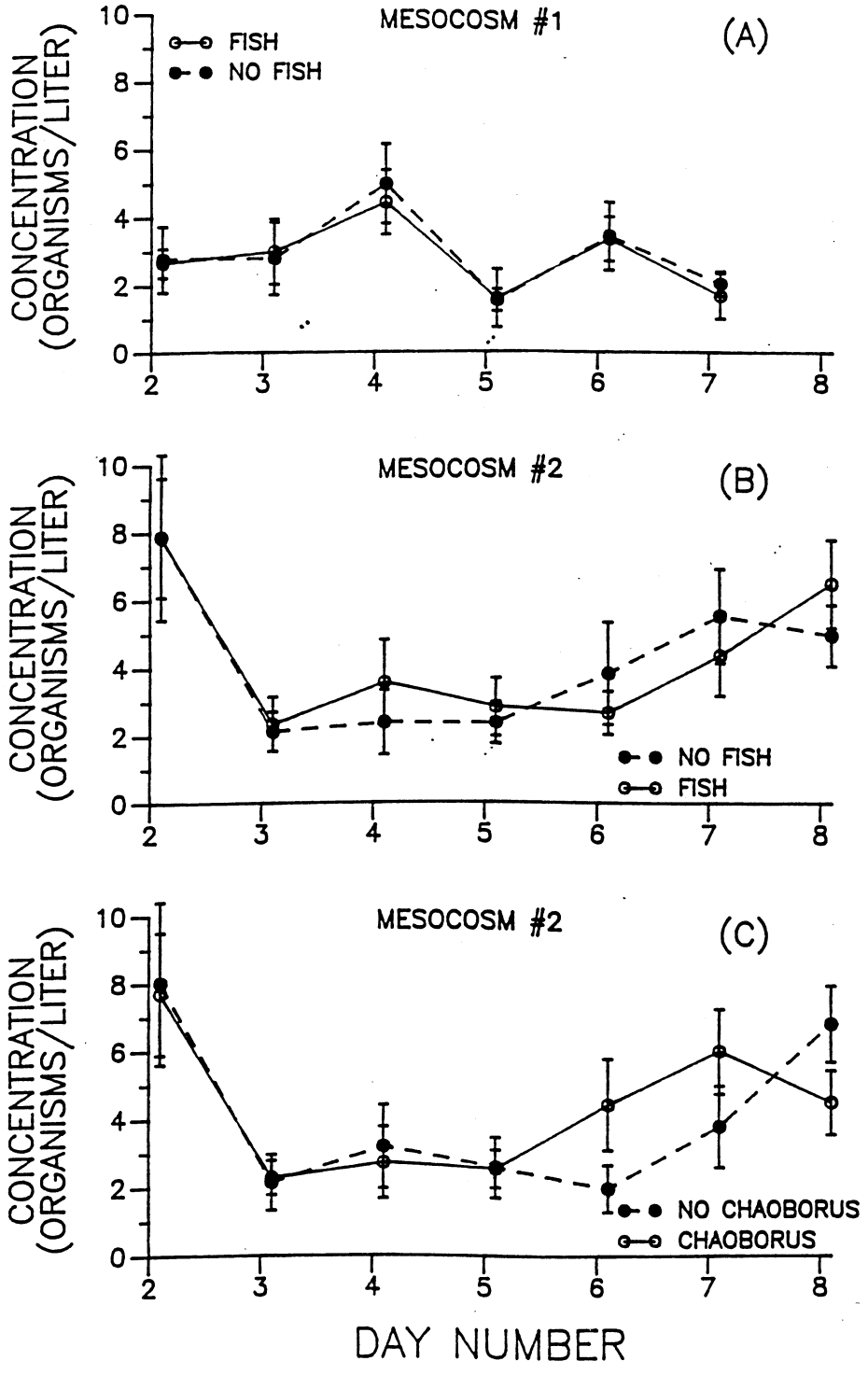

FIGURE 22

CYCLOPOID COPEPODS

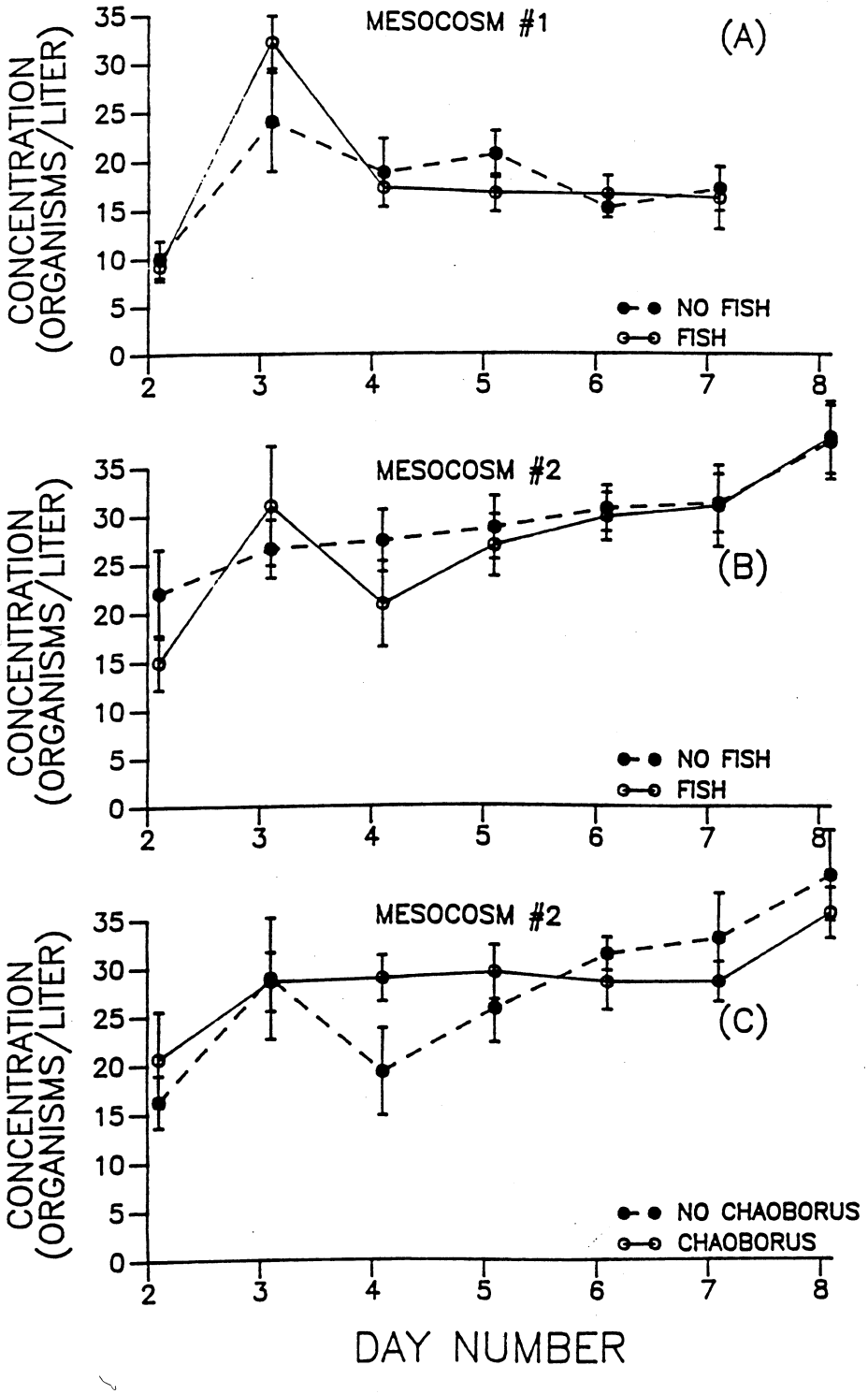

FIGURE 23

NAUPLII

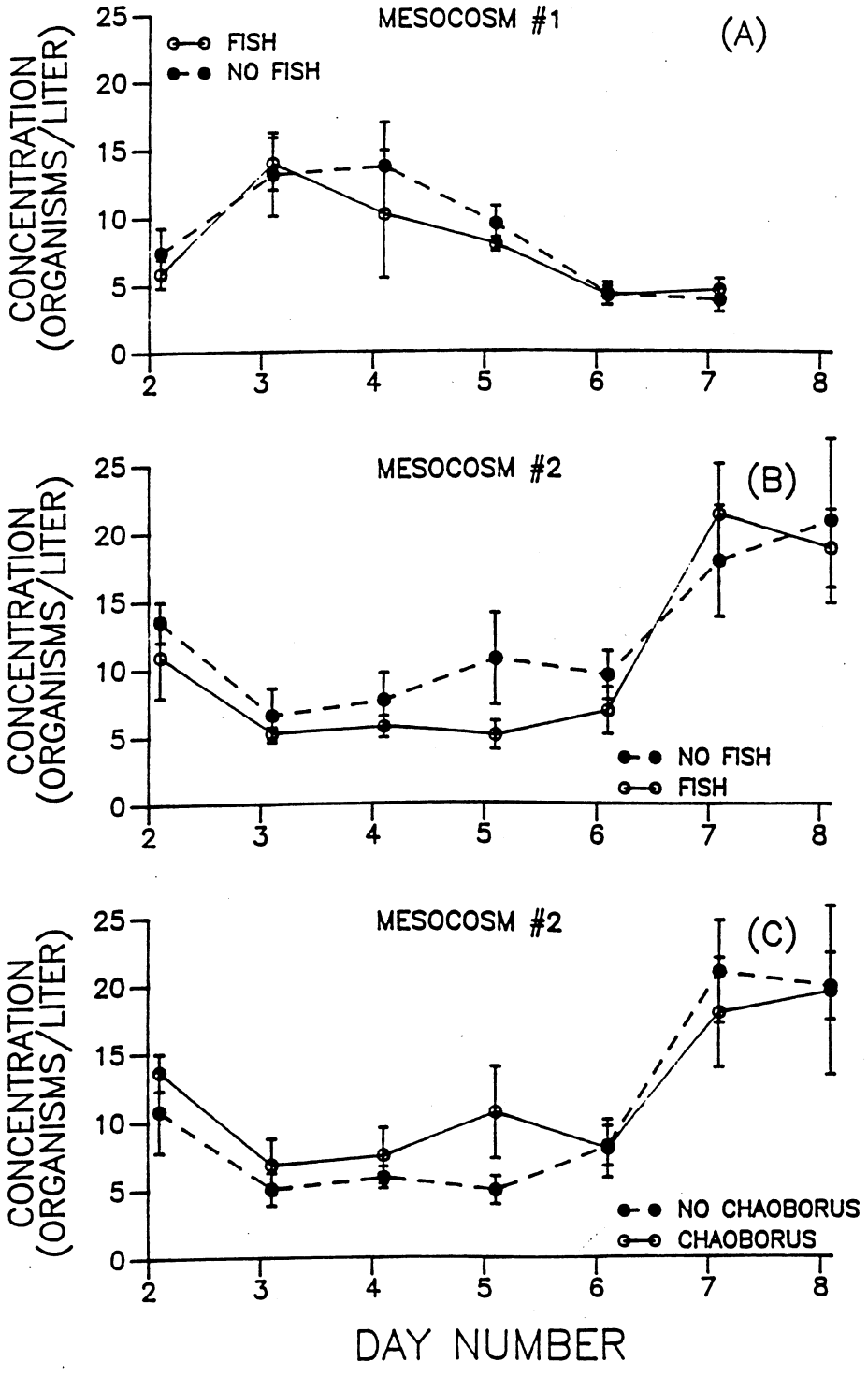

FIGURE 24

CERIODAPHNIA

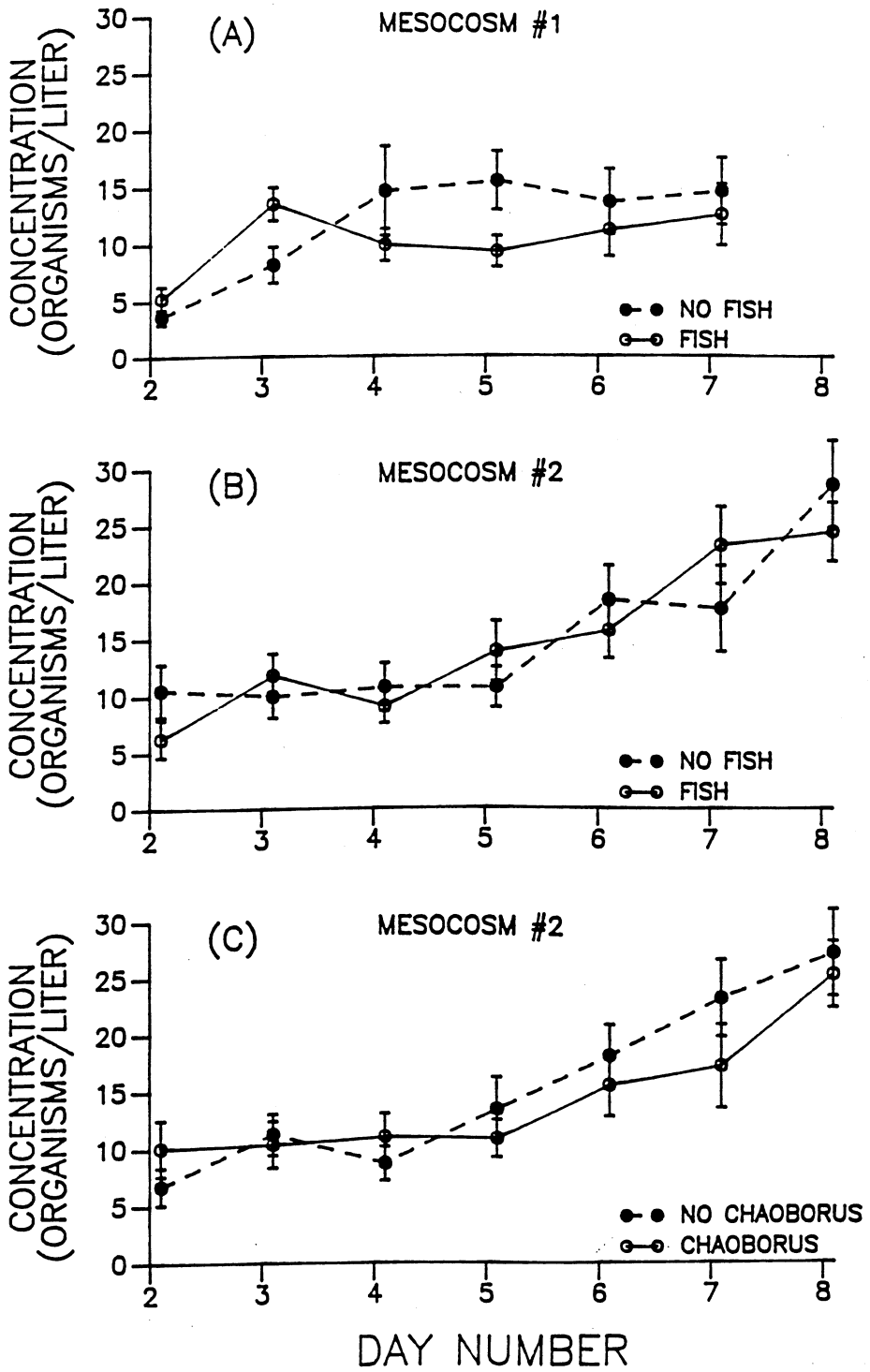

FIGURE 25

DIAPHANOSOMA

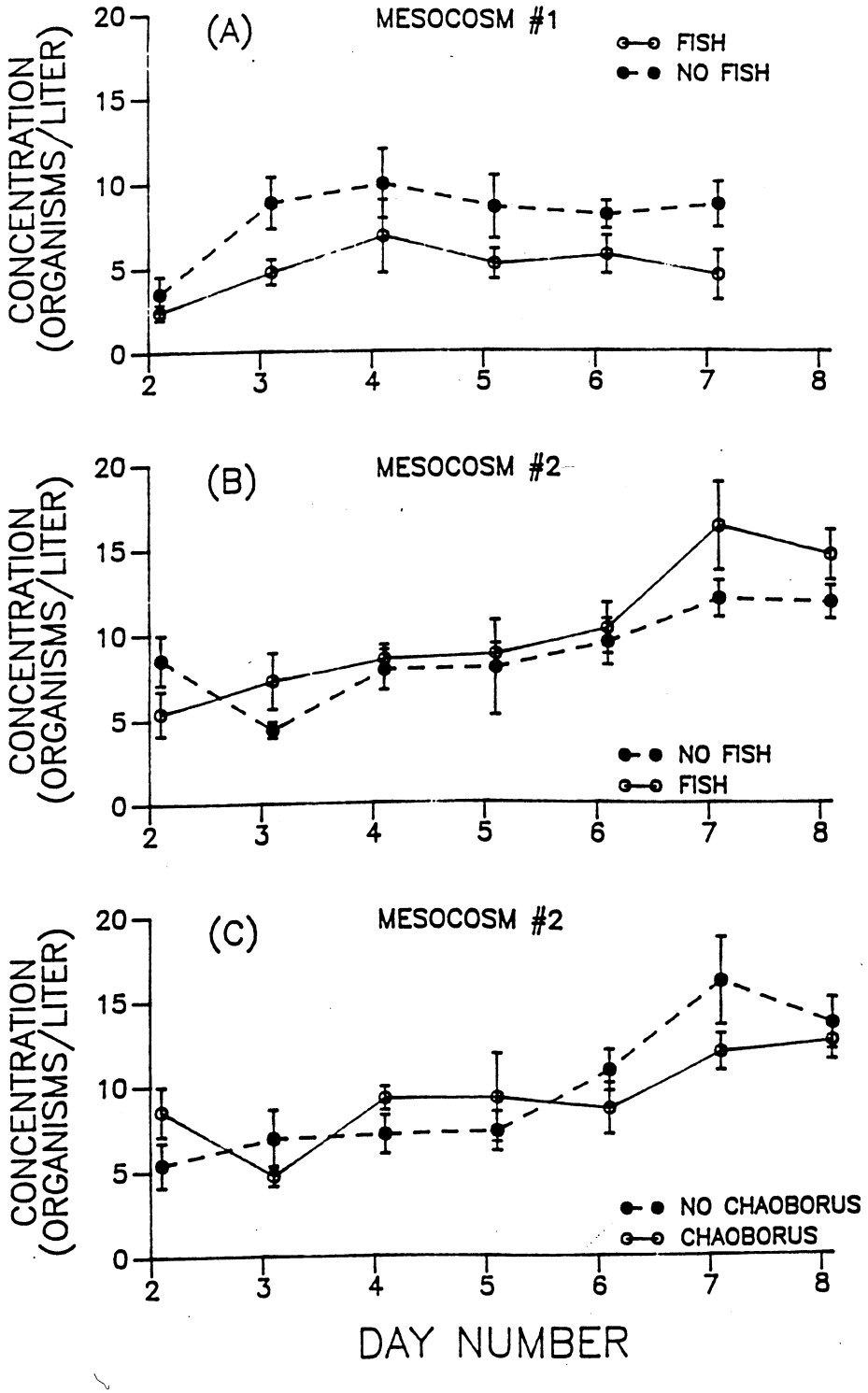

FIGURE 26

ASPLANCHNA

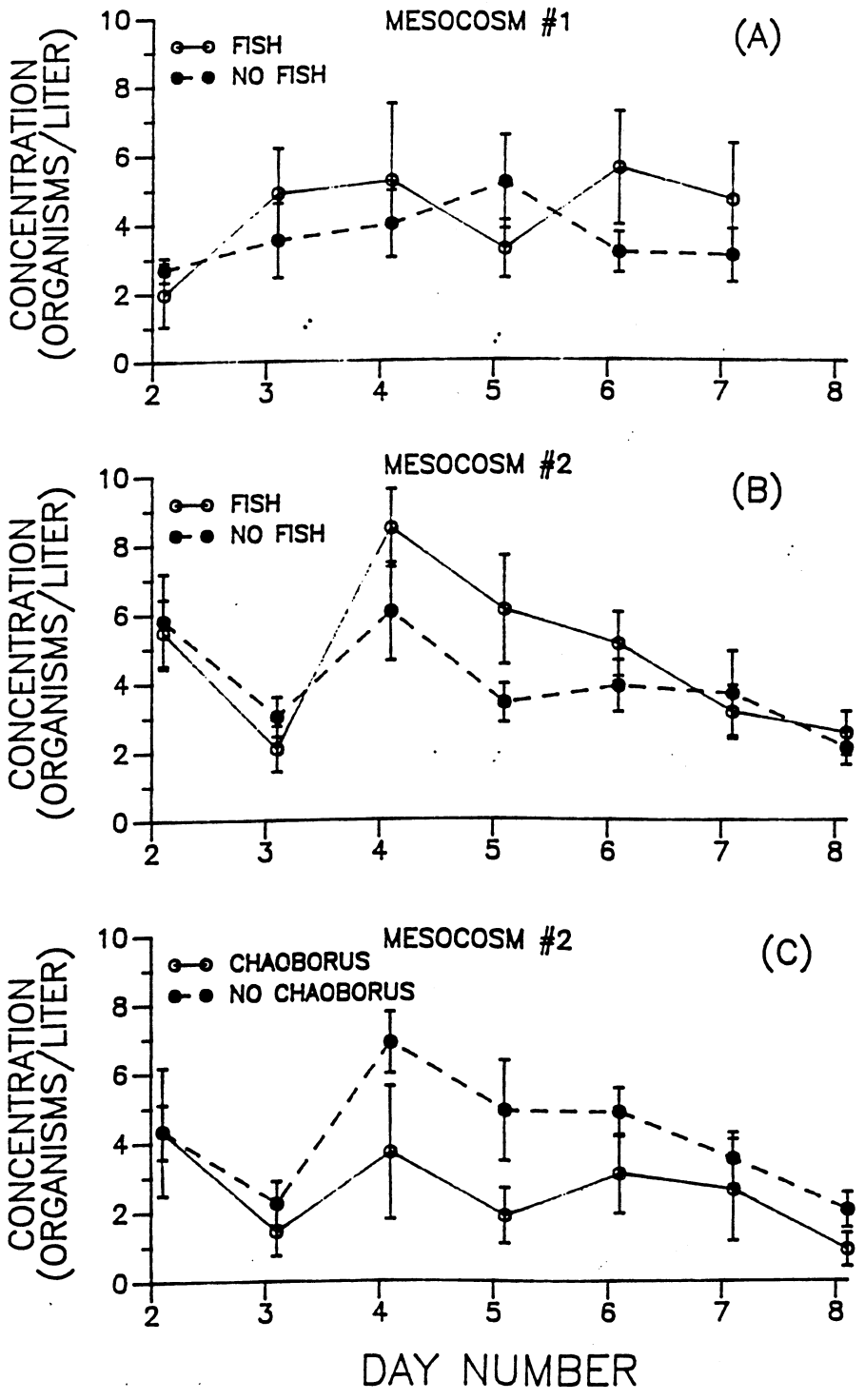

FIGURE 27

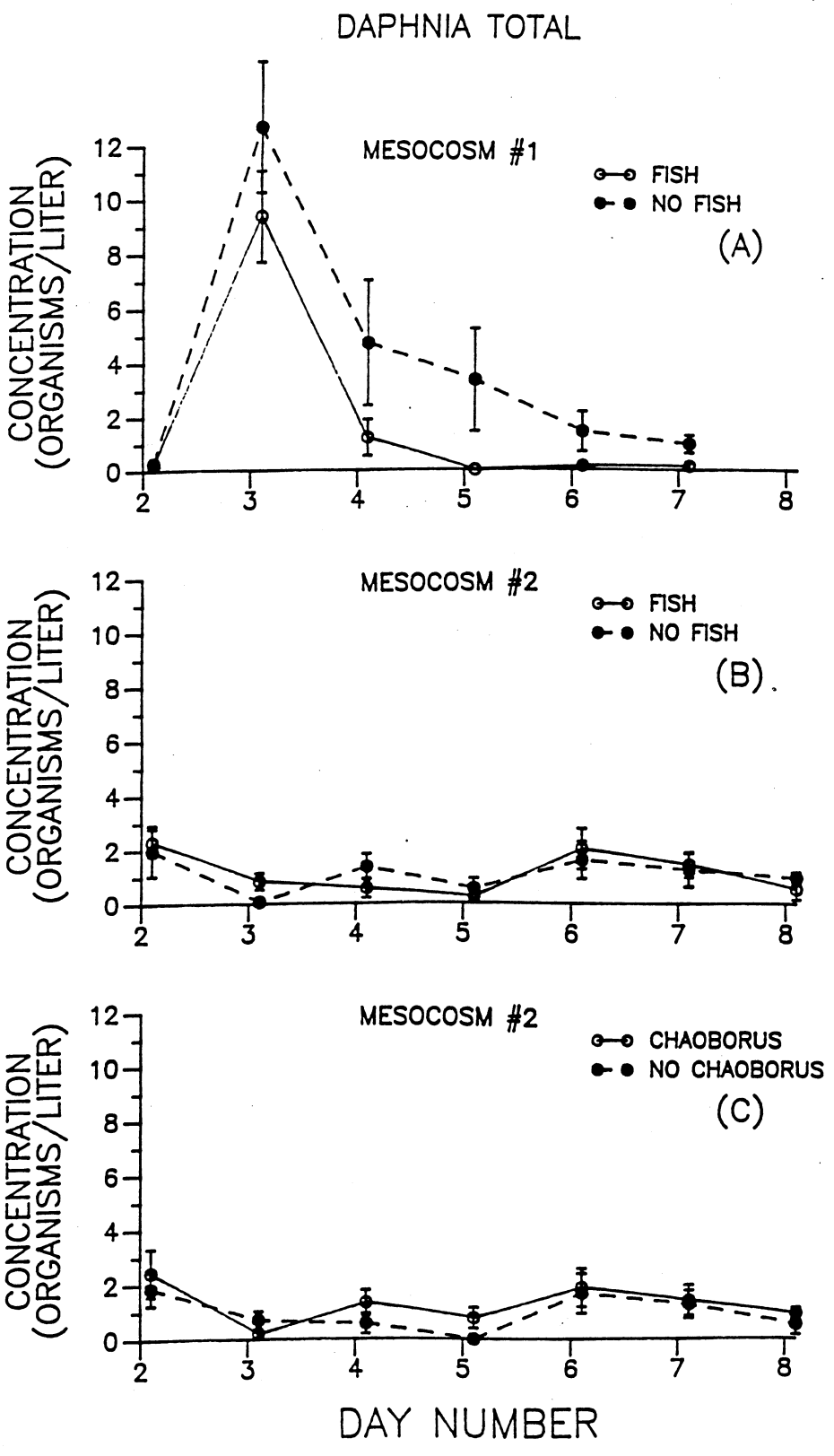
DAPHNIA TOTAL
MESOCOSM #1
FISH
NO FISH
(A)
CONCENTRATION (ORGANISMS/LITER)
MESOCOSM #2
FISH
NO FISH
(B)
MESOCOSM #2
CHAOBORUS
NO CHAOBORUS
(C)
DAY NUMBER

FIGURE 28

CHAOBORUS

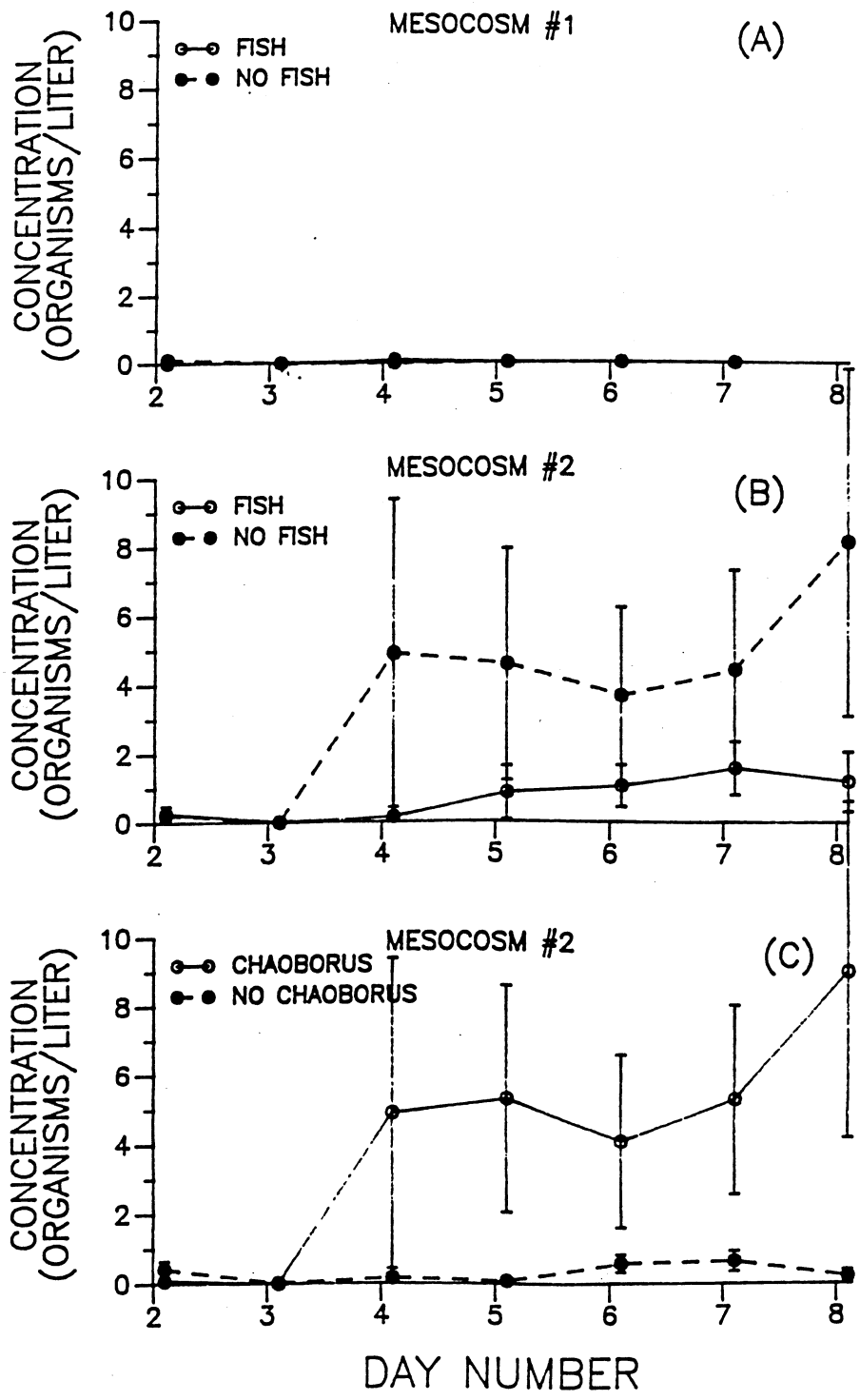

FIGURE 29

BOSMINA

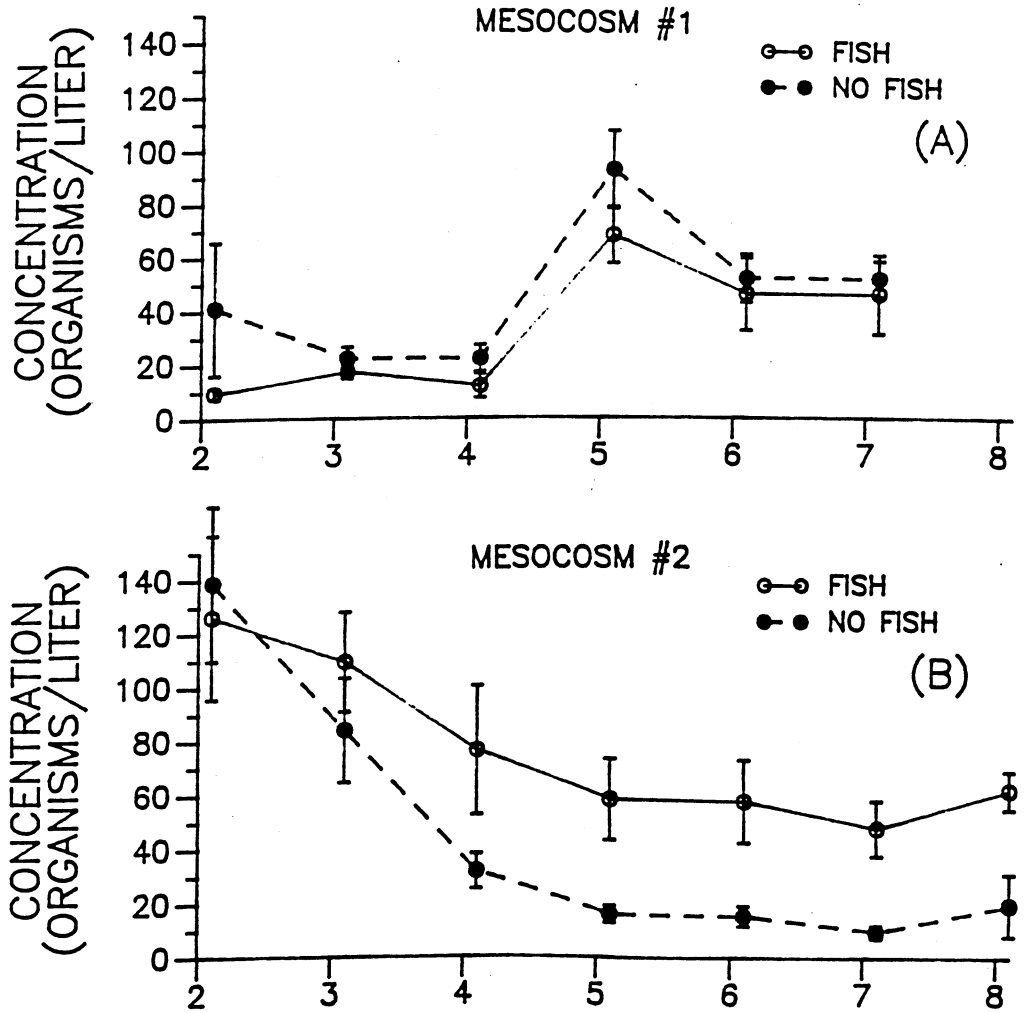

FIGURE 30

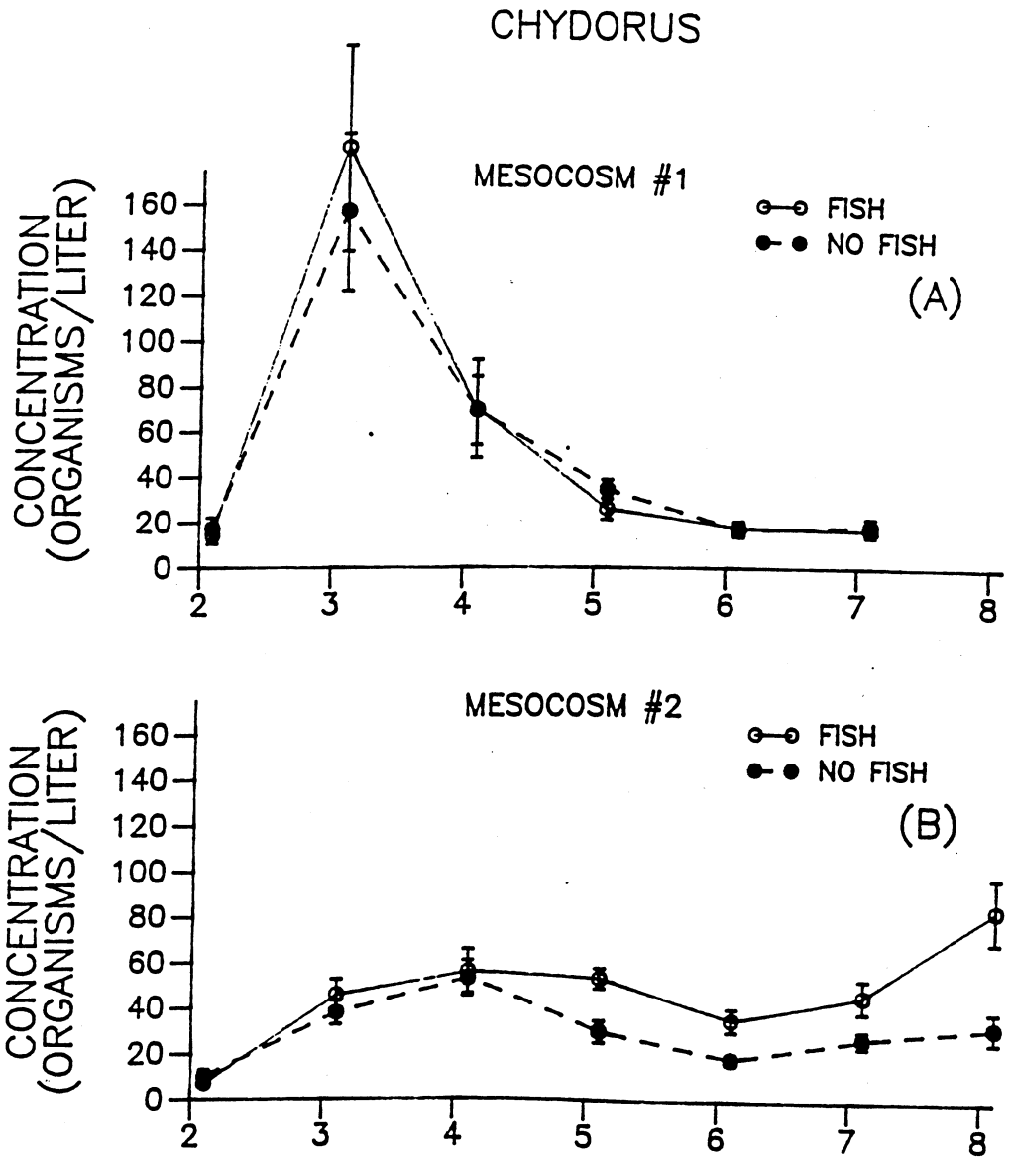
CHYDORUS
MESOCOSM #1
FISH
NO FISH
(A)
CONCENTRATION (ORGANISMS/LITER)
160
140
120
100
80
60
40
20
0
2
3
4
5
6
7
8
MESOCOSM #2
FISH
NO FISH
(B)
CONCENTRATION (ORGANISMS/LITER)
160
140
120
100
80
60
40
20
0
2
3
4
5
6
7
8

FIGURE 31

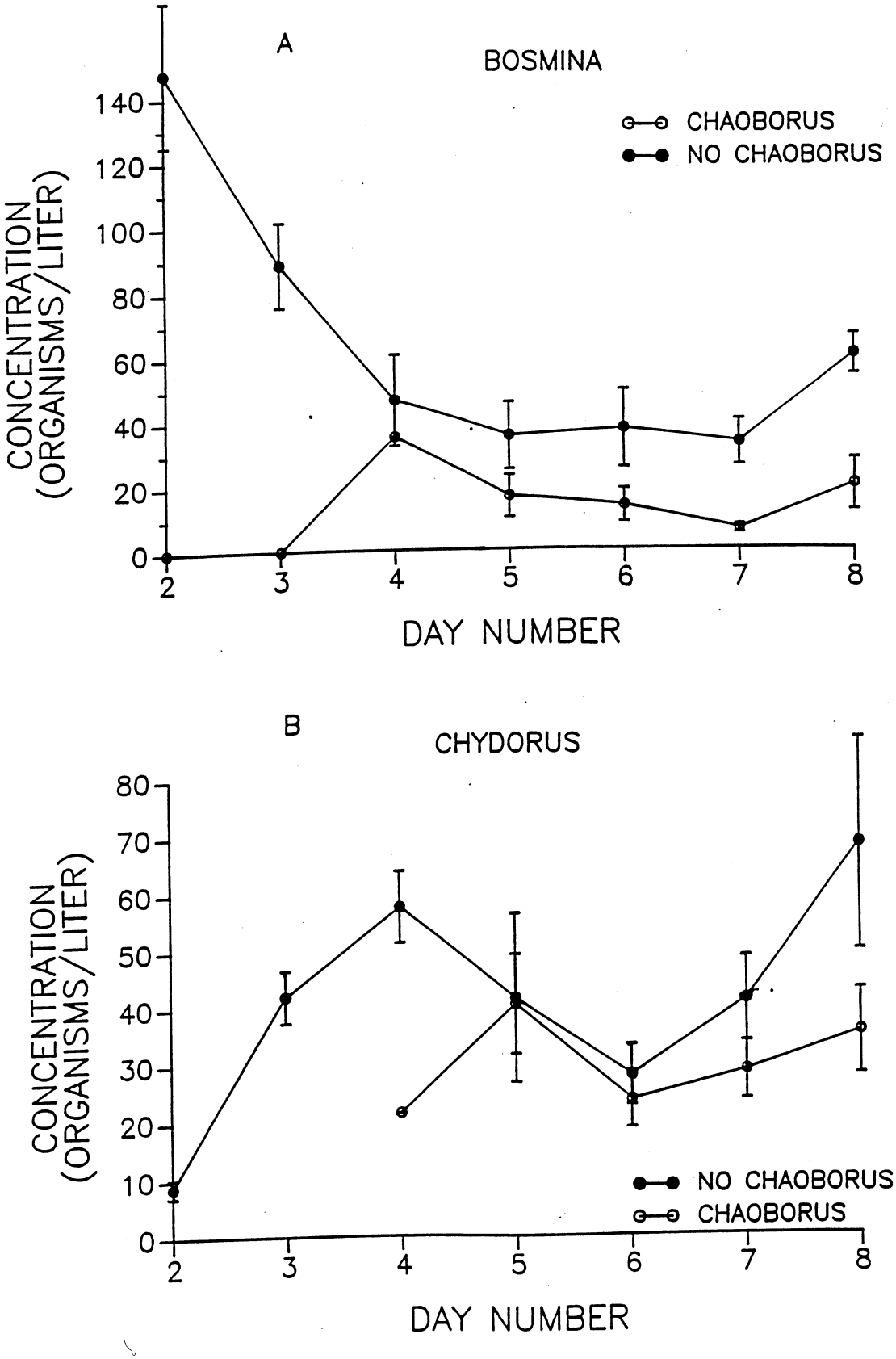
A
BOSMINA
CHAOBORUS
NO CHAOBORUS
CONCENTRATION (ORGANISMS/LITER)
140
120
100
80
60
40
20
0
2
3
4
5
6
7
8
DAY NUMBER
B
CHYDORUS
CONCENTRATION (ORGANISMS/LITER)
80
70
60
50
40
30
20
10
0
NO CHAOBORUS
CHAOBORUS
2
3
4
5
6
7
8
DAY NUMBER

FIGURE 32

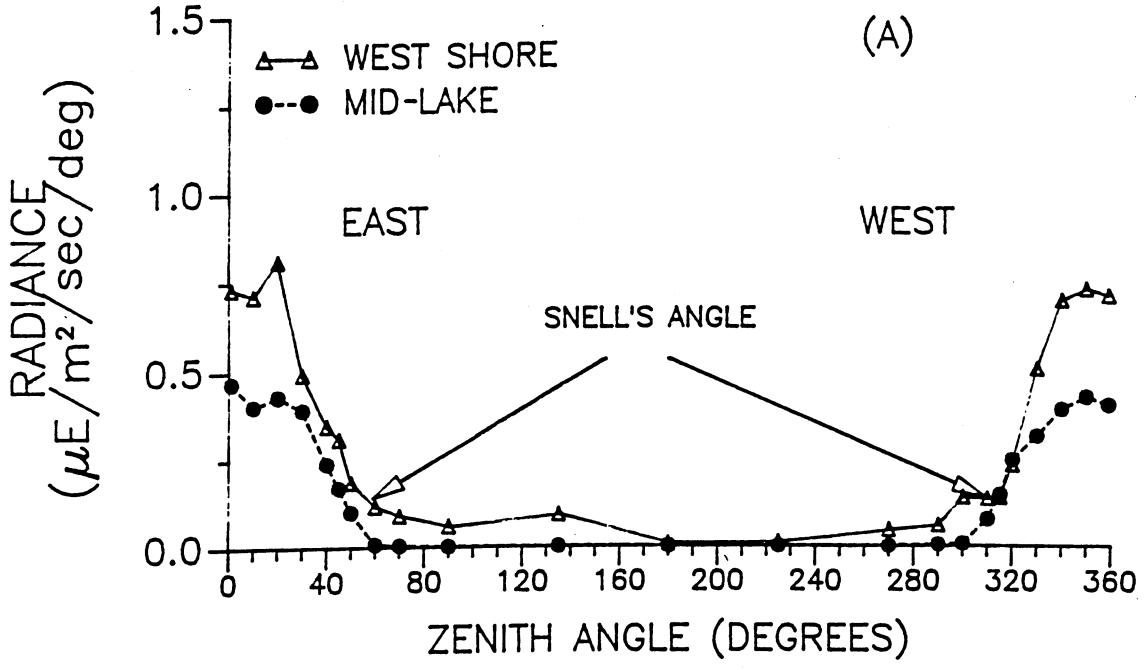
(A)
WEST SHORE
MID-LAKE
EAST
WEST
SNELL'S ANGLE
RADIANCE (μE/m²/sec/deg)
1.5
1.0
0.5
0.0
0
40
80
120
160
200
240
280
320
360
ZENITH ANGLE (DEGREES)

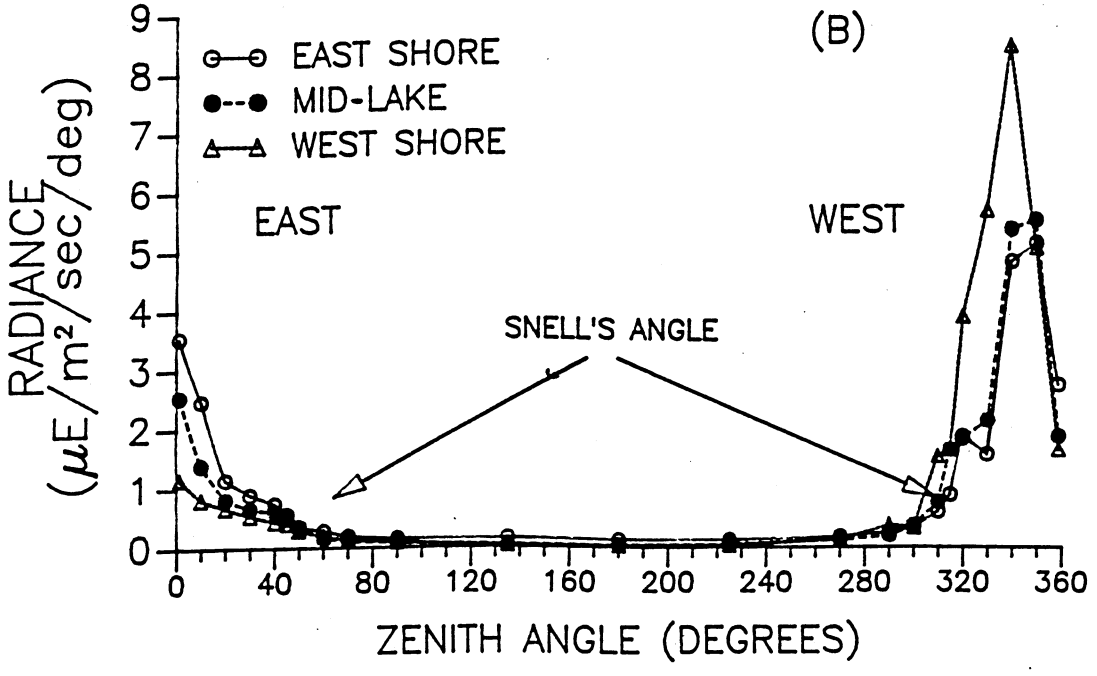
(B)
EAST SHORE
MID-LAKE
WEST SHORE
EAST
WEST
SNELL'S ANGLE
RADIANCE (μE/m²/sec/deg)
9
8
7
6
5
4
3
2
1
0
0
40
80
120
160
200
240
280
320
360
ZENITH ANGLE (DEGREES)

FIGURE 33

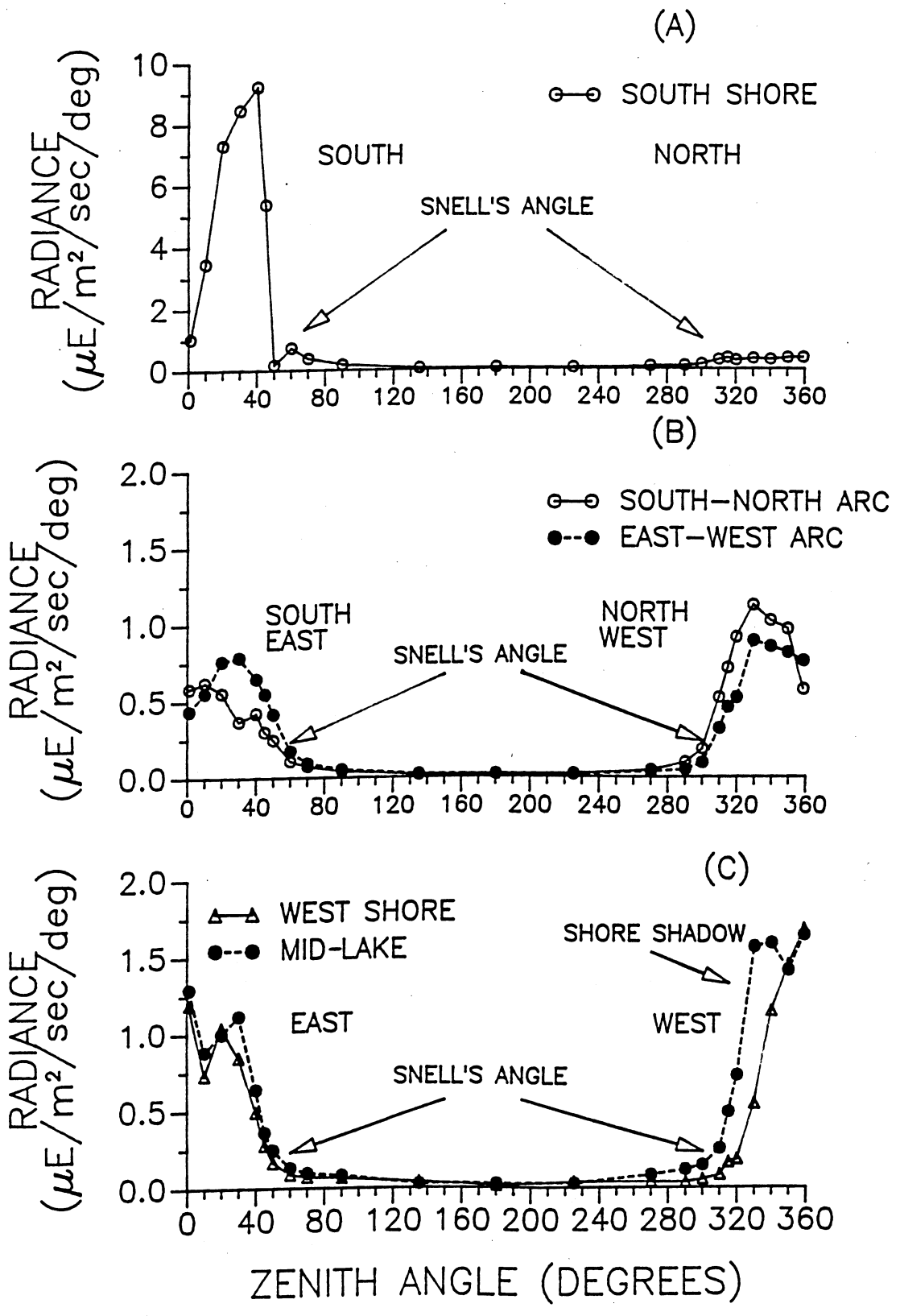
(A)
SOUTH SHORE
SOUTH
NORTH
SNELL'S ANGLE
RADIANCE (μE/m²/sec/deg)
10
8
6
4
2
0
0 40 80 120 160 200 240 280 320 360
(B)
SOUTH–NORTH ARC
EAST–WEST ARC
SOUTH EAST
NORTH WEST
SNELL'S ANGLE
RADIANCE (μE/m²/sec/deg)
2.0
1.5
1.0
0.5
0.0
0 40 80 120 160 200 240 280 320 360
(C)
WEST SHORE
MID-LAKE
SHORE SHADOW
EAST
WEST
SNELL'S ANGLE
RADIANCE (μE/m²/sec/deg)
2.0
1.5
1.0
0.5
0.0
0 40 80 120 160 200 240 280 320 360
ZENITH ANGLE (DEGREES)

FIGURE 34

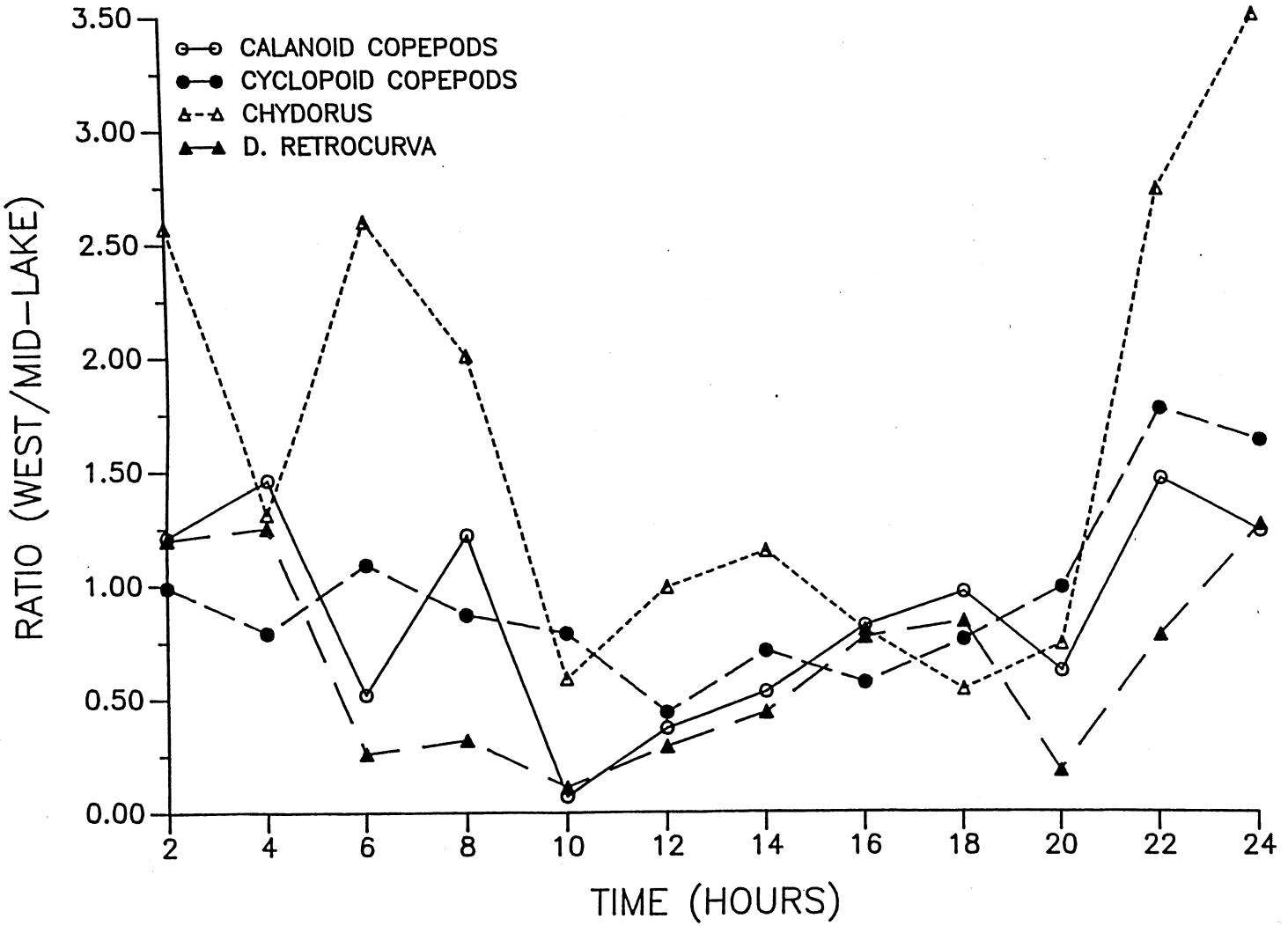
CALANOID COPEPODS
CYCLOPOID COPEPODS
CHYDORUS
D. RETROCURVA
RATIO (WEST/MID-LAKE)
3.50
3.00
2.50
2.00
1.50
1.00
0.50
0.00
2
4
6
8
10
12
14
16
18
20
22
24
TIME (HOURS)

FIGURE 35